Statistical Analysis of Passenger Car Use to Model the Impact of Electric Vehicle Take-up on the Power Distribution Network

Sikai Huang

A thesis presented in fulfilment of the requirements for the degree of Doctor of Philosophy

Institute of Energy and Environment
Department of Electronic and Electrical Engineering
University of Strathclyde
Glasgow G1 1XW
Scotland, UK

October 2014

This thesis is the result of the author's original research. It has been composed by the author and has not previously been submitted for examination which has led to the award of a degree.

To my parents, Jiankang Huang and Jingliang Tang

Table of Contents

List of Figures

List of Tables

Abbreviations

ASCBR	Acceptable Shifting Convergence Band Rule
CB	Confidence Band
CL	Confidence Level
CDF	Cumulative Distribution Function
DNO	Distribution Network Operator
DSM	Demand Side Management
D2D	Day to Day
EV	Electric Vehicle
GIS	Geographic Information System
h2h	Home to Home
ICE	Internal Combustion Engine
LV	Low Voltage
MC	Monte Carlo
MV	Medium Voltage
NG	National Grid
NHTS	National Household Travel Survey
NTS	National Travel Survey
OpenDSS	Open Distribution System Simulator
PDF	Probability Density Function
PHEV	Plug-in Hybrid Electric Vehicle
RV	Random Variable
SOC	State of Charge
TUS	Time of Use Survey
UKERC	United Kingdom Energy Research Centre
V2G	Vehicle-to-Grid

Abstract

The market for plug-in electric vehicles is expected to grow significantly over the next few years as a number of automobile manufacturers have released electric vehicle models onto the market. The charging demand of wide-scale use of EVs may have a significant impact on domestic electricity loads and could risk overloading the power distribution system unless appropriate charging strategies are applied to prevent this.

In order to quantify the future electric vehicle charging demand, it is necessary to gain a good understanding of current privately owned car use. In this thesis, domestic car use patterns have been studied in detail by analysing the United Kingdom Time of Use Survey 2000 data. The key findings show that weekday car use patterns are rather different than weekend ones. The majority of domestic cars are used for commuting to work during week days. Car activities, such as depart from home and arrive home are highly correlated and dependent on time of the day. Cumulative driving times are significantly dependent on the car arrival time. In most research, the relationship among these types of events are often ignored, which leads to errors in the calculation of charging demand. Three high resolution Monte Carlo simulation models are structured based on these domestic car use statistics in order to represent the weekday car use patterns; they represent three different approaches to trying to capture the complex dependencies associated with car use. The return time dependent Monte Carlo model utilise car returning home probabilities and the cumulative driving period dependent on arrival home time statistics. The single time increment Monte Carlo model uses two-state probability distributions of car departure and arrival to reproduce the weekday car location status. Although the correlation between car departure and arrival home events are not explicitly captured in this model, the multiple time increments Monte Carlo model captures this relationship by sampling from car away and parking period time dependent probability distributions.

Validation of the simulation results shows that all three models generate acceptably accurate car use patterns with home as the primary parking location.

In the later part of the thesis, assessments the impact of electric vehicle home charging on the distribution network have been performed for two case studies; one focuses on the peak load impact on substation transformers, and the other one examines individual household voltages (at 230V low voltage level). For the specific network considered, it is shown that distribution substation transformers (i.e. primary and secondary) will face increasing peak load due to electric vehicle charging in the case that householders start charging as soon as they arrive home. It is recognised for the first time that domestic car use behaviour has effects on the household electricity consumption model and to reflect this the household electricity model has been modified to account for the changes in occupancy associated with car movements. In the low voltage case study, the household voltage issue has been investigated for this specific network by performing power flow calculations, and shows that a household, located at the end of a long service cable, suffers under voltage before the substation feeder reaches its thermal limit.

In the last part of the thesis, several vehicle charging strategies have been developed to mitigate the problem of overloading the substation transformer. It is shown that a simple time delay to charging strategy creates an additional peak load on the substation loading profile; however, with a random time delay, overloading of the substation can be avoided. The potential role of EVs as responsive demand has been explored with the aim of utilising vehicle charging to support local power system operation with surplus wind generation. An algorithm is proposed that can effectively shift vehicle charging by implementing a linear cost function to track the surplus wind generation.

Acknowledgements

The development of this PhD thesis over the last couple years has been one of the most challenging but at the same time rewarding experience of my life. This research could not have been achieved without the help and encouragement of many people, to whom I want to offer my warmest gratitude:

First, I would like to thank my academic supervisor Professor David Infield for his priceless guidance and for his invariable support and positive attitude throughout my PhD. I will always be thankful for the opportunity of starting, developing and completing this PhD under his supervision.

I gratefully acknowledge the funding for this research provided by the EPSRC Transition Pathways to a Low Carbon Economy (TP) Consortium. Also, I am grateful for the collaboration of my colleagues at the TP consortium.

I would also like to thank Damien Frame, Julian Feuchtwang and Susan Yue Wang for their academic support.

And thank you to Shimeng for all her support over the past couple years. It won't be possible without her.

1. Chapter 1: Introduction

With wider deployment of the plug-in electric vehicles (EV), Distribution Network Operator (DNO) would expect increasing domestic demand due to large numbers of vehicles charging. Additional EV charging load could lead potentially to overloading of power system assets unless appropriate demand side management is in place. This thesis is primarily concerned with the quantification of the potential impact of domestic electric vehicle charging on the power distribution system.

This chapter first assesses the existing literature on modelling electric vehicle charging and analysing the impact on the distribution system. It then introduces relevant analysis techniques and outlines the objectives and methodology of the thesis. Finally, it enumerates the main contributions of the thesis.

1.1. Thesis background

1.1.1. Electric Vehicle Deployment Contributions and Concerns

The need to reduce carbon emissions is driving significant changes to the way electricity is generated and used. Transport poses particular challenges to decarbonisation but one approach that is finding favour in European countries is a move to replace a proportion of cars with EVs, [1.1]. Transport is a significant and growing source of domestic carbon emissions, presently representing 21% of total UK domestic carbon emissions, where passenger cars account for 58% of this, [1.2]. Wide deployment of electric vehicles can offer significant environmental benefits for reducing carbon emissions compared with existing internal combustion engine (ICE) vehicles. The UK government provides incentive schemes for domestic consumers to purchase electric vehicles. The UK Department for Transport (DfT) released a document, "Low carbon and electric vehicles", in 2009, [1.3]. It states that the government plans to create a £250m scheme to reduce the price of electric and plug-in hybrid cars, from 2011 onwards, to help consumers purchase them. Approximately £20m of the £250m will be used to develop an electric vehicle charging infrastructure framework, helping to create a UK network of electric car cities. The number of the electric vehicles deployed in the UK up to 2050 has been forecast by John et al [1.4]. The predicted number of EVs up to 2050, under the market leading 'Market Rules' scenario, is presented in that work; in particular it is assumed that there would be 1.1 million electric vehicles on the road in the UK by 2020.

The electricity supply industry, including the DNOs, concerned that the increasing deployment of electric vehicles will lead to significant additions to electricity load that could be difficult to meet, [1.5], [1.6]. There is also particular concern that much of this additional load may occur at times when the electricity supply system is already heavily loaded. These challenges will apply across the entire power system. It is likely that EVs will not be evenly distributed geographically since their limited range will make them more attractive in urban than rural areas. In the early days of deployment it is also quite possible that certain cities will see higher penetrations as a result of local planning and incentive schemes, and measures to discourage the use of conventional vehicles, for example through the establishment of centre city non-pollution zones. National Grid (NG), the UK transmission network operator, has created two different 'Future Energy Scenarios' (FES) – Slow Progression and Gone Green – to meet the energy demands of this century, [1.7]. At the moment, there are around 5,000 electric vehicles on the road in the UK. In Gone Green, there are expected to be 3.2 million cars in the UK by 2030 and in Slow Progression there will be 0.9 million. On a cold winter day, the average electricity customer currently consumes 13 kWh. FES analysis assumes an average EV charge of approximately 6.3kWh per day, which means an increase in consumption of almost 50% for a typical home. As the transmission system owner and operator, NG has to understand what the future demand is at peak times so as to ensure that the network has adequate capacity in place to meet the demand.

1.1.2. Studies on Electric Vehicle Use Modelling and Charging Impact on the Distribution Network

Several PhDs, [1.8] to [1.13] have been recently completed that focus on resolving the challenges of integrating electric vehicles into power systems. Some of the researchers analysed the potential impact of electric vehicle charging on the distribution network, [1.8], [1.9] and others focused more on developing control strategies for EV charging in order to either mitigate the impact or to utilise them as responsive load[1.10], [1.12]. In [1.8], the thesis illustrates the EV charging impact on medium voltage distribution network as results of power flow analysis with various charging strategies. Another thesis focuses on impact analysis of EV charging specifically on the Irish LV network as well as the development of control strategies for EV charging, [1.9]. The development of control strategies for EV charging as demand response in order to prevent stress on the power distribution system, [1.10]. In [1.11], part of thesis deals with the EV charging impact at a national level as well as at low voltage level under a 2030 EV deployment scenario. The thesis explores the opportunities for EV charging providing ancillary services for intermittent energy sources, such as photovoltaic generation are explored in [1.12]. Another UK thesis illustrates the capability of a developed tool to assess the EV charging impact on the national load profile based on the statistical analysis of household car use data as well as EV models currently available on the market, [1.13].

A number of electric vehicle trials have been performed by the automobile manufactures, electricity utilities and academic researchers, often undertaken collaboratively, in order to learn from EV user adaption as well as assess EV charging impact on the electricity grid, [1.14] to [1.17]. In addition to providing valuable practical experience to the companies, these studies provide data on EV use patterns. However, due to the limited nature of the trials, these data are of restricted generality. For example, in [1.9], the EV charging model has been structured from limited trial vehicle usage data. Most research though has focused on predicting the impact of EV take up on the electricity system, the best of this based on substantial data quantifying vehicle use. A Finnish study modelled plug-in hybrid electric vehicle (PHEV) charging based on the National Travel Survey published by the Finnish

Transport Agency, [1.18]. It states that half of the driven journeys in Finland are shorter than 50km. This paper also highlights the challenges and limitations of the National Travel Survey data, in particular that a driver can operate multiple cars during the same survey diary day. Papers [1.19] to [1.21] derive from the on-going multi-year EPRI study into plug-in electric vehicles, this being the most comprehensive approach to EV impact analysis undertaken to date, and serves to underline the importance of this area of analysis. In [1.22], US National Household Travel Survey has been studied in detail in order to quantify the PHEV charging load for summer and winter cases. Although this study comes after [1.10], more precise assumptions and careful considerations of future PHEV deployment enables much more accurate impact analysis on the distribution network, which is rather different than the previous study. Two Dutch studies derived statistics for vehicle use patterns from a survey conducted by the Dutch Ministry of Transportation, [1.23] and [1.24]. Both Verzijlbergh and Lojowska present probability distributions for vehicle movements based on the Dutch survey, and these are used in stochastic modelling; the main weakness of these studies is their hourly time resolution. Large volumes of information regarding short distance vehicle movements have thus been neglected due to the course time resolution, although these short trips constitute the bulk of domestic journeys and would make significant contributions to EV charging loads. Yunus *et al*, [1.25], presented a stochastic model for EV charging and impact on the distribution transformer. This work illustrated the merit of the stochastic method (sampling from probability distribution) compared with a deterministic approach (using assumptions) to EV modelling. The main concern with this study though is its assumption that cars only make one trip away from home each day and associated with this that the departure times from home and the return time are normally distributed about their mean values chosen to be 7am and 6pm respectively for weekdays, which is highly simplistic as compared with the data presented in this thesis, and therefore likely to produce misleading results. Moreover the rather low charging rates used in the study can lead to underestimates of the potential impact on the grid, even though different sizes of battery capacities have been considered. Qian *et al*, [1.26], present in detail their modelling of vehicle movements making use of UK data on vehicle utilisation as a function of time of day. However, a log-normal probability distribution is simply used to represent the daily distance travelled and although this is not totally unreasonable it does not take account of the fact that in practice journey lengths depend strongly on when those journeys occur during the course of the day, as will be shown in the next part of this thesis.

Other than the time resolution issue, another interesting relationship that has often been neglected in earlier research is the link between car arrival time and the time of the subsequent departure from the home. These two parameters are critical when determining the available time period for EV charging. One Monte Carlo model structured in this thesis has treated these events as statistically independent in the approach implemented, although it is possible to evaluate the correlations between these events, [1.27] and [1.28]. In [1.27], a mathematical formulation, called a copula function, was used to evaluate an approximation to the relationship between car departure and arrival home and is limited to a maximum of two home-to-home (h2h) journeys per day. No validation is presented in the paper; therefore, it is not possible to know the accuracy of the driving patterns represented in the paper. In [1.28], a curve fitting technique was applied to the hourly distribution of the last arrival time home dependent on car departure time to generate the required time dependent distribution. However, as the car arrives home, the synthetic driving cycles are randomly assigning to the temporal distribution. In fact, the driving activity is highly dependent on the car arrival time, and this is ignored in [1.28]. Both approaches have shown the challenges of determining the mathematical relationship between car departure from home and arrival back home.

Pecas Lopes *et al*, [1.29], have examined in detail the impact of EVs on the electricity distribution system; they refer to the situation where owners charge their vehicles without constraints when they return home as "dumb charging" but little detail on modelling of the vehicle movements is provided. Electric vehicle charging impact can be assessed by performing load flow such as in [1.30]. Putrus *et al* presents the three supply-demand matching scenarios charging impacts on substation transformer loading as well as voltage issues at 11kV and 400V level as results of power flow calculation. The impact on the LV network voltage has been illustrated for the EV acting as distributed generation through vehicle-to-grid technology; and for that particular network, the system can couple up to 30% of households with EVs before the local voltage drops below the statutory limits. Additionally, power quality and phase imbalance issues due to vehicle charging have also been investigated. In contrast to small-scale distribution network analysis, a Spanish research team analysed electric vehicle charging impacts on large-scale real distribution areas from medium voltage 20kV to low voltage 6kV voltage levels, which includes more than 6,000 LV residential customers, and an industrial and residential area with over 61,000 customers, [1.31]. The advantage of having this large-scale distribution model enables distribution system operators to forecast the required network investment with different future levels of PEV penetration. Although the EV penetration level is adapted from the EPRI study, the large-scale distribution planning model has simulated that required incremental investment can be avoided if smart charging strategies are implemented compared to the default charging regime; and the energy losses with maximum EV penetration level could significantly be increased even when majority of vehicles charging at off-peak hours. As part of analysis of network constraints, Quiming *et al*, [1.32] performed a study focusing on the potential impact on residential distribution transformer life due to vehicle charging.

Several EV studies have been published on vehicle charging strategies developed to meet system constraints, reduce EV charging costs, or help absorb renewable generation in the distribution system, [1.33] to [1.36]. Control strategies have been applied to EV charging activity in order to prevent either overload the system or voltage droop, such as in [1.37]. In paper [1.34], load scheduling and dispatch for vehicle charging are adjusted to reduce EV charging costs based on an electricity price signal. Deilami and his colleagues, [1.35], proposed a novel load management solution for coordinating the charging of EV fleets. By identifying three prioritised time zones, vehicle charging can be shifted to times of day with less intensive system loading in order to manage system distribution system constraints and reduce costs. However, this modelling approach has the weakness of using fixed and generalised household demand profiles; therefore, the change of the household demand profiles would lead to different prioritised time zones for vehicle charging.

1.2. Thesis Objectives

The main question this thesis attempts to answer is:

- What will be the impact of electric vehicle charging on the UK power distribution network in the future and how can this charging be controlled to improve distribution network operation?

Answering this question requires the statistical analysis of data for current domestic car use, the development of stochastic models for future electric vehicle charging, and the development of a power distribution network model which enables distribution network operators assessing the impact. Finally, charging strategies need to be developed that can be applied to these vehicle charging loads in order to mitigate the impact and help absorb surplus renewable generation.

To answer the main thesis question, the following activities have been undertaken:

1. Review the existing literature on modelling electric vehicle charging and impact assessment on the power distribution system to identify the research gap.
2. Identify main car use data sources and calculate privately owned car use statistics with home as primary parking location, especially for weekdays. To understand the use patterns of domestic car driver.
3. Develop stochastic models to simulate weekday car driving patterns.
4. Analyse simulation results against the data source statistics to check the consistency of the model output.
5. Establish case studies to quantify the impact of vehicle charging on primary (11kV) and secondary (11kV/400V) distribution substation transformers.

6. Develop a low voltage network model with real network parameters to perform assessment on the vehicle charging impacts.
7. Identify a suitable individual household electricity consumption tool and generate house by house electricity consumption profiles for a hypothetical residential community.
8. Investigate the impact of vehicle charging on low voltage network in terms of feeder loading and voltage deviation.
9. Develop control strategies for vehicle charging in order to mitigate the impact on the substation transformer loading.
10. Develop control strategy for vehicle charging to absorb local surplus renewable generation.

1.3. Contributions to Knowledge

The thesis delivers a number of important contributions to engineering in terms of both knowledge and the development of novel techniques:

1. It provides a detailed analysis of UK privately owned car use based on the United Kingdom Time of Use Survey 2000 data. From this data, key statistics of weekday car usage have been identified and from these, key probabilities and probability distributions of weekday car usage, such as departure time, arrival time, cumulative driving period dependent on arrival time, etc. have been estimated. These statistics reveals the driving behaviour of domestic car user in UK. In different European countries, the driving habits of people are different; UK domestic car user has different driving distance than the Finnish drivers. This particular contribution is presented in Chapter 2.

2. High resolution time-series Monte Carlo (MC) models enable simulating privately owned car daily use patterns have been developed. A return time dependent MC model utilises only car arrival time and the associated cumulative driving period. Both fixed time increment and multiple time increments MC models follow weekday car movements, such as time of departure and arrival, duration of parking at home and time away from home, and the cumulative driving period. A comprehensive analysis has been performed to check the modelling results with Time of Use Survey statistics. Three Monte Carlo models are present in detail in Chapter 3.

3. An individual household electricity consumption model has been modified to include the electricity consumption changes due to EV use through active occupancies in the household. Details of individual household electricity consumption modelling is presented in Chapter 4.

4. An impact assessment of future EV charging has been performed on primary and secondary substation transformers of a UK specific network that structured based on real network parameters. Power flow analysis has been performed on a typical low voltage (11kV/400V) distribution network based on real network parameters. Impact results are presented in Chapter 4.

5. Opportunities to use EV charging as responsive load in the power distribution system have been explored with 'time-shifting' charging strategies. The potential benefit of utilising EVs to absorb surplus wind generation in the system have been investigated based on the consideration of the numbers of EVs parked at home and available for

charging at any time of day. Details of developed charging strategies has been presented in Chapter 5.

1.4. Publications Arising from This Thesis

Through the development of this thesis, the author has contributed the following journal articles as co-author:

J. Barton, **S. Huang**, D. Infield, M. Leach, D. Ogunkunle, J. Torriti, M. Thomson, The Evolution of Electricity Demand and the Role for Demand Side Participation, in Buildings and Transport, *Energy Policy Special Section: Transition Pathways to a Low Carbon Economy*, vol. 52, pp, 85-102, January 2013.

D. Pudjianto, P. Djapic, M. Aunedi, C. K. Gan, G. Strbac, **S. Huang**, D. Infield, Smart Control for Minimizing Distribution Network Reinforcement Cost due to Electrification, *Energy Policy Special Section: Transition Pathways to a Low Carbon Economy*, vol 52, pp, 76-84, January 2013.

The author has also contributed to the following conference papers either as main author or co-author:

X. Zhong, A. Cruden, D. Infield, **S. Huang**, Assessment of Vehicle to Grid Power as Power System Support, *Proceedings of the 44th International Universities Power Engineering Conference (UPEC)*, Glasgow, 2009.

S. Huang, D. Infield, The Potential of Domestic Electric Vehicles to Contribute to Power System Operation through Vehicle to Grid Technology, *Proceedings of the 44th International Universities Power Engineering Conference (UPEC)*, Glasgow, 2009.

S. Huang, D. Infield, The Impact of Domestic Plug-in Hybrid Electric Vehicles on Power System Loads, *Proceedings of International Conference on Power System Technology (POWERCON)*, Hangzhou, 2010.

S. Huang, D. Infield, Demand Side Management for Domestic Plug-in Electric Vehicles in Power Distribution System Operation, *The 21st International Conference and Exhibition on Electricity Distribution (CIRED)*, Frankfurt, 2011.

D. Frame, G. Ault, **S. Huang**, The Uncertainties of Probabilistic LV Network Analysis, *IEEE Power and Energy Society General Meeting (PESGM)*, San Diego, 2012.

S. Huang, D. Infield, Potential of Plug-in Electric Vehicles for Supporting Regional Power Distribution System Operation with High Penetration of Wind Generation, *Proceedings of International Conference on Sustainable Power Generation and Supply (SUPERGEN)*, Hangzhou, 2012.

S. Huang, R. Carter, A. Cruden, D. Densley, T. Nicklin, D. Infield, Potential Impact of Uncoordinated Domestic Plug-in Electric Vehicle Charging Demand on Power Distribution Networks, *European Electric Vehicle Congress (EEVC)*, Brussels, 2012

S. Huang, L. Wu, D. Infield, T. Zhang, Using Electric Vehicle Fleet as Responsive Demand for Power System Frequency Support, *Vehicle Power and Propulsion Conference (VPPC)*, Beijing, 2013.

S. Huang, D. Infield, A. Cruden, D. Frame, D. Densley, Plug-in Electric Vehicles as Demand Response to Absorb Local Wind Generation in

Power Distribution Network, *Proceedings of the 27th International Electric Vehicle Symposium & Exhibition (EVS)*, Barcelona, 2013.

1.5. Thesis Structure

The structure of this thesis mirrors the development of the concepts – from initial scoping, through development of the Monte Carlo model, to impact assessment and demand side management for electric vehicle charging.

Chapter 2 first describes the different sources of survey data for UK transport statistics, which includes privately owned car use information. This part of chapter also explains the advantages of using The United Kingdom 2000 Time Use Survey (TUS) compared to the National Travel Survey 2002-2008 (NTS). The second part of this chapter describes the methodological steps to derive the required statistical information relevant to privately owned car use. The third part of ***Chapter 2*** describes in detail the car use statistics derived from the TUS data, including time of departure and arrival back home, purpose and duration of journeys, and locations of parking, etc. This chapter provides statistical information that will be used for the Monte Carlo simulation (MC) modelling of privately owned car use presented in ***Chapter 3***. The last part of the chapter discusses the challenges faced in assessing car use statistics.

Chapter 3 presents in detail the Monte Carlo modelling of privately owned car use and the implementation of the inverse-transform method and illustrates the different approaches taken to modelling car use. The basic concept of MC simulation is explained in the first section. A MC model that uses only statistics of time arrival and the total driving journey distribution at these times is developed; this is referred as the return time dependent MC model. The main advantage of this return time dependent MC model is that it only requires the two types of car use statistics mentioned and despite this can produce accurate forecasts of cumulative driving period for cars returning home. Next two MC models following car locations approach are structured by following the logical sequence through the day when cars park at home, depart from home, arrive home, and the total journey driven as a function of the arrival time. One is called single time increment MC model, which only uses probabilities of car departure home and car arrival home. Although the correlation between car departure and arrival home events are ignored in this model, the multiple time increments Monte Carlo model captures this relationship by sampling from car away and parking period time dependent probability distributions. It is assumed that the charging facility is only available at home; therefore, the parking location analysed in the MC models is no other than the primary house. Simulation results from these MC models have been analysed in detail so that the outputs of these MC models are consistent with TUS data statistics calculated in ***Chapter 2***.

Chapter 4 presents two case studies illustrating the impact of EV charging on the power distribution network, including the increase in primary substation (11kV/400V) peak power, secondary substation (400V/230V) feeder thermal limits as well as voltage deviations at monitored households. In the first case study, the EV charging profiles are calculated based on the outcome of the return time dependent MC models, and both standard (13A) and fast (32A) single-phase charging are considered. The simple 'plug and charge' strategy enables charging the battery starting as soon as the EVs arrive home, and no constraints on the charging duration. These vehicle charging profiles have been used to assess the impact on the primary substation loading. Results shows that the EV charging increases the existing peak load on substation transformers. As contrast, the multiple time increments MC model limits the EV charging in relation to the car departure statistics, and charging profiles have been used in the second case study. The LV network model is based on a hypothetical residential community but makes use of real network parameters. Results present that the impact of EV charging on the low voltage network, especially 230V. The assessment of EV charging impact has been undertaken on distribution feeder line and examines thermal limits and voltage deviations. Power flow (also known as load flow) analysis has been performed for calculating excessive feeder current and the deviation of voltage due to EV charging on the network.

Chapter 5 explores the potential of privately owned EVs to act as responsive demand in the context of local power distribution network operation. The first section presents the opportunity of electric vehicle participating in the demand side management (DSM). Case study 1 introduces several different charging strategies that modify the EV charging impact on the power distribution network. In case study 2, electric vehicles are used to absorb local wind generation so that the maximum amount of surplus wind can be utilised driven by a wind dependent cost function for vehicle charging. The outcome illustrates that EVs can be utilised to improve the operations of the distribution network, and reduces the cost of recharging the EVs.

Chapter 6 concludes the thesis and brings together the learning from each of the chapters. It justifies the contributions to knowledge listed above and answers the key thesis question. Finally, important future work is identified.

1.6. References

[1.1] European Commission, 'Clean transport, Urban transport – Electric vehicles', [online], http://ec.europa.eu/transport/themes/urban/vehicles/road/electric_en.htm accessed on 09/03/2014.

[1.2] The Secretary of State for Transport. (2009). *Low Carbon Transport: A Greener Future, A Carbon Reduction Strategy for Transport*, Crown Office [online]. Available https: https://www.gov.uk/government/publications/low-carbon-transport.

[1.3] Department for Transport, *Low carbon and electric vehicle*, 2009. Available at: http://www.dft.gov.uk/pgr/scienceresearch/technology/lowcarbonelecvehicles/

[1.4] J. Barton, S. Huang, D. Infield, M. Leach, D. Ogunkunle, J. Torriti, M. Thomson, The Evolution of Electricity Demand and the Role for Demand Side Participation, in Buildings and Transport, *Energy Policy Special Section: Transition Pathways to a Low Carbon Economy*, vol. 52, pp, 85-102, January 2013.

[1.5] National Grid, "Operating the Electricity Transmission Networks in 2020," June 2011. Available online: http://www.nationalgrid.com/uk/Electricity/Operating+in+2020/

[1.6] Scottish and Southern Energy, "SSE Annual Report 2012", available online: http://www.sse.com/uploadedFiles/Controls/Lists/Reports_and_Results/SSE_AnnualReport2012.pdf

[1.7] National Grid Connecting, 'Journey of discovery - Electric vehicles, energy demand, future energy scenarios', http://www.nationalgridconnecting.com/journey-of-discovery/

[1.8] K. Qian, "Modelling of Electrical Distribution Systems with High Penetration Level of Distributed Generation and Electric Vehicles", Ph.D. thesis, School of Engineering and Computing, Glasgow Caledonian Univ., Glasgow, UK, 2010.

[1.9] P. Richardson, "Integration of Distributed Energy resources in Low Voltage Electricity Networks", Ph.D. thesis, School of Electrical, Electronic and Communications Engineering, Univ. College Dublin, Dublin, Ireland, 2012.

[1.10] S. Shao, "An Approach to Demand Response for Alleviating Power System Stress Conditions due to Electric Vehicle Penetration", Ph.D. thesis, Virginia Polytechnic Institute and State University, Virginia, US, 2011.

[1.11] P. Papadopoulos, “Integration of Electric Vehicles into Distribution networks”, Ph.D. thesis, School of Engineering, Cardiff Univ., Cardiff, UK, 2012.

[1.12] F. Marra, “Electric Vehicles Integration in the Electric Power System with Intermittent Energy Sources – The Charge/Discharge Infrastructure”, Ph.D. thesis, Dept. Elect. Eng., Technical Univ. Denmark, Denmark, 2013.

[1.13] E. L. Parry, “Electricity load estimation and management for plug-in vehicle recharging on a national scale prior to the development of third party monitoring and control mechanisms”, Ph.D. thesis, Dept. E. E. E., Univ. of Bath, Bath, UK, 2013.

[1.14] R. Carter, A. Cruden, D. Densley, and T. Nicklin, "Timed Charging Points for Electric Vehicles: User Behaviour and Potential Impacts to Low Voltage Networks," in *European Electric Vehicle Congress*, Brussels, Belgium, 2011, p. 7.

[1.15] Coventry and Birmingham Low Emission Demonstrators (CABLED). Online: http://www.arup.com/Home/Projects/CABLED.aspx

[1.16] M. Wikstrom, E. Sunerstedt, “Experiences from the operation of 50 EVs during one year in Sweden,” in *European Electric Vehicle Congress*, Brussels, Belgium, 2012, p. 5.

[1.17] P. Cocron, Bu, x, F. hler, I. Neumann, T. Franke, *et al.*, "Methods of evaluating electric vehicles from a user's perspective - The MINI E field trial in Berlin," *Intelligent Transport Systems, IET,* vol. 5, pp. 127-133, 2011.

[1.18] A. Rautiainen, S. Repo, P. Jarventausta, A. Mutanen, K. Vuorilehto, and K. Jalkanen, "Statistical Charging Load Modeling of PHEVs in Electricity Distribution Networks Using National Travel Survey Data," Smart Grid, IEEE Transactions on, vol. 3, pp. 1650-1659, 2012.

[1.19] A. Maitra, J. Taylor, D. Brooks, M. Alexander, and M. Duvall, "Integrating plug-in- electric vehicles with the distribution system," in *20th International Conference and Exhibition on Electricity Distribution (CIRED 2009), 8-11 June 2009*, Stevenage, UK, 2009, p. 1029 (5 pp.).

[1.20] J. Taylor, A. Maitra, M. Alexander, D. Brooks, and M. Duvall, "Evaluation of the impact of plug-in electric vehicle loading on distribution system operations," in *2009 IEEE Power & Energy*

Society General Meeting (PES), 26-30 July 2009, Piscataway, NY, USA, 2009, p. 6 pp.

[1.21] J. Taylor, A. Maitra, M. Alexander, D. Brooks, and M. Duvall, "Evaluations of plug-in electric vehicle distribution system impacts," in *Power and Energy Society General Meeting, 2010 IEEE*, 2010, pp. 1-6.

[1.22] S. Shafiee, M. Fotuhi-Firuzabad, and M. Rastegar, "Investigating the Impacts of Plug-in Hybrid Electric Vehicles on Power Distribution Systems," Smart Grid, IEEE Transactions on, vol. 4, pp. 1351-1360, 2013.

[1.23] R. A. Verzijlbergh, Z. Lukszo, E. Veldman, J. G. Slootweg, and M. Ilic, "Deriving electric vehicle charge profiles from driving statistics," in *Power and Energy Society General Meeting, 2011 IEEE*, 2011, pp. 1-6.

[1.24] A. Lojowska, D. Kurowicka, G. Papaefthymiou, and L. van der Sluis, "From transportation patterns to power demand: Stochastic modeling of uncontrolled domestic charging of electric vehicles," in *Power and Energy Society General Meeting, 2011 IEEE*, 2011, pp. 1-7.

[1.25] K. J. Yunus, M. Reza, H. Zelaya-De La Parra, and K. Srivastava, "Impacts of Stochastic Residential Plug-In Electric Vehicle Charging on Distribution Grid," in *Innovative Smart Grid Technologies (ISGT), 2012 IEEE PES*, 2012, pp. 1-8.

[1.26] Q. Kejun, Z. Chengke, M. Allan, and Y. Yue, "Modeling of Load Demand Due to EV Battery Charging in Distribution Systems," *Power Systems, IEEE Transactions on,* vol. 26, pp. 802-810, 2011.

[1.27] A. Lojowska, D. Kurowicka, G. Papaefthymiou, and L. Van der Sluis, "Stochastic Modeling of Power Demand Due to EVs Using Copula," *Power Systems, IEEE Transactions on,* vol. 27, pp. 1960-1968, 2012.

[1.28] L. Tae-Kyung, Z. Bareket, T. Gordon, and Z. S. Filipi, "Stochastic Modeling for Studies of Real-World PHEV Usage: Driving Schedule and Daily Temporal Distributions," *Vehicular Technology, IEEE Transactions on,* vol. 61, pp. 1493-1502, 2012.

[1.29] Pecas Lopes, J. A., Soares, F. J. and Almeida, P. M. R., "Integration of Electric Vehicles in the Electric Power System," Proc. IEEE, vol. 99, no. 1, pp. 168-183, 2011.

[1.30] G. A. Putrus, P. Suwanapingkarl, D. Johnston, E. C. Bentley, and M. Narayana, "Impact of electric vehicles on power distribution networks," in *Vehicle Power and Propulsion Conference, 2009. VPPC '09. IEEE*, 2009, pp. 827-831.

[1.31] F. Pieltain, x, L. ndez, Roma, x, T. G. S. n, et al., "Assessment of the Impact of Plug-in Electric Vehicles on Distribution Networks," Power Systems, IEEE Transactions on, vol. 26, pp. 206-213, 2011.

[1.32] G. Qiuming, S. Midlam-Mohler, V. Marano, and G. Rizzoni, "Study of PEV Charging on Residential Distribution Transformer Life," Smart Grid, IEEE Transactions on, vol. 3, pp. 404-412, 2012.

[1.33] S. Bashash and H. K. Fathy, "Robust demand-side plug-in electric vehicle load control for renewable energy management," in *American Control Conference (ACC), 2011*, 2011, pp. 929-934.

[1.34] W. Di, D. C. Aliprantis, and Y. Lei, "Load Scheduling and Dispatch for Aggregators of Plug-In Electric Vehicles," *Smart Grid, IEEE Transactions on,* vol. 3, pp. 368-376, 2012.

[1.35] S. Deilami, A. S. Masoum, P. S. Moses, and M. A. S. Masoum, "Real-Time Coordination of Plug-In Electric Vehicle Charging in Smart Grids to Minimize Power Losses and Improve Voltage Profile," *Smart Grid, IEEE Transactions on,* vol. 2, pp. 456-467, 2011.

[1.36] S. Shao, M. Pipattanasomporn, and S. Rahman, "Demand Response as a Load Shaping Tool in an Intelligent Grid With Electric Vehicles," Smart Grid, IEEE Transactions on, vol. 2, pp. 624-631, 2011.

[1.37] D. Johnston, E. Bentley, M. Narayana, J. Tianxiang, P. Suwanapingkarl, and G. Putrus, "Electric vehicles as storage devices for Supply-Demand management," in *Vehicle Power and Propulsion Conference (VPPC), 2010 IEEE*, 2010, pp. 1-6.

[1.38] N. Leemput, F. Geth, J. Van Roy, A. Delnooz, J. Buscher, and J. Driesen, "Impact of Electric Vehicle On-Board Single-Phase Charging Strategies on a Flemish Residential Grid," *Smart Grid, IEEE Transactions on,* vol. 5, pp. 1815-1822, 2014.

2. Chapter 2: Household Car Use Data Analysis and Identification of Relevant Probabilities and Probability Distributions

For the purposes of quantifying the potential impact of widespread electric vehicles charging on the UK's power distribution system, it is essential to obtain relevant statistical data on vehicle usage. Since EV ownership is presently very limited, these data will inevitably be for internal combustion engine (ICE) vehicles, and in particular privately owned cars. This should not be an issue since the limited journey distances that will be dealt with in this work could easily be undertaken by an EV. Different sources that provide data on the use of household cars are presented and compared. Particular attention is paid to the United Kingdom 2000 Time of Use Survey as it contains detailed and valuable statistical information about household car use. This database has been analysed to obtain detailed car use statistics, such as probability of a car departure from home, probability of a car arrival home, probability distributions of individual journey time, etc. In this chapter, household car use behaviour is discussed in detail.

2.1. Private Owned Car Use Data Sources

In order to build up the probabilistic models[1] for privately owned car use, The United Kingdom 2000 Time Use Survey (TUS) has been selected as the main data source, [2.1]. There are other data sources available for verifying key statistics, such as time of day of car departure and arrival home, average daily driving journey time and length, car parking locations, and the journey purpose; in particular the National Travel Survey 2002-2010 (NTS), and Focus on Personal Travel 2005, [2.2] and [2.3].

2.1.1. The United Kingdom 2000 Time of Use Survey

The Time of Use UK Survey (TUS) 2000 is concerned with how people in the United Kingdom spend their time. The survey is based on diaries kept by 12,000 participants describing their day-to-day (D2D) activities with a ten-minute time resolution. In particular, the survey provides detailed data on privately owned vehicle use. Individuals in sampled households are asked to complete a two separate one day travel diaries for each week over the 15 months that they are participating in the survey, where the days are chosen at random over the whole week. Each diary runs from 4.00am to 3.50am the next day to minimise activity at the beginning and end of diaries. These diaries provide details of trips undertaken, including the purpose, method of travel, time of day that journey takes place, and the destination. Specific number codes are used to denote these household activities (i.e. sleeping, eating, etc.) and these will be made use of at a later stage in order to perform statistical analysis. The way data was recorded enables unambiguous identification of car movements, the purpose of the journey (e.g. travel to work, travel to

[1] A ***probability model*** is a mathematical representation of a random phenomenon. It is defined by its ***sample space***, ***events*** within the sample space, and ***probabilities*** associated with each event.

shopping centre, travel to school, etc.) and the location where the car is parked (e.g. home, friend's home, workplace, etc.) when it is not being driven.

2.1.2. National Travel Survey 2002-2008

The purpose of National Travel Survey is to monitor long-term changes in travel patterns and provide a better understanding of the use of transport facilities made by different sectors of the population. A similar survey methodology is applied as for the TUS: participating households are asked to fill in a seven-day travel diary, and the time resolution of the survey data is thirty minutes in this case. Additionally, the survey also provides general information on personal and company vehicle travel and also the driving speed for urban and other areas. As stated in the report, car access is one of the most important factors in determining the amount of travelling people do. Overall, there were 34.2 million licensed vehicles registered in Great Britain at the end of 2008, which included approximately 28 million cars. Among these 28 million cars, 89% of them are privately owned.

2.1.3. Focus on Personal Travel 2005 Edition

This survey is designed to bring together information about personal travel in Great Britain and highlight some of the key issues. It aims to provide readers with an introduction to the major trends in personal transport and a greater depth of understanding of some of the current areas of interest, debate and development. It includes the report of the National Travel Survey 2002/2003.

2.1.4. Other Available Car Use Data Sources

Besides UK data sources mentioned above, there are several studies with good quality analysis utilising overseas car use data sources in order to capture the characteristics of privately owned or domestic car driving patterns. In papers [2.4] and [2.5], the authors simulate electric vehicle's plug-in time by analysing

US National Household Travel Survey (NHTS) 2001 data, [2.6]. NHTS data is collected on daily trips taken in a 24-hour period, and various attributes are recorded, such as purpose of the trip, means of transportation used, and how long the trip took, etc. The 2001 NHTS sample comprised 26,038 samples and 43,779 households in nine areas, based on a total of 69,817 interviewed households. For long trips, a four-week recall period was used and data was collected on all trips of 50 miles or more from home. The definition of a travel day trip was modified to explicitly exclude stops to change mode of transportation. The time resolution is 1-min over 24-hour period, starting from 04:00 to 03:59 next day hours.

In [2.7] and [2.8], driving patterns were extracted from the transportation data for the year 2008 provided by the Dutch Ministry of Transportation, [2.9]. The Mobility Research Netherlands report gives a large dataset of individual trips by various transport means. The data is collected by means of a survey of roughly 40,000 people in the Netherlands. The dataset consists of over 130,000 individual movements (one way trips), from which approximately 40,000 are car movements involving roughly 18,000 individual cars. The most important variables that have been used to construct the different charge profiles in this study are (for each of the 18,000 individual cars): daily driving distance, home arrival time and home departure time. The time resolution, shown in [2.7] and [2.8], is hourly from 0000 to 2400 hours.

2.1.5. Advantage of Analysing United Kingdom Time Use Survey 2000 Data

The main advantage of using TUS as the main data source is the ten-minute time resolution compared to the NTS data, despite the rather similar approaches to collecting data, and the nature of the records, including departure and arrival time of day, duration of journey, etc. The amount of energy required to charge electric vehicle batteries is calculated based on the total length of journeys starting from and returning back home. Thirty-minute or lower time resolution data certainly loses critical information on commonly made short journeys, such as trips to local shops (see Section 2.3.3) with the result that the amount of energy required to charge EV batteries for these frequent journeys would be neglected. Figure 2.1 illustrates three examples of household journey activity that can be identified from the TUS data and the corresponding journey codes.

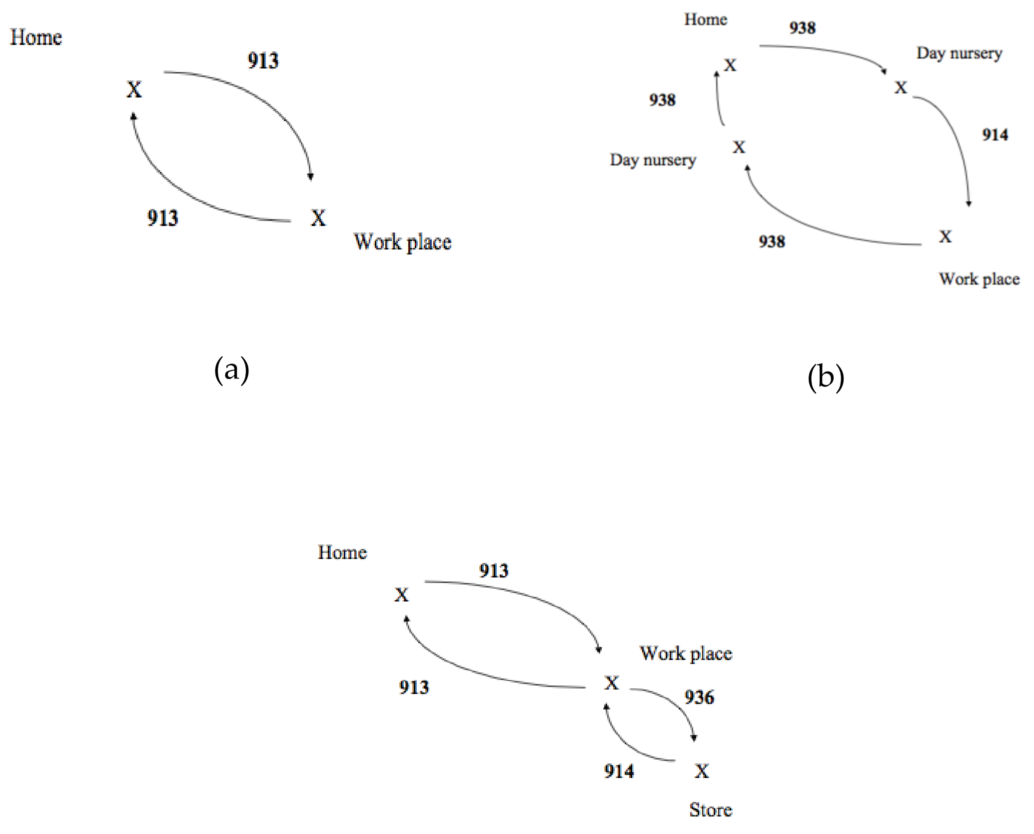

(c)

Figure 2.1 Examples of household journey activities. (a) home-to-work; (b) home-to-work with an errand en route; (c) home-to-work with a shopping trip from work.

As shown in Figure 2.1, specific code numbers are assigned in order to reflect the purpose of each journey. For example, Figure 2.1a shows the straightforward journeys to work and back home from work, coded as 913. TUS data indicates that many people in paid work start from home in the morning and return home in the evening. The first journey is defined by its purpose, which in this case is to go to work. If the journey back home in the evening was defined in the same way it should be a journey home from work, but instead, it is defined as another journey that relates to work. The code does not differentiate between journeys to and from work although this distinction can be deduced from the sequence. If an errand or additional driving activity occurs before one to/from working place, these driving activities tend to be rather short journeys. Detailed statistics of these errands or additional activities are explained in Section 2.3.5. Figure 2.1b gives the defined journeys to and from work including an errand or additional activity; suppose now that an errand is carried out on the way to work and from work, e.g. a child is left at the day nursery in the morning and picked up in the afternoon. Since the commute to work is no longer straightforward, the 913 code is no longer used. The first part of the journey is now connected with childcare (i.e., the reason to go to the day nursery) and the second part is connected with work. However, since the work portion of the journey is no longer straight from home, this is given the code for travel to/from work from a place other than home (code 914). The first part of the way back home is also connected with childcare, coded as 938. The final part of the journey is also coded to childcare since the journey's destination is home, coded as 938. In the Figure 2.1c, the journey includes an errand during lunch break at work, but still the starting place and final destination is home. Code 913 applies since the purpose of the journey is commuting as in the first case. The journeys to and from work are unaffected. The trip to the store is a journey of its own. The trip to the store is coded according to the purpose of the trip (code 936); the trip to work is classified according to the destination and the fact that the journey is not undertaken from home. Such detailed journey information is valuable for calculating total journey length when the car returns home and enables a Monte Carlo simulation model based on this data to produce accurate and valid charging demand calculations. Comparing the daily car usage patterns defined as the probability that a car is in use at different times of the day[2] for the TUS and NTS data it is clear that the two data sets are in reasonable agreement for the trend of weekday household car use as shown in Figure 2.2a. The weekend data of household car use shows that TUS data gives a higher proportion of cars in use than NTS data; however, the focus of the research here is on the weekday household car use. Household electricity consumption is suspected to impose the largest temporal demands on the distribution system. Additionally, electric vehicles are more likely to be used for short-range journeys (<100 miles) rather than long-range journeys (> 100 miles) which are more likely to take place at weekends.

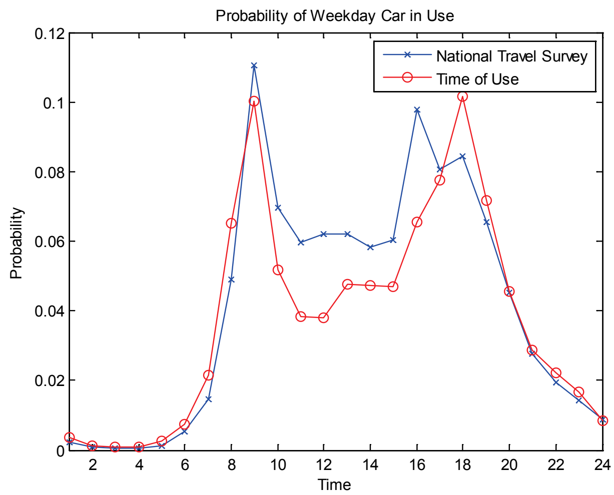

(a)

[2] Note that these are not probability distributions (sometimes called probability density functions – PDFs) in the formal sense even though they involve probabilities.

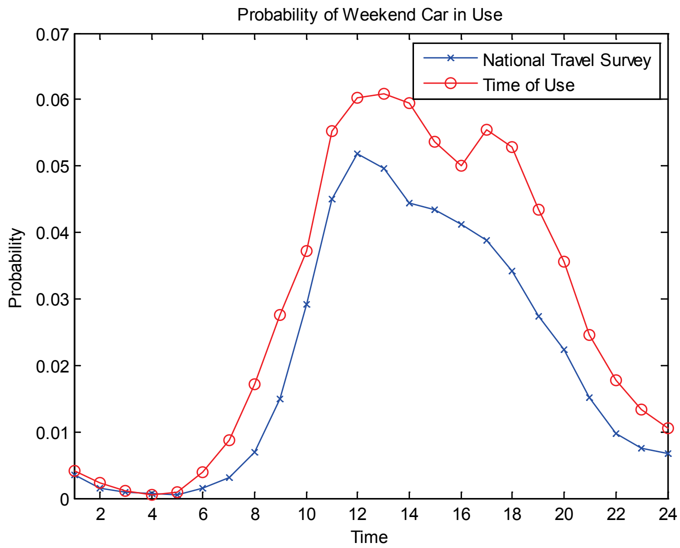

(b)

Figure 2.2 Comparison of NTS and TUS data. (a) weekday; (b) weekend.

A further advantage of the TUS data is that it has already been used to build an electricity consumption model for domestic households, [2.10], that can be used alongside the vehicle modelling. This household electricity consumption model, developed at Loughborough University, calculates demand based on active occupancy; this being the number of occupants who are active (i.e. not sleeping) in the household at a given time of day.

2.2. Methods Used for Calculating Car Use Statistics

This section explains the procedures for extracting the driving related data from the TUS database, such as car location, car being driven on the road, etc. These driving related data are all available in terms of time of day, reflecting the diary structure, and the time resolution is ten-minutes. Different stages of data processing are illustrated in Figure 2.3. The first step is raw data processing, which extracts and converts the original TUS data into more usable data compatible with Microsoft Excel. The next step is data post processing, and the outcome dataset contains household diaries together with car ownership information. These processed datasets have been further analysed in order to obtain statistics for the use of privately owned cars in a form useful for the subsequent Monte Carlo modelling.

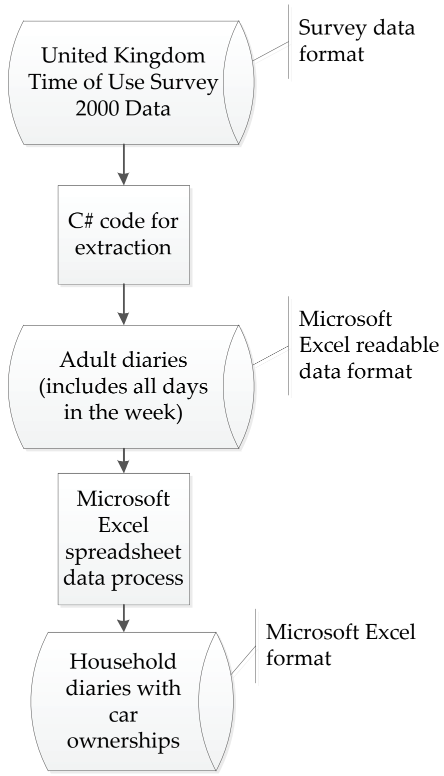

Figure 2.3 Stages of TUS data processing. The data format has been converted into a Microsoft Excel readable format at the end of the process.

2.2.1. Raw Data Processing

Several pre-requisite procedures are needed in order to process the database before more detailed analysis is undertaken. The first step is to extract the relevant data from the original TUS database. A C# code has been developed to extract the location, mode of transport and purpose for travel from the database. The function of the C# code is to locate the required variable label and extract the whole variable value for each diary entry. These diaries record every household's daily activities. Each diary contains the specific code denoting people actually driving their car (there are separate codes for passengers in transit). The extracted data is saved as a new Excel readable file for further data analysis. The resulting new database contains more than just driving information; it includes household reference number and number of persons in the house, day of the week, cars ownership etc. In total, 18,469 daily diaries (for both adults and children) were analysed. A total of 5,158 cars were identified as owned by the sample population in question. The nature of each stage of data processing is shown in Figure 2.4.

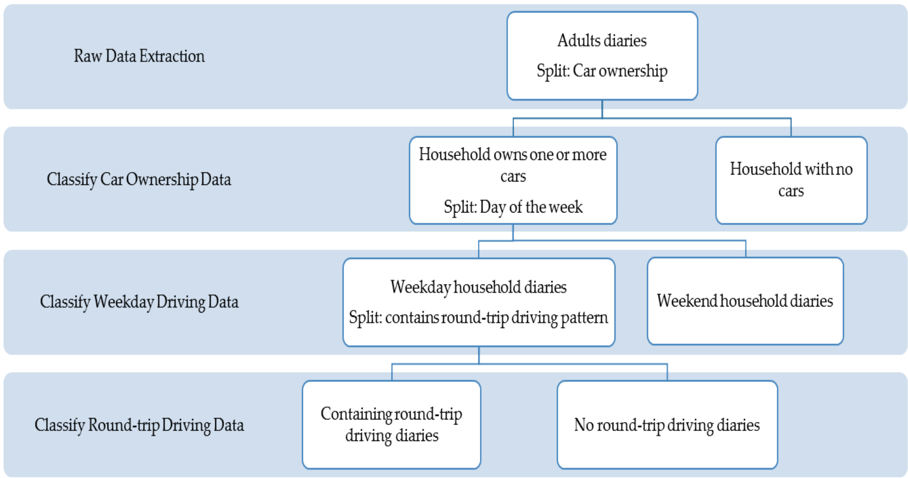

Figure 2.4 The structure at each data processing stage.

After filtering out the child diaries at the outset (not shown in Figure 2.4) , the remaining 14,443 adult diaries, which are recorded for each ten-minute period throughout the day, were arranged into two sub-databases, depending on whether weekdays or weekends are being considered. The numbers of weekday and weekend diaries returned were 7,219 and 7,224 respectively. This separation was performed as driving habits are self-evidently different at weekends. Both databases contain a specific code that indicates that the diary owner is travelling in a car as the driver (inherited from the original TUS data base). These diaries also distinguished the purpose and mode of travelling. Details of processed TUS data regarding code dictionary can be found in Appendix A.

2.2.2. Post Data Processing

After extracting driving related data, a new dataset is formed that also contains relevant household information. Summing up the number of unique household reference numbers gives the total number of households in the survey; this was found to be 4,972. Table 2.1 provides the relevant numbers for TUS data. For the population outlined above, the task is now to obtain exact car use patterns in the form of appropriate statistics and probability distributions. By searching for this specific driving code for each ten-minute interval, the probabilities of cars being parked or driven on the road at given time of day can be calculated. All calculated probabilities are all functions of time but do not themselves constitute a probability distribution. They have been classified into weekday and weekend profiles (as for example were shown in Figure 2.2). Detailed analysis of the weekday profiles helps build up the probabilistic models of these privately owned cars. There are a number of parameters for which time of day dependent probabilities are calculated; note that some of these are conditional probability events. For example, at given time of day, the probability that a car leaves home is self-evidently under the condition that it has been parked at home in the immediately preceding time step. Probabilities for each ten-minute time interval, t, are estimated from the survey data. These are listed below:

1. Probability of a car being parked at home
2. Probability of a car being away from home
3. Probability of a car departure home
4. Probability of a car arrival home

5. Probability distribution for time away from home conditional on time of departure
6. Probability distribution for time parking at home conditional on time of arrival to home
7. Probability distribution for cumulative time driving conditional on time away from home
8. Probability distribution for total driving time during round trip – conditional on arrival time

Table 2.1. Households and Diary Numbers in the TUS data.

	Numbers in TUS data
Households	**4,972**
Population of Adults (Households with 1+ cars)	**7,565**
Households with Cars	**3,623**
Weekday Diary Households	**3,606**
Weekend Diary Households	**3,608**
Weekday Diary	**7,219**
Weekend Diary	**7,224**
Weekday Diary contains Driving	**3,716**
Cars in Weekday Diary Data	**5,158**

2.3. Identification of Key Probabilities and Probability Distributions

Probabilistic characterisations of privately owned vehicle usage cover time of use, duration of use and distance covered as well as car ownership are outlined below. The results presented here represent UK privately owned driving behaviour based on the TUS survey sample.

2.3.1. Household Car Ownership

The population of adults whose household has at least one car in this study is 7,565, and this subset of the adult population is distributed over 3,623 households. Of this subset, 3,606 are covered by weekday diaries and 3,608 by weekend diaries; Figure 2.5 shows a Venn diagram of the households showing coverage of weekdays only, weekends only, and coverage of both. As already mentioned, all participants return at least 2 diaries, but there would seem to have been required a requirement for roughly equal numbers of weekdays and weekend diaries.[3] As a result there is a small number of adults who only return weekday diaries, and a similarly small number who only return weekend diaries. A consequence of this is that some households with at least one car are exclusively described in terms of weekend activity, and some only in terms of weekday activity. Fortunately the vast majority of households with at least one car (over 99%) are described in terms of both weekday and weekend activity, and car use in particular. It is also fortuitous that the numbers of weekday and weekend diaries are almost equal. These issues are important for some of the car status probability calculations, as will be described below.

[3] It is stated in the report for The United Kingdom 2000 Time Use Survey that there is a roughly equal number of week and weekend day diaries completed.

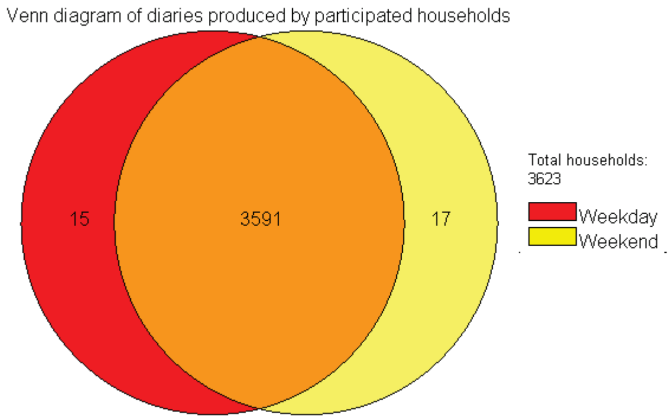

Figure 2.5 Venn diagram showing diary information for households with more than one car.

The number of cars per household is also analysed and classified by car ownership as shown in Figure 2.6a. The largest group of households in the survey have just one car. Just over one-fourth of total households have two cars. 25% of households in the original database do not have a car, as shown in Figure 2.6b. The average car ownership per household is just over one for the entire sample population.

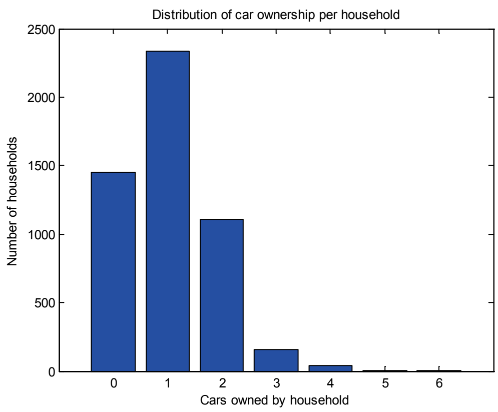

(a)

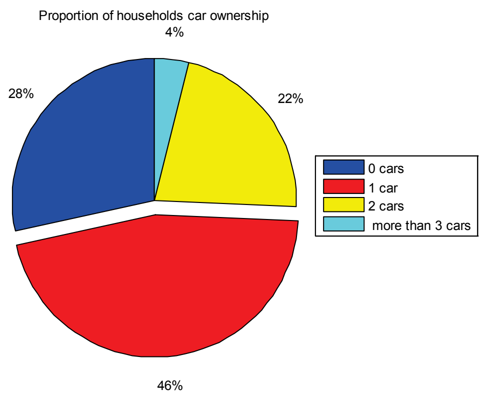

(b)

Figure 2.6 Cars ownership per household. (a) frequency distribution; (b) pie chart.

For the population outlined above, the task is now to calculate the exact patterns of vehicle use. After filtering out the child diaries, the remaining adults' diaries, which are recorded for each ten-minute period throughout the day, were arranged into two sub-databases, depending on whether weekdays or weekends are being considered. By searching for this specific driving code for each ten-minute interval, the probability of cars being driven on the road at any time can be calculated, as explained in detail in the following sections.

2.3.2. Time of Day Car in Use

The time of day when people use their cars as main driver (i.e. not as passenger) is important as it determines when EV batteries are being discharged and by how much, and consequently will affect when battery charging is likely to occur. The exact timing of battery charging is essential to determine the added load on the electricity distribution system, in itself important to ensure the provision of adequate electricity supply capability (both generation, transmission and local distribution) to charge future electric vehicles whilst supplying the remainder of the demand. Without further analysis, including other system loads, it is not possible to identify when the most critical time periods will be. As defined in the survey data, a car is driving on the road at a particular time of day when the diary gives the household adult activity for that ten-minute period as "driving a car as main driver" (code 15 in TUS). The probabilities for a car being in use for weekdays and weekends are calculated as follows:

1. For each ten-minute time step, count the number of diaries where an adult is driving (code 15), n_{drive}, over all weekday or weekend diaries: summing over all weekday 7,219 diaries with a value of 1 assigned to

all code 15 entries, and zero otherwise, and denoted by the logical variable $val(15)$:

$$n_{\text{drive}}(t) = \sum_{i=1}^{i=n_{ds}} val(15), t = 1,2,3,..,t_{\text{day}} \tag{2.1}$$

The integer t denotes the time of day in terms of the number of ten-minute periods and runs from 1 to 144 to cover 24 hours, and where $t = 1$ is the time period 4.00am to 4.10am. t_{day} is equal to 144. i denotes the diary index and n_{ds} represents the number of total diaries in the weekday or weekend data.

2. Dividing n_{drive} by the total number of cars[4], n_{ds}, the probability of a car being in use, $\mathrm{P}_{\text{drive}}(t)$ is calculated for both weekday and weekend subsets:

$$\mathrm{P}_{\text{drive}}(t) = \frac{n_{\text{drive}}(t)}{n_{\text{ds}}}, t = 1,2,3,...,t_{\text{day}} \tag{2.2}$$

Where n_{drive} gives the total number of cars in use (actually being driven) at any time. Note that this is different from cars simply being away from home at a given time. This summation is repeated for all weekday or weekend diaries. These probabilities are presented as a function of time of day in Figure 2.7. It should be noted that these probabilities will be underestimates since diaries for the houses with more than one car may not always cover situations where more than one car is being driven at the same time. These probabilities give a good idea of car use throughout the week but in fact are not used in the Monte Carlo simulation so that accuracy is not a particular issue. To be clear, these

[4] Although, as discussed previously, not all households are separately covered by both weekday and weekend diaries the coverage is sufficiently complete (over 99%) that no significant errors are introduced if the figure for total number of cars is used to calculate these probabilities rather than the number of cars that would be calculated by summing over all the houses with weekday or weekend diaries.

are time dependent probabilities but are not probability distributions. There is nothing in principal to stop the probabilities remaining high throughout the day, or conversely low. The integral over time is not constrained to be unity as with a probability density function (PDF).

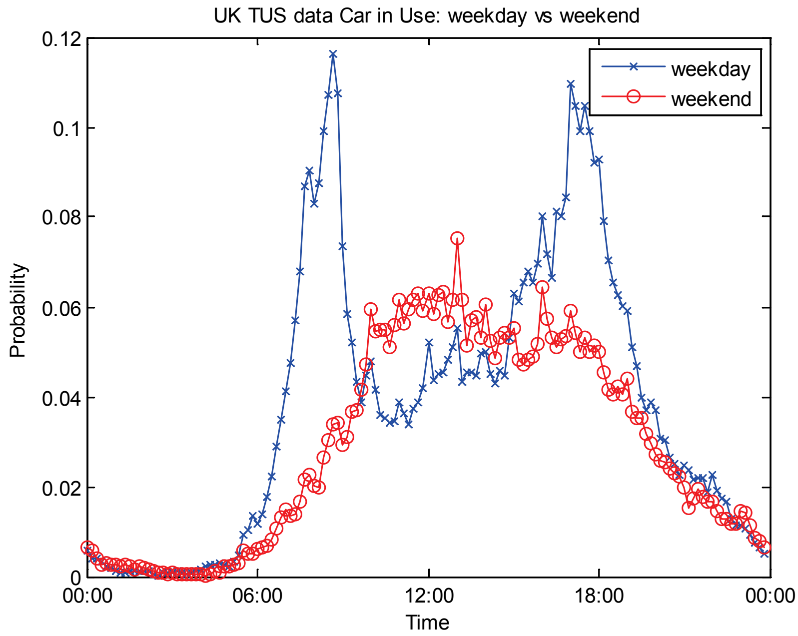

Figure 2.7 Probabilities that a car is being driven during weekdays and weekends as a function of time of day.

Figure 2.7 show the varying probability through the day that a random car is being driven, and exhibits the expected peaks occurring in the weekday morning and evening. In contrast, driving over the weekend is more widely spread over the day. Specifically the results confirm that the peak driving time for weekdays is over the period 7:30 to 9:20 in the morning and 16:45 to 18:40 in the evening as might be expected from known commuting behaviour, and that the pattern over the weekend is very different, justifying the disaggregation of the data. If a significant proportion of cars are assumed to be electric at some time in the future, it will be essential to ensure provision of adequate electricity supply capability (both generation, transmission and local distribution) to charge these electric vehicles whilst of course supplying the remainder of the demand. Without further analysis, including other system loads, it is not possible to identify when the most critical time periods will be, although already there should be concern about EVs returning to home after work at about the same time the electricity load tends to peak. Detailed results from the modelling are presented in Chapter 4.

2.3.3. Average Daily Driving Period

The average daily driving period reflects the amount of time people spent on driving over 24-hour period, and it is a crucial parameter that can be obtained from the TUS data. From analysis of both the weekday and weekend datasets, the average daily driving period can be calculated as following:

1. Calculate the average driving period for a single diary day:

$$\bar{T}_{\text{driving}}(i) = \frac{T_{\text{drive}}(i)}{T_{\text{day}}} \tag{2.3}$$

T_{drive}, is the total number of 10 minute time slots occupied by driving counted in the i^{th} diary over the day. T_{day} is the total number of time slots in a day, 144. After calculating the average driving period for each diary, the average driving period for the whole TUS activity dataset, including weekday and weekends, can be calculated as following:

2. Divide the sum of average driving period by the number of driving diaries[5] in the TUS data:

$$\bar{T}_{\text{TUS\_driving}} = \frac{1}{n_{ds}} \times \sum_{i=1}^{i=n_{ds}} \bar{T}_{\text{driving}}(i) \tag{2.4}$$

[5] Driving diaries represent the diaries containing driving activity in the dataset.

As already noted, there are 6,670 driving diaries for 5,158 cars in the TUS dataset. The corresponding figures for weekdays and weekends[6] are 5.24% and 5.04% respectively indicating, as might have been anticipated, that cars spend a higher proportion of the time driving during the week than weekend.

2.3.4. Car Parking Locations

Data about the locations where people park their cars is important for the analysis of the impact of EV charging since this determines future charging opportunities, and from the point of view of the power distribution network operators, will determine the impacts from future EV charging on their system, as well as the opportunities for utilising these parked electric vehicles as responsive demand. The home and the work place are considered as the primary and secondary locations for future vehicle charging points, and there is also expected to be a growth in other charging locations such as public car parks. In the case of the TUS data, the weekday dataset has been analysed and probability of a car parking at home at a given time of day has been calculated. Figure 2.8, gives the probability of cars parking at home as a function of time of day. This parking information is derived from the TUS weekday dataset by counting the number of cars parking at home at time for each ten-minute time interval t. Recall that the total number of cars in the TUS dataset is 5,158; however, the available number of adult diaries with driving information for weekdays is only 3,716 (this is a subset of the 7,219 adult weekday diaries where there has been some driving activity during the day). The difference between the total car population and the number of available diaries that include at least one period where the car is being driven, Δn_{ds}, is equal to 1,442 as (5,158 minus 3,716). These missing driving related diaries have been

[6] There are 3,716 driving diaries in the weekday dataset and 2,956 driving diaries in the weekend dataset.

excluded when calculating the probabilities, and this is thought to be a reasonable way to prevent overestimating the probability of car use. It assumes that all cars in a household can be treated equally. This may not fully capture the way a household utilises their cars but without more information, there is no alternative way to analyse the TUS data. On the positive side the sample number of diaries used (weekdays) at 3,716 is statistically significant. The weekday probability that a car is parked at home (or conversely is away from home, either driving or parked elsewhere) at time interval t can be calculated as follows:

1. For each ten-minute time step, count the number of diaries where an adult is staying at home (code 1), n_{home}, over all driving diaries, $n_{ds} = 3,716$, in the weekday data subset[7] with denoted by the logical variable $val(1)$:

$$n_{\text{home}}(t) = \sum_{i=1}^{i=n_{ds}} val(1), t = 1,2,3,...,t_{\text{day}} \tag{2.5}$$

2. Dividing n_{home} by n_{ds}, the probability of a car parking at home at time t, P_{home} is calculated below for weekday datasets:

$$P_{\text{home}}(t) = \frac{n_{\text{home}}(t)}{n_{ds}}, t = 1,2,3,...,t_{\text{day}} \tag{2.6}$$

3. Similarly the probability of a car being away from home, P_{away}, is calculated as below:

$$n_{\text{away}}(t) = n_{ds} - n_{\text{home}}(t), t = 1,2,3,\ldots,t_{\text{day}} \tag{2.7}$$

[7] Code '1' is interpreted as the status of "car parking at home" in the post data processing. The original TUS code '2' definition was designating that person stays at home. These two can be considered equivalent given that the car is associated with the person who identifies his or herself as the driver in their diary.

$$P_{\text{away}}(t) = \frac{\mathrm{n}_{away}(\mathrm{t})}{n_{ds}}, t = 1, 2, 3, ..., t_{\text{day}} \tag{2.8}$$

where n_{home} is the number of diaries that a car parks at home, and n_{away} is the number of diaries that a car is away from home. Again n_{ds} is the total available weekday diaries that include some driving activity, 3,716. From this point on analysis will concentrate on weekday car use and thus the subset of 7,219 weekday diaries. The probabilities cars parking at home or being away from home are denoted as P_{home} and P_{away}.respectively. Because n_{away} is defined as $n_{\text{ds}} - n_{\text{home}}$, P_{away} is simply $1 - P_{\text{home}}$ for all t, as is clear and how these probabilities vary through the day is compared in Figure 2.8. It is useful to think of these probabilities as applying to cars (or individual drivers), rather than households. Figure 2.8 shows that majority of cars are parked at home during night time and early evening when they could play an important role in demand side management scheme, such as easing the integration of renewable or offsetting other loads on the system.

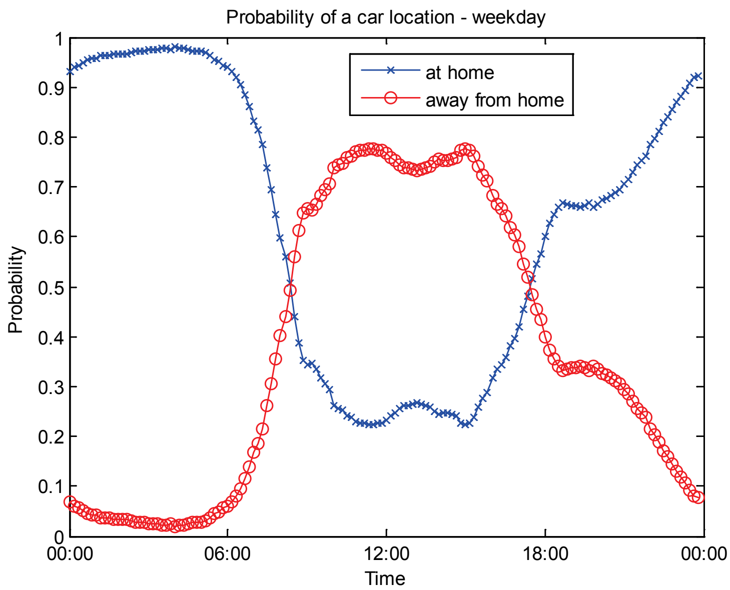

Figure 2.8 Probabilities of car locations calculated from weekday subset data.

In the TUS data, other parking locations have been coded, such as at schools, supermarkets, and hospitals and the average parking period at these locations could be calculated. These places may well become available for fast charging in the future as charging stations are installed more widely, [2.11]. This however, is beyond the scope of the present study. Nevertheless it is interesting to briefly look at the probabilities of parking at the workplace, $P_{\mathrm{park\_work}}$. These are calculated as follows:

$$P_{\mathrm{park\_work}}(t) = \frac{n_{\mathrm{park\_work}}(t)}{n_{ds}}, t = 1, 2, 3, \ldots, t_{\mathrm{day}} \tag{2.9}$$

$n_{\mathrm{park\_work}}$ is the total number of diaries where a person is at work (code 1110) that a car parks at work over all weekday diaries. It is calculated by sum value of 1 assigned to all code 1110, and zero otherwise, which is denoted by the logical variable $val(2)$ [8].

Figure 2.9 shows these probabilities superimposed on the probabilities of parking at home as previously calculated. It can be seen that, following the morning commute to work, a significant proportion of cars, but clearly not all of the cars that leave home in the morning, are subsequently parked at the workplace for much of the working day. The probability of parking at work is approximately half from 9am until 3pm but with a short dip between 11:30 am and 2pm where the car has been used for some additional activity such as driving to lunch or shopping.

[8] In the TUS data, code '1110' is defined that a person is 'working time in main job'.

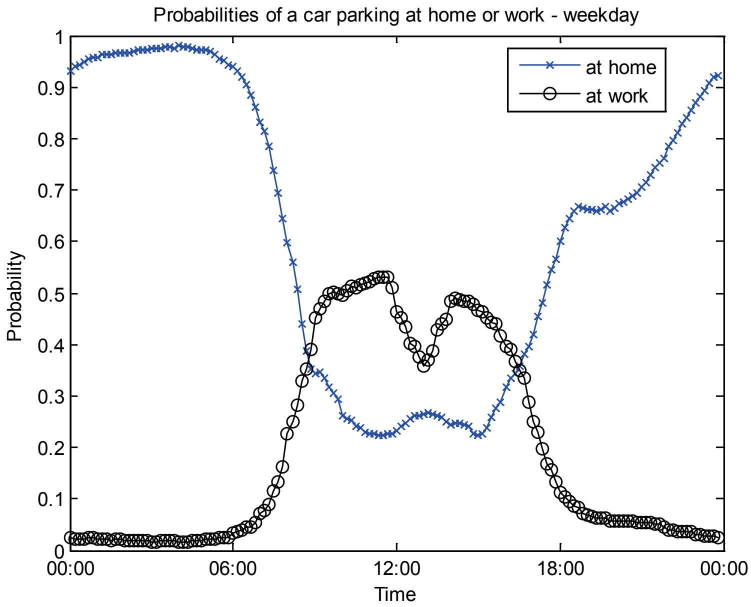

Figure 2.9 Probabilities of cars being parked at home and at work on a weekday.

2.3.5. Purpose of Journeys

Driving is generally undertaken for a specific purpose, such as getting to work, taking children to school (also known as 'school run'), etc. By extracting and analysis of the data for weekdays, the probabilities of travel to/from work and the parking location of cars at different times of the day have been calculated as function of time. The probability of driving to work at time t is calculated from:

$$P_{\text{drive\_work}}(t) = \frac{n_{\text{work}}(t)}{n_{\text{ds}}}, t = 1, 2, 3, \ldots, t_{\text{day}} \tag{2.10}$$

where n_{work} is the number of weekday diaries that have driving to work (code 913) recorded at time t.

Figure 2.10 illustrates the probabilities of cars being driven on the road through the day for the purpose of getting to/from work compared the probability of the car being in use for any purpose, as already given in Figure

2.7. Well over half of the morning rush hour domestic traffic is involved with commuting to work. To be more specific, at 7:40 in the morning on a typical weekday, the probability of cars being on the road travelling to (or from) work is around 20% less than the probability of driving for all purposes. In other words, during the morning peak, about 80% of privately owned cars on the road are being used for commuting. During the evening peak however, the reasons for driving are a little more diverse with 34% of cars being used in connection with the workplace. The key conclusion, perhaps not unexpected, is that most cars contributing to the morning rush hour are commuting to work. The evening peak in contrast reflects a greater diversity of reasons for being on the road. One point to note though is that the design of the survey, and in particular the ten-minute resolution, makes it difficult to distinguish when cars are being driven to drop off children at school en route to work. The higher time resolutions that most researchers work with will of course encounter more pronounced difficulty in this regard.

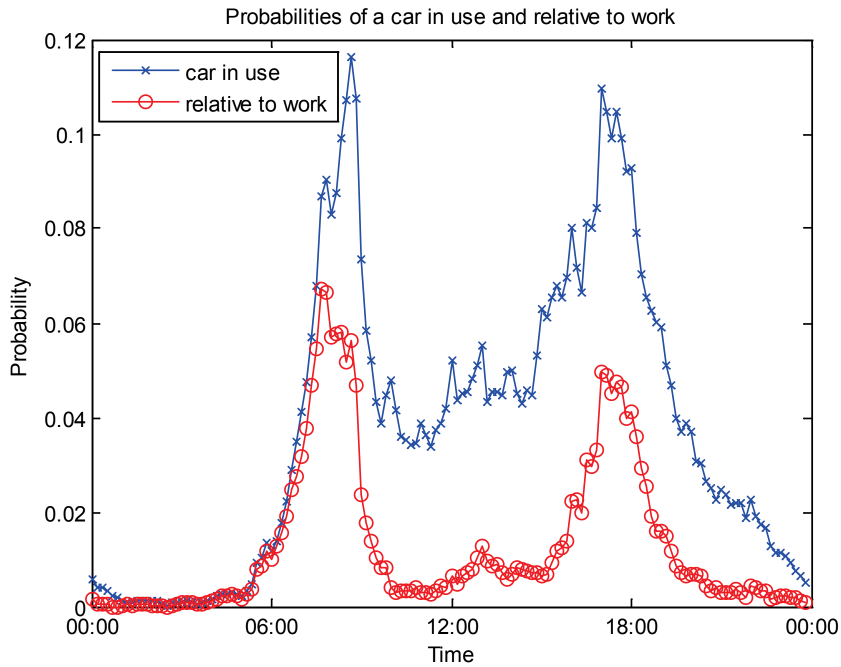

Figure 2.10 Comparison of probabilities that a car is used for commuting to/from work with car in use for weekdays.

2.3.6. Further Investigation of Weekday Driving Patterns

Since electricity use profiles have a distinct diurnal characteristic, it is important to capture the daily pattern of vehicle use, and in particular the probability of journeys commencing at particular times of the day, and their expected duration. For the interests of this research, weekday daily driving patterns related to home only have been analysed and in the most recent electric vehicle trials, users mainly drive electric vehicles during weekdays and use conventional ICE cars for longer weekend journeys, [2.14].

2.3.6.1. Car Departure and Arrival Time in Relation to Home

A random sample of 100 TUS weekday diaries showing driving activity as shown in Figure 2.11. In this example, each dot represents a ten-minute driving period and an unbroken series of dots means a continuous driving event. For each individual driving event, the start and end times together with the diary codes will also allow the locations of the cars to be determined. In the previous section, probabilities of cars parking at home or the work place at given time were calculated. Now the focus is to obtain the probability that car starts a driving event from home and then ends the driving event at home.

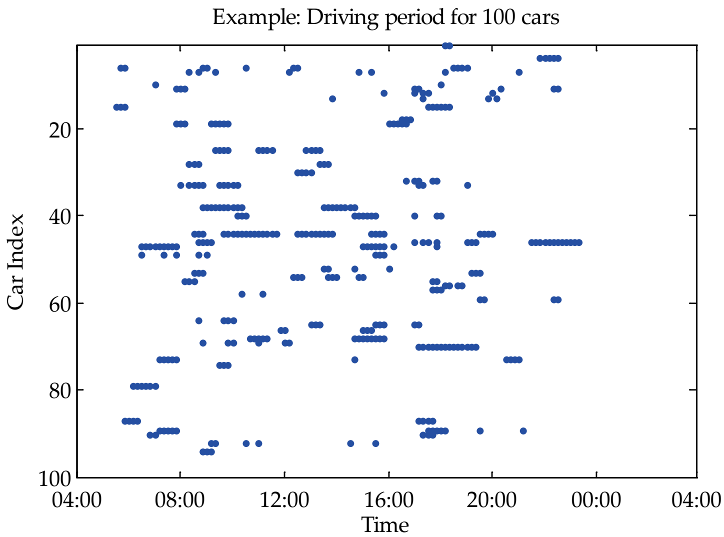

Figure 2.11 Individual weekday driving periods for a population 100 cars.

A car status transition plot is shown in the Figure 2.12 for a random sample of 100 weekday diaries. It illustrates the times when the car status changes from home to away, or vice versa; these are the times when a car departs or arrives back home respectively. The blue crosses mark car departures from home and the red stars represent arrivals home. For example, in diary number 1890, a car departs home at $t = 21$ (i.e. 07.30 am) and arrives back home the same day at $t = 45$ (11.30am). Note that there are instances where a car departs from home during the diary day but does not return home during that same diary day (i.e. up to 3.50am the next day). Conversely, there can be instances where the diary only records a return during the diary day with no corresponding departure on that diary day. This illustrates what is perhaps the main limitation of the TUS data and is a consequence of the limitation to single day diaries. All the adult weekday diaries, the focus of this study, have been analysed to count how many such instances arise. The results indicate 555 diaries (14.95%) show the car not arriving home in the same diary day, i.e. being away at 3.50am next day ($t = 144$); and 424 diaries (11.41%) show the first event during the diary day as a car arriving home; this implies that the car status is away at the beginning of the diary day (4.00am and $t = 1$). It cannot be known the exact reason for the car either not arrives home or not departs from home in the same day; it is possible that a car was away from home for several days. Therefore the relationship between when a car departs from home and arrives back home within the diary day period (4:00am to 3:50am next day) has been investigated. The numbers of cars arriving back home, given their departure time, has been recorded and illustrated in Figure 2.13. The numbers of cars arriving home for a given departure time are indicated in the figure by the colour of the points. There are two major trends evident: first, the majority of cars are clustered along the diagonal line; second, for cars departing from home around 8am in the morning, the arrival home time lies generally between 4pm in the afternoon and 8pm in the evening. Clearly cars cannot arrive home before they depart; this explains the diagonal feature. How the diary characteristics illustrated in the figure are dealt with in the Monte Carlo simulation is discussed in Chapter 3, Section 3.3.

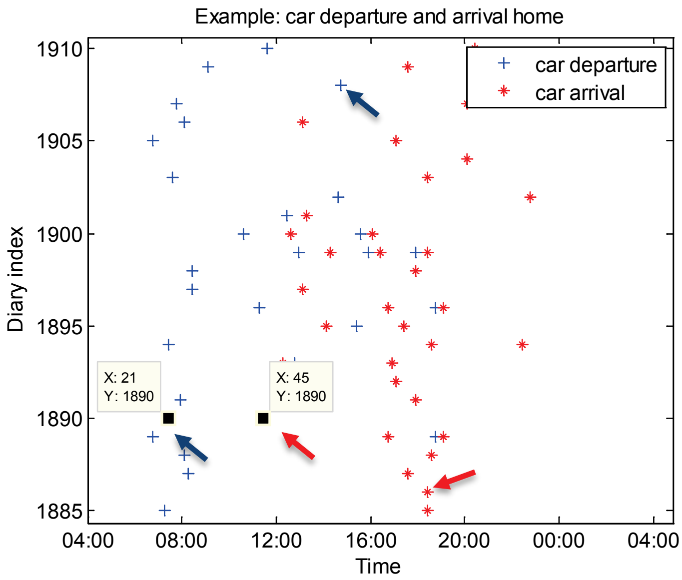

Figure 2.12 Examples of car departure times and arrival home. The blue crosses represents car departures from home, red stars represent car arrivals.

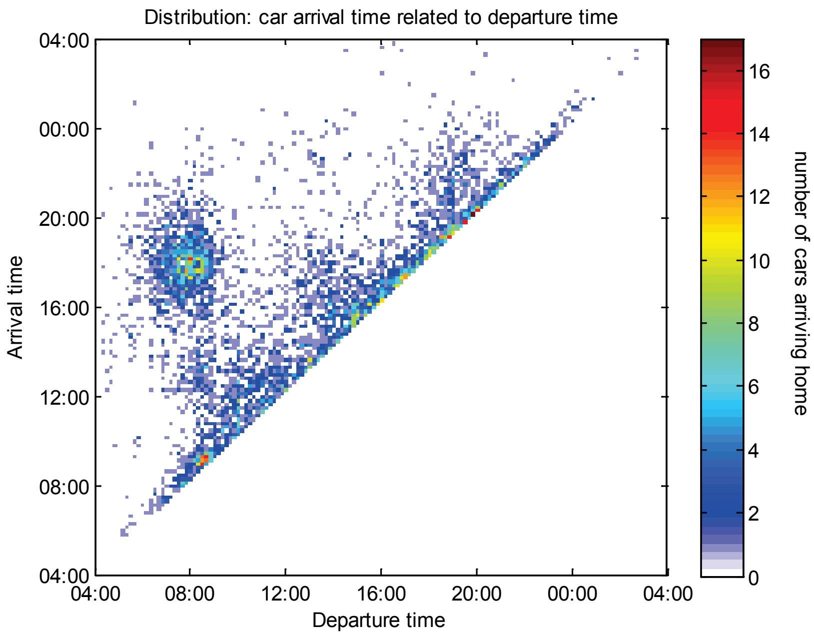

Figure 2.13 Relationship between car departure time and subsequent arrival time during the diary day for all journeys.

For a specific car to depart home at given time t, it must already be at home (i.e. it must be at home at $t-1$). If a car is parked at home at time t , it is possible that the car departs home or alternatively remains parked at home during the next 10 minute interval $(t+1)$. The same logic applies to cars arriving home. For a certain population of cars, the probability that a single car departs or arrives home is therefore conditional upon whether the car is parked at home[9]. Therefore, the probability that a specific car departs or arrives home at time t, should be calculated as the probability conditional on the car status at time $t-1$, [2.12]. For each ten minute time interval throughout the 24 hours, the probability of a given car departing from home, $P_{\text{departure}}$, is calculated for weekday data directly from:

1. For each ten-minute time step, counting the number of diaries where a car departs from home (code 915), $n_{\text{departure}}$, over all weekday data subset[10] with a value of 1 assigned to all code 915 entries, and zero otherwise, and denoted by the logical variable $val(915)$:

$$n_{\text{departure}}(t) = \sum_{i=1}^{i=n_{ds}} val(915), t = 1,2,3,\ldots,t_{\text{day}} \tag{2.11}$$

2. The probability of a car departs from home at time t as condition of parking at home at time $(t-1)$, $P_{\text{departure}}(t)$ is calculated below for weekday datasets:

$$P_{\text{departure}}(t) = \frac{n_{\text{departure}}(t)}{n_{\text{home}}(t-1)}, t = 1,2,3,\ldots,t_{\text{day}} \tag{2.12}$$

[9] The primary parking location considered in this research is home.
[10] Code '915' is defined as the status of car departs from home in the post data processing.

where $n_{\text{departure}}$ is the total number of diaries with cars depart from home at time t and n_{home} is the total number of diaries with cars parking at home at time $t-1$. n_{ds} is the total number of diaries in the weekday dataset, which is 3,716. In a similar manner, for each ten minute time throughout the diary day, the probability of a given car arriving back home at time t, P_{arrival}, conditional on the car being away from home at time $t-1$, is calculated for all weekday data, directly from:

1. For each ten-minute time step, counting the number of diaries where a car arrives back home (code 159), n_{arrival}, over all weekday data subset[11]. Value of 1 assigned to all code 159 entries, and zero otherwise, and denoted by the logical variable $val(159)$:

$$n_{\text{arrival}}(t) = \sum_{i=1}^{i=n_{ds}} val(159), t = 1,2,3,...,t_{\text{day}} \tag{2.13}$$

2. The probability of a car arrives back home at time t as condition of being away from home at time $t-1$, $P_{\text{arrival}}(t)$ is calculated below for weekday datasets:

$$P_{\text{arrival}}(t) = \frac{n_{\text{arrival}}(t)}{n_{\text{away}}(t-1)}, t = 1,2,3,...,144 \tag{2.14}$$

where n_{arrival} is the number of diaries with cars arriving home at time t calculated as the sum of the $val(159)$. n_{away} is the number of cars being away from home at time $t-1$. n_{ds} is the total number of diaries in the weekday dataset as before. Therefore, the probabilities of a car departs and arrives

[11] Code '159' is defined as the status of car arrives back home in the post data processing.

home at given time, $P_{\text{departure}}$ and P_{arrival}, is plotted against time of day in Figure 2.14.

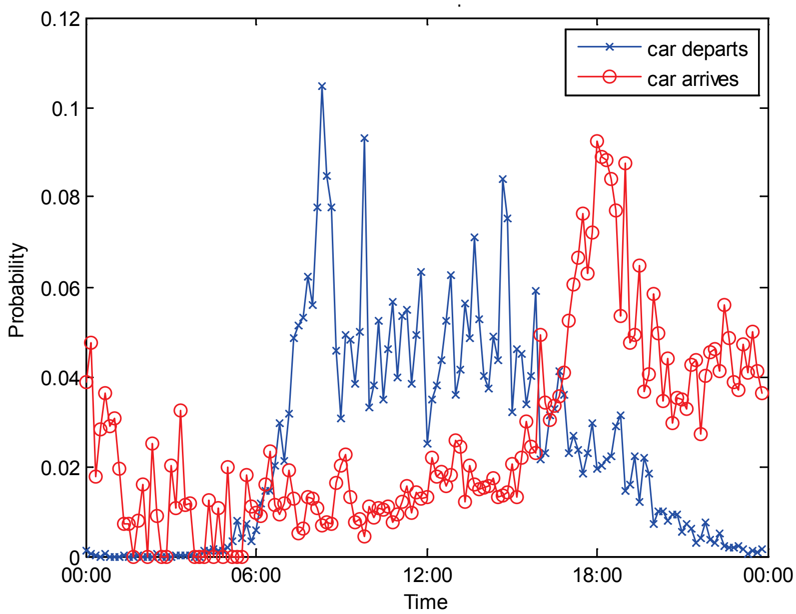

Figure 2.14 Time dependent probabilities of a car departs from home and arrives back home.

The probability that a random car departs from home peaks at about 8:20am (during the morning commuting period); whilst the probability that a car returns home peak at around 6pm. This peak in returning vehicles coincides almost exactly with weekday peak in the existing household electricity demand, [2.10]. This information is critical for the determination of the timing of EV battery charging as this is most likely to occur when immediately after the EVs arrive home.

For a car returning a specific household, the probability of a car arriving back home at a specific household, $P_{\text{arrival\_household}}$, is calculated as follows:

$$P_{\text{arrival\_household}}(t) = \frac{n_{\text{arrival}}(t)}{n_{\text{household}}}, t = 1,2,3,\ldots,144 \tag{2.15}$$

where $n_{\text{household}}$ is the total number of households in the weekday dataset, which is equal to 3,606. There is an uprising trend of car returning household from 6am in the morning, and majority of cars returning to household is 6pm in the evening as shown in Figure 2.15. The probability then decreases to near zero between 1am and 5am in the early morning, which signifying extremely low car returning to household activity.

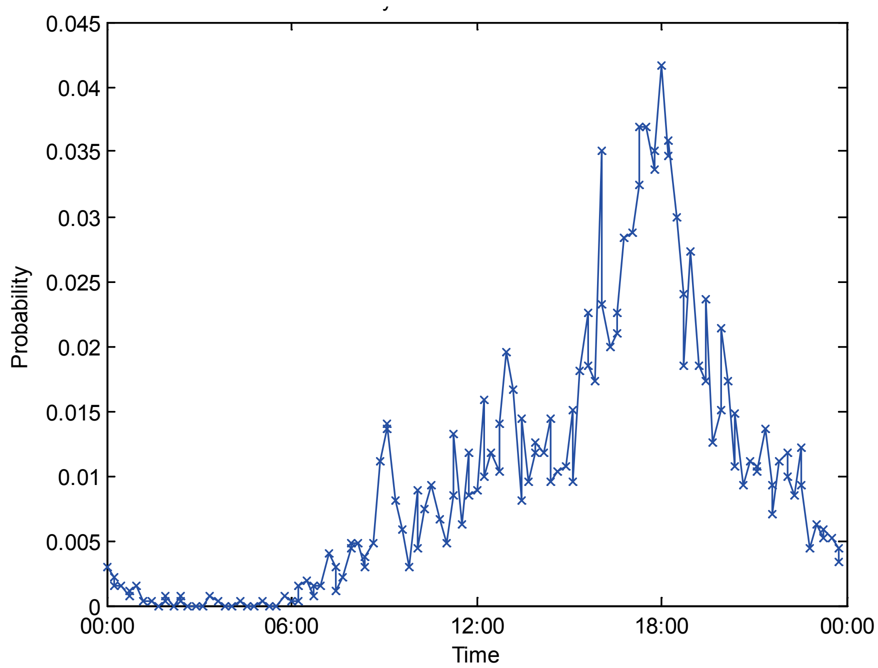

Figure 2.15 Probability of a car returning to the household.

2.3.6.2. *Car Away from Home Period*

The amount of time a car spends away from home is defined as the number of time intervals between a car departure from home and its arrival back. This away period information is associated with the time period, $t_{\text{departure}}$, when car departs home (it could equally have been defined as dependent on the car arrival time as in the previous section). Figure 2.16 shows the probability distribution that a car away from home based on a total sample of 5,422 car away from home events.

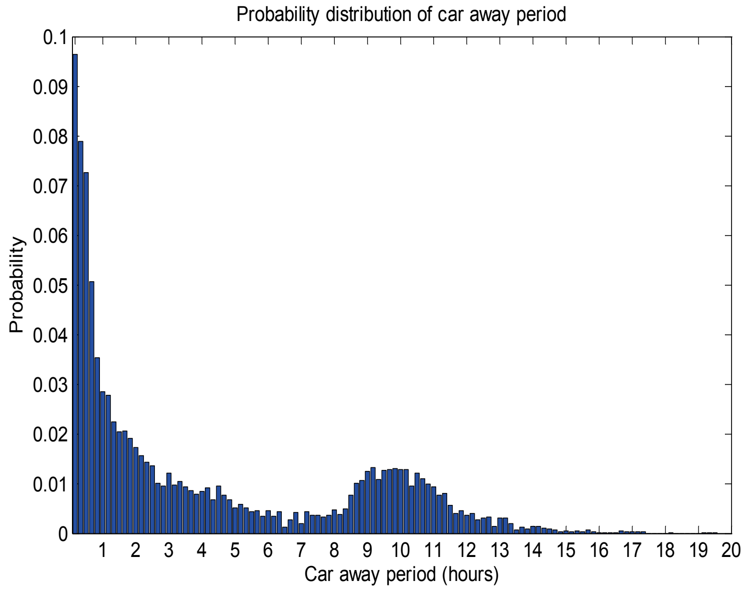

Figure 2.16 Probability distribution of car away home period calculated from TUS weekday data.

From the distribution it can be seen that, not surprisingly, the highest probability is associated with round trip journeys of ten minutes or less. The longest is round trip is over 19 hours (not actually visible on the graph as the probability is less than 1.8×10^{-4}). Between these extremes a local peak in probability can be identified at around 10 hours. A possible explanation for this, is that during weekdays, the main daily activity is commuting to work and typically cars are parked there until being driven back home. This local peak can be fitted well by a Gaussian curve, as shown in Figure 2.17, for data between $t = 43$ and $t = 74$. The mean of this fitted distribution is $t = 58$, and the standard deviation is 1 hour and 36 minutes. The car away period (round trip journey time), has been divided into eight groups. Short round trip journeys lasting from 10 minutes up to 30 minutes constitute the largest group with approximately 25% of the total journeys. The rest of round trip journey groups have been designed to have fairly equal proportions of the total, expect for the final round trip journey group (fifteen hours up to maximum recorded away period) that has only 0.6% of the total. The 'six to ten hours' away period group is the second largest with approximately 17%, and reflects the peak in the away period distribution occurs at around 10 hours as shown in Figure 2.18. It would be helpful if the purpose of the journey (such as travel to work, shopping, education, etc.) could be associated with the length of these away period; but this is beyond the scope of this research reported here.

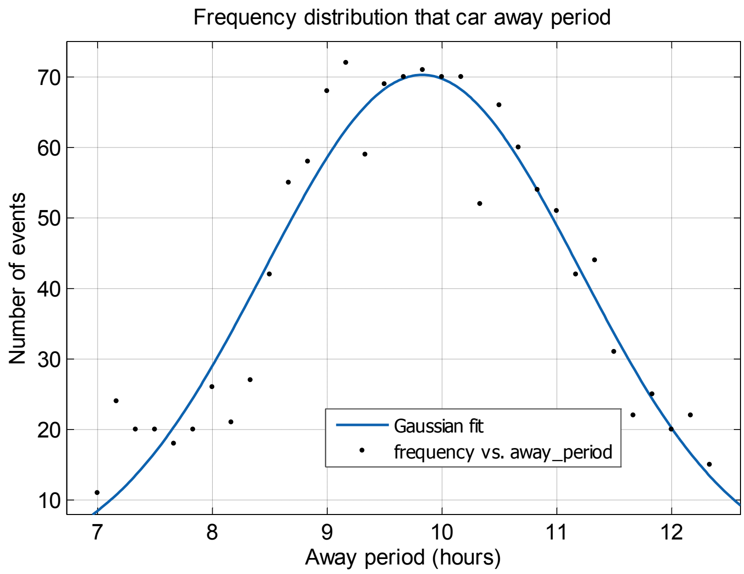

Figure 2.17 Frequency distribution for car away period for duration between 7 hours and 12 hours 20 minutes.

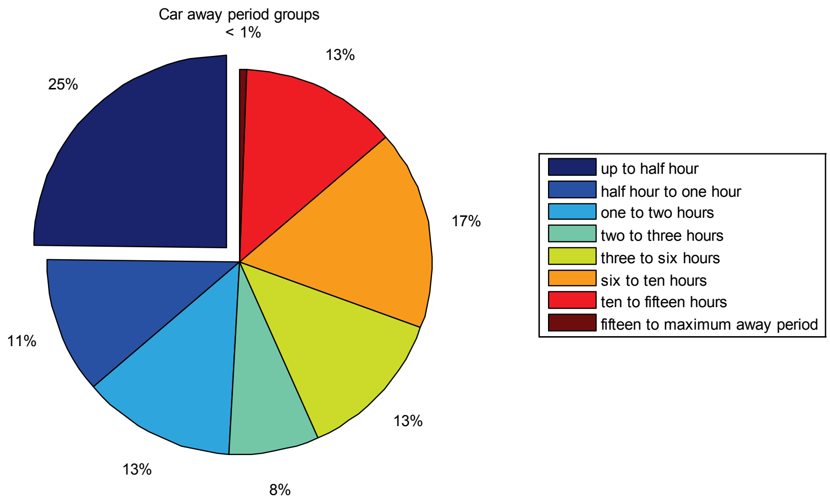

Figure 2.18. Percentage of car away period.

A joint probability distribution for round trip durations and time of day when the vehicle departs from home as shown in Figure 2.19. This joint PDF is not used directly but in future research a suitable analytic joint distribution function could be fitted to the data. In this work, it is regard the probability distribution of a car away period as a series of 144 time dependent marginal PDFs. The ten-minute time resolution data provides sufficient statistics to describe domestic car use probability distributions without the use of curve fitting. The risk of curve fitting to such probability distributions can lead to overgeneralisation of event occurrences and also can result in biased statistics. As shown in the figure, there is a concentration of data points for which cars depart from home between 6am and 9am. The corresponding round trip journey times fall mainly between four and half hours and twelve and half hours. This confirms the previous comment (Section 2.3.5) that majority of journeys are related to work. Another phenomenon apparent from Figure 2.19 is that the later in the day a car departs from home, the less likely it will be away for long period of time. In other words, shorter journeys tend to take place in the evening and night time, rather than during the morning and afternoon.

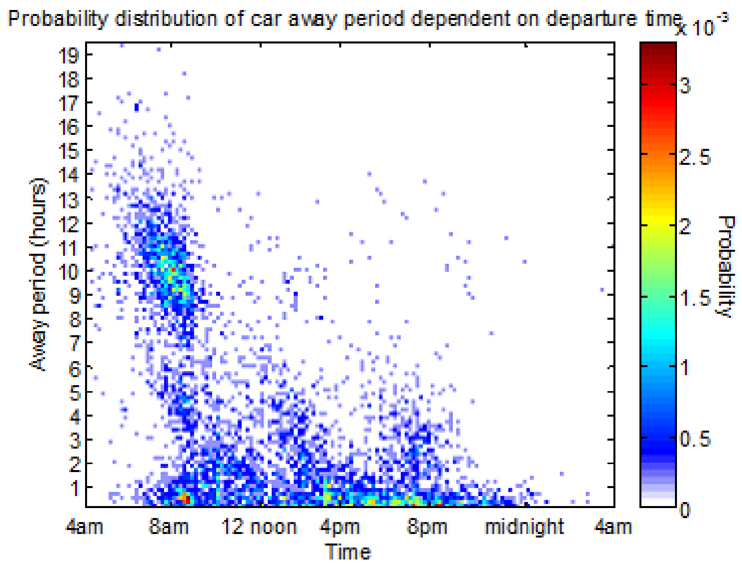

Figure 2.19 Joint probability distribution for round trip durations.

2.3.6.3. *Car Being Parked at Home Period*

The amount of time a car spends parking at home is defined as the number of time intervals between a car arrival time and its next departure. The parking duration information is associated with the time period, t_{arrival}, when the car arrives back home. However, due to the structure of TUS data, the calculation of parking period has been performed with a 'loop-back' technique[12]. This technique is explained in detail in the Appendix A. Figure 2.20 shows the probability distribution for time parking at home based on a total sample of 4,799. From the distribution it can be seen that, the highest probabilities are associated with parking periods up to 30 minutes. The longest is parking period considered is 24 hours, which signifies that a car parks at home for the entire survey day. A local peak in probability can be identified at around 14 hours. It can be understood that during weekdays, the majority of households park their overnight at home after returning from main daily activities, such as working at main job during daytime.

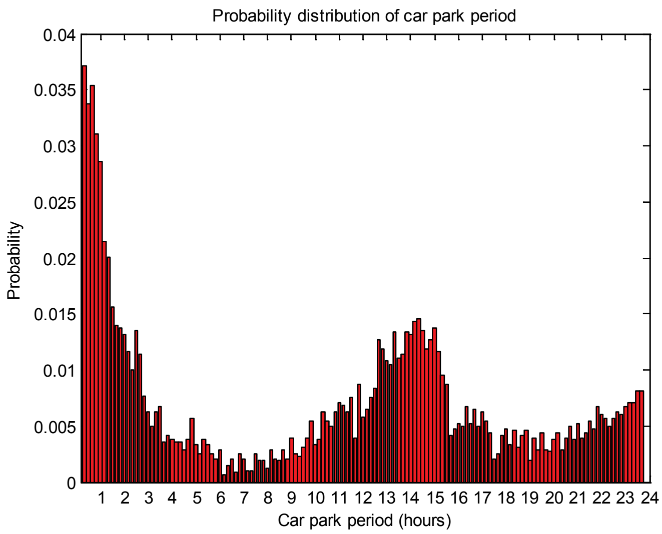

Figure 2.20 Probability distribution of car away home period calculated from TUS weekday data.

[12] The 'loop-back' technique counts the number of time slots occupied by parking activity from the arrival time to the end of diary and then from the beginning of the same diary. TUS data only covers 24 hours period from 4am to 3:50pm next day.

A joint probability distribution for round trip durations and time of day when the vehicle departs from home is shown in Figure 2.21. These series of 144 time dependent marginal PDFs has been used as inputs of fixed time increment and multiple time increments Monte Carlo models (see Chapter 3 section 3.3.2.3). As shown in the figure, there is a linear concentration of data points for cars arriving back home between 4 and 8pm. The corresponding parking duration are 16 hours and 11 hours respectively. This confirms the previous comment that the majority of households park their cars at home after returning from their main daily activities. For example, if a car arrives back home at 4pm, it will then be parked at home for 16 hours (i.e. this car departs from home at 8am next day). Another phenomenon apparent from the figure is that there are number of short parking periods (less than 2 hours) occurring between 8am and 8pm. This reveals the fact that households are likely to park their cars at homes for a couple hours during daytime, although the purpose of stay is unclear. These parking durations are important for calculating EV home charging.

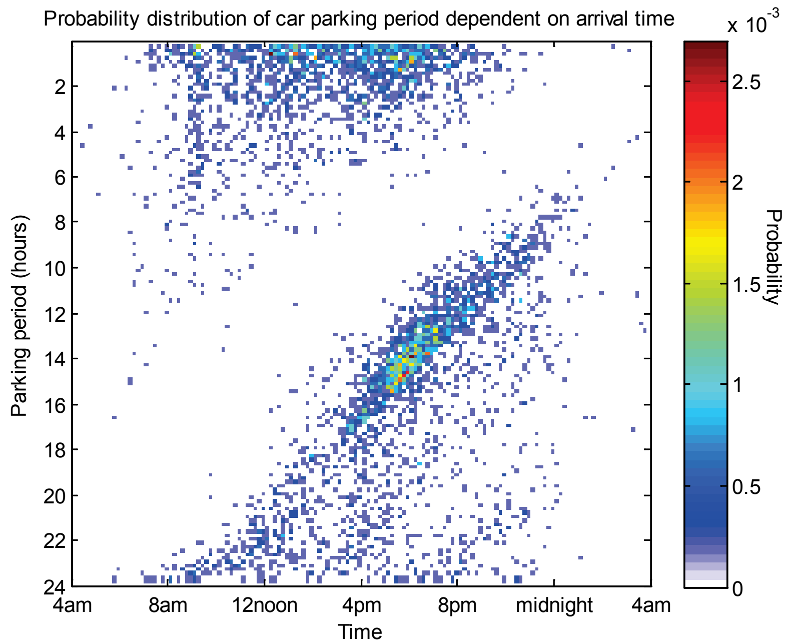

Figure 2.21 Joint probability distribution for home parking durations.

2.3.6.4. *Car Drive Period*

The amount of time people spend on actual driving is important for calculating the amount of energy used by the EV, the state of charge (SOC), and the re-charging period required. Across the entire fleet of EVs it will determine the amount of electricity required to replace the equivalent number of conventional ICE cars. Up-to-date electric vehicle specifications indicate that it is not possible to completely replace ICE cars with electric vehicles due to range limitations. By counting the number of individual driving periods in the weekday diaries, a probability distribution of the length of individual journeys can be deduced. This is shown in Figure 2.22 and confirms that a large proportion of driving activities are very short (ten minutes or less), and that occasionally very long journeys are made. Note that driving period is only accurate to the nearest ten-minutes due to the time resolution of TUS diaries recorded. If a car has actually been driven for a time less than 5 minutes, it will be recorded as a ten-minute journey. This is considered the simple way to interpret the TUS data, but it will provide some minor bias to the journey time statistics, particularly for short journeys.

Most individual weekday driving events are short journeys; for example, driving events of ten-minutes (or less) account for approximately 38% of all journeys, and 23% for twenty-minute driving events (more details see Appendix A). The occasional long aggregated round trip distance driving period events can be found. For example a journey with a total 420 minutes (7 hours) driving duration has been calculated by aggregation; however these long journeys are rare (less than 1% of such journeys last more than 400 minutes). It can be seen that journeys up to 30 minutes in length account for over 78% of all journeys. For weekday TUS dataset, there are 3,716 diaries containing driving information and the average driving period is 0.052% over

24-hour period, i.e. the average domestic car is only driving on the road for approximately one hour a day.

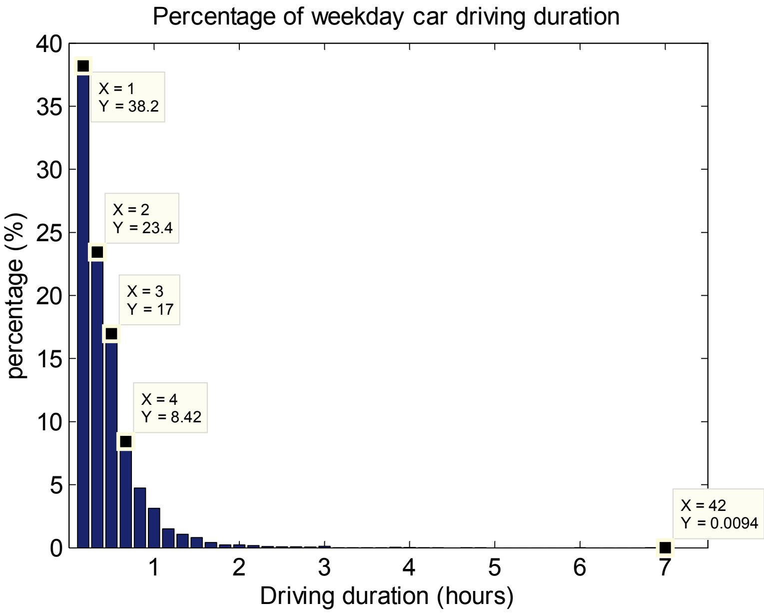

Figure 2.22 Percentage of weekday journey durations.

2.3.6.5. *Driving Period Dependent on Car Arrival Home Time*

As discussed in the previous section, home is regarded as the primary location for EV charging. Attention is now turned to the aggregate or cumulative time driving during any period away from home. For a given value of time t, this is found simply by summing up all the individual journey durations within the time period between a departure from home and the next arrival back home at time t, and then calculating the probabilities for each of the durations so as to give the probability distribution of aggregate driving duration for journeys arriving back home at time t. This process is repeated for all time steps (i.e. $t = 1$ to 144). The resulting 144 PDFs for every ten-minute time step describe the time dependence of the process and can be viewed probabilities conditional on arrival time: $P\left(T_{\text{drive\_arrival}} \mid t_{\text{arrival}}\right)$. Numerically the calculations are undertaken by the following three steps:

1. For each car arriving home at time, t_{arrival}, sum individual driving period, $t_{\text{driving\_period}}$, between its departure and arrival time:

$$T_{\text{driving}}\left(t_{\text{arrival}}\right)=\sum_{t_{\text{departure}}}^{t_{\text{arrival}}} t_{\text{driving\_period}} \tag{2.15}$$

2. To calculating the conditional probability of the cumulative driving period, T_{driving}, for each car dependent on its arrival time t, the number of occurrences for each cumulative driving period, $n\left(T_{\text{driving}}\right)$ is divided by the number of cars arriving home at time t_{arrival}, denoted n_{arrival}:

$$P(T_{\text{driving}} \mid t_{\text{arrival}})=\frac{n\left\{T_{\text{driving}}(t_{\text{arrival}})\right\}}{n_{\text{arrival}}(t_{\text{arrival}})} \tag{2.16}$$

Figure 2.23a, a isometric view of the conditional probability of driving period given the time of arrival at home, shows that at the beginning of the diary day (4am) and its end (3:50am next day), the probability is equal to 1. This is the result of the very small sample sizes at such times of day since very few cars arriving home then. For example, for a car arriving home at 4:10am, there is only one diary record, so that the calculated probability is unity for the one round trip journey involved, in this particular case it was equal to twenty minutes. Similar arguments apply to other small samples sizes, giving probabilities of 0.5, 1/3, 0.25, etc.

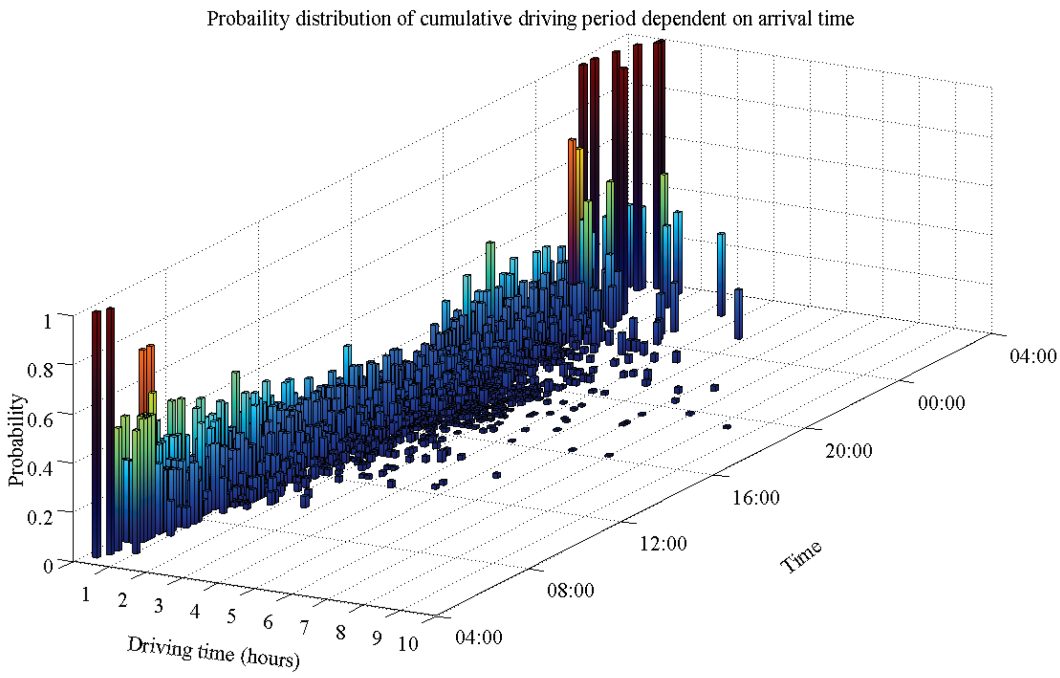

(a)

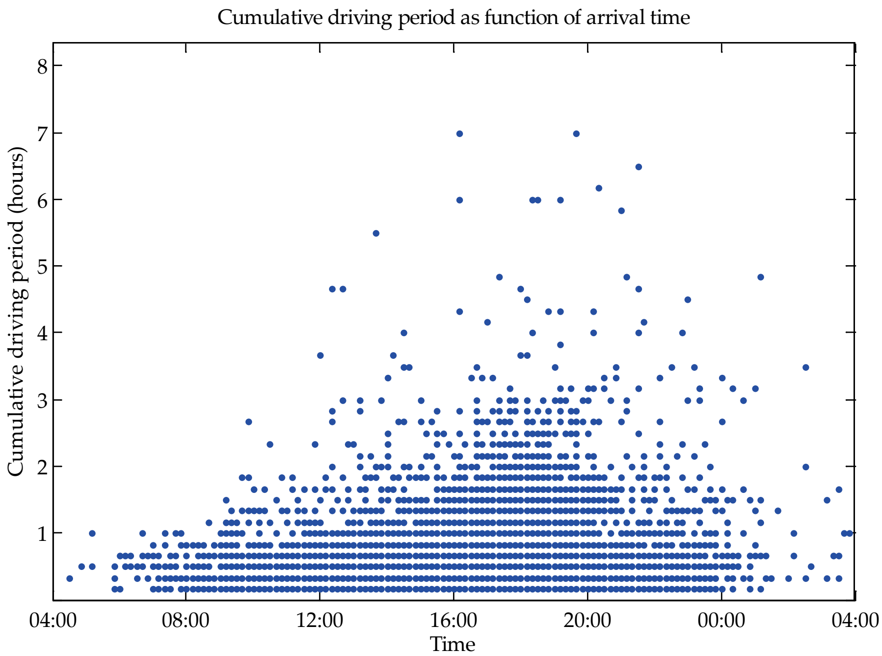

(b)

Figure 2.23 Distributions that cumulative car driving period dependent on the arrival home time. (a) conditional PDF; (b) scatter plot.

Figure 2.24, some example probability distributions are presented for the cumulative driving periods for cars arriving home at different times of day. For each time t, a single probability distribution of journey length, $P(T_{\text{driving}} \mid t_{\text{arrival}})$, can be used to calculate the mean distance travelled by each car when it arrives back home. T_{driving} represents the total round trip driving duration, is a discrete random variable and equals the number of ten minute periods. It is important to note that these probabilities are for total round trip driving duration, not time away from home. In fact the duration of the round trip is not needed explicitly for calculation purposes, but it is implicit in the probabilities calculated. However, for the purposes of this research, the PDFs are required for Monte Carlo simulation. A clear trend is apparent in that as the day progresses, typical journey times are longer. This is not really surprising as more time is available for car driving activity. Figure 2.25c, shows that for journeys ending at 6.00pm, journey times can be up to 270 minutes, approximately 4.5 hours, but such long journeys are rare. Figure 2.25d shows signs of rather small data sets, which indicates less cars arriving back home at that particular time.

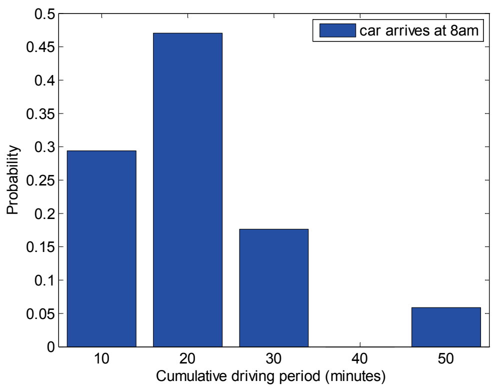

(a)

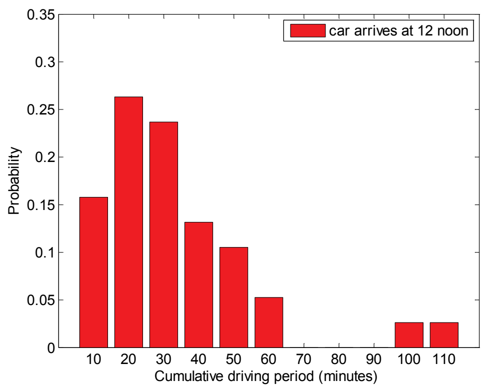

(b)

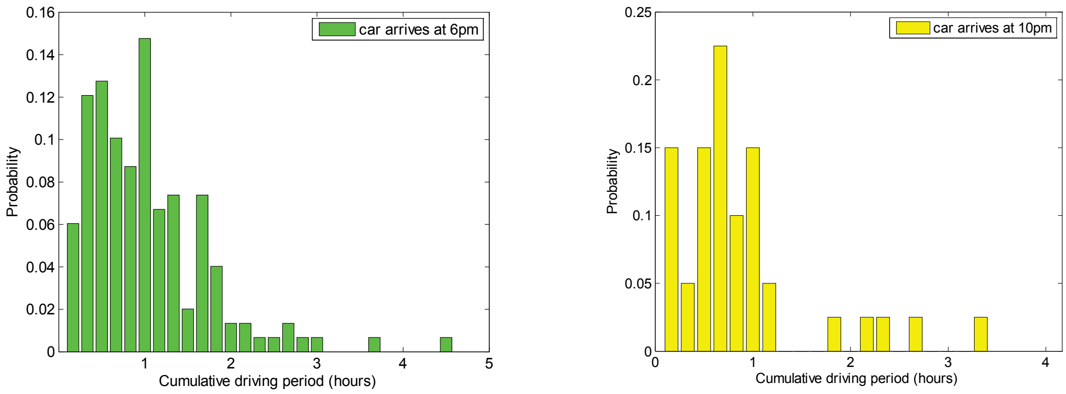

(c) (d)

Figure 2.24 Probability distributions of round trip aggregate driving period dependent on when the cars arrive home for: (a) morning period; (b) noon period, (c) evening period, (d) night-time period.

2.3.6.6. *Driving Period Dependent on Car Away from home Period*

The total time driving depends on the period that the car is away from home, and clearly is less than or equal to the away period. In the previous section, the cumulative driving period has been calculated when car arrives home. This can be related, point by point, to the total time driving. Since there is a one to one relationship between the car arrival times and the car departure times, the car away period can be calculated when car departs from home. Figure 2.25 and Figure 2.26 show this relationship and reflects the obvious constraint that driving time is less than or equal to away time. Ideally the relationship between time away from home and total time driving would be identified for each value of t throughout the day. Although TUS data is in ten-minute resolution, it is impossible to establish relationship cumulative driving period and car away period for every possible condition unless there is sufficient data available. For example, at 8am, the probability distribution for the duration that the car is away from home, as shown in Figure 2.25, has data only for 53 entries out of the 117 away periods (total of 146 samples), with the bulk of the diary entries clustered around 580 minutes, i.e. 9 hours and 33 minutes.

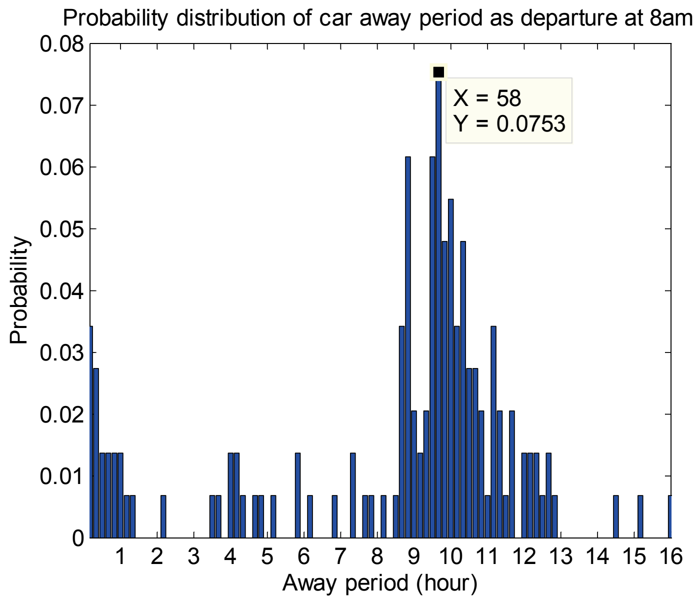

Figure 2.25 Probability distribution of car away period for departures at 8am in the morning.

The given aggregated driving period data associated with these away periods is not sufficient to produce accurate probability estimates to cover every given possible away period. For example, the car away period of 580 minutes is taken as a sample from the probability distribution of car away period dependent on departure at 8am. There are a maximum of 58 possible values for driving period associated with this away period[13]. This means that when calculating the probability for each driving period dependent on the away period, there will be 58 potential driving period values that can occur. In fact, as shown in Figure 2.26, only 33% (19 out of 58) of all possible values exist in the data set due to the limited total number of diaries in the TUS data. It is clear that there are insufficient data samples for reliably calculating the

[13] Driving period is less than or equal to away period.

required probabilities. It is possible to resolve this issue by fitting a parametric distribution to the histogram of cumulative driving dependent on car away period. However, the concern of sampling from the fitted distribution is the overfitting of the cumulative driving period dependent on car away period. It is beyond the scope of this research to investigate the effects of using parametric distribution to represent the cumulative driving period.

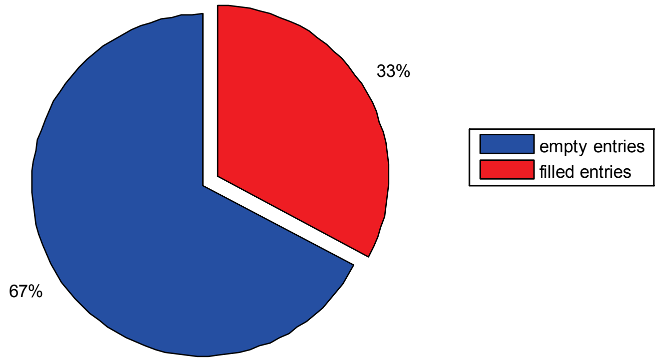

Figure 2.26 Available driving period entries for cars departing at 8am.

To resolve this issue, clustering technique has been used to group the away period data into blocks, [2.13], as discussed above. Eight groups are used as shown in Table 2.2. The first group is defined to cover away periods from ten-minutes up to 30 minutes, and the last group covers the wide time range from 15 hours up to 19.5 hours. The intention is to ensure that all cluster groups have sufficient data to facilitate acceptable probabilistic calculations in the Monte Carlo simulations.

Table 2.2 Groups of car away period

Groups	Away period (ten-minute)
I	1~3
II	4~6
III	7~12
IV	13~18
V	19~36
VI	37~60

VII	61~90
VIII	91~117

These grouped blocks of away period data can now be combined with the associated driving period data to estimate the conditional probabilities of cumulative driving period dependent on a specific away period range at a given time of day. For example, in the TUS data, a particular car is away for ten minutes and being driven for ten minutes; this ten-minute driving period is added to the ten-minute of less driving group conditional upon car away period being in cluster Group I. After clustering, the number of driving period entries in cluster Group I, for cars departing at 8am, is shown in Table 2.3. Note that the resulting conditional probability is function of time with ten-minute resolution. These cluster based probabilities are used as input to some of the Monte Carlo simulation models explored in Chapter 3.

Table 2.3 Number of driving period entries in cluster Group I for cars departing at 8am.

Away period (minutes)	Driving period entries
10	4
20	0 1
30	0 1 3
Group I (10~30)	4 2 3

2.4. Summary of Chapter 2

This chapter discusses the car use data sources available in the United Kingdom, the United States and European countries. The reasons for choosing United Kingdom Time of Use 2000 survey data as the main data source for this research was explained, in particular its much higher time resolution than other UK sources such as the National Travel Survey. In fact the time resolution, at ten minutes, is better than data sets available to most researchers around the world, where hourly data is the most commonly used.

Household car use statistics has been calculated from the TUS survey data, especially weekday car use has been presented in detail. Preliminary analysis shows that privately owned cars are utilised only 5.2% of the time for transportation, thus making them, in principal, available for the remaining 94.8% of time providing ancillary services to the power system. The methodology used to extract relevant data has been presented. Key findings showing high time resolution car use patterns have been presented, including probabilities of car use and parking status for both weekday and weekends. The focus though is on car use during the working week as this is where most power network problems are anticipated. Probabilistic characterisation of car usage during weekdays has been undertaken that covers time of use, and duration of use dependent on the time that a car arrives home, and also as dependent on the round trip duration, and both of these as a function of the time of day. These probabilities will be used as the basis for Monte Carlo simulations of car use in Chapter 3.

Various challenges have been encountered in the search for good quality data on the use of privately owned cars. The first challenge is to identify a reliable source of car use data, since there are various options available for different countries and for UK in particular. Both TUS and NTS data provide good quality car use information; however, the focus of these two data sets are very different. For TUS data, the focus is on the activities of the people living in various households; and therefore, it is highly relevant to the integration of EV charging loads with other domestic appliances electricity loads. On the other hand, NTS data provides more information regarding geographic and speed related information, and the primary limitation is the lower time resolution. The second challenge is to do with the process of extraction and post-processing of the car use information required for Monte Carlo modelling, and this regard the TUS data, although highly detailed, is incomplete and sometimes difficult to interpret. With the TUS data, numerical codes are used to distinguish the activities of the house occupants, and a sub-set of these codes relate specifically to car use. During the extraction of car related data, various conditions need to be considered. For example, a person drives the car as its main driver and the purpose of the driving activity is take a child or children to school (technically in TUS: a place of education). Two sets of codes in the TUS diaries represent the activity itself, and the separately the purpose of activity. A significant challenge faced in this research was the calculation of probabilities of car use from TUS data. Due to the survey diary format, the starting point of all diaries is at 4am in the morning and the end point is 3:50am next day. This was chosen by TUS because the household activity reaches a minimum at around this time in most cases. This together with the fact the diaries are kept two distinct, non-contiguous, days during each week the survey period means that it is not possible to properly capture certain probabilities of car use, such as a car departing home and then staying away from home until beyond 3.50 the next day. There is no way of knowing exactly when that particular car actually returns home and thus the round trip journey duration, and aggregate associated driving time cannot be determined in these instances. Fortunately there are only limited numbers of such occurrences evident in the diaries. Nevertheless there is no proper way to deal with these and the resulting statistics and probabilities will be to a small extent in error.

Another issue that follows from the high time resolution is the lack of sufficient data at each time of day, to confidently estimate all the required probabilities and probability distributions. Again, it is possible to resolve this issue by fitting a parametric distribution to the histogram of car use statistics. However, the concern of sampling from the parametric distribution is the overfitting of the car use statistics, which produce non-realistic car use patterns. It also is beyond the scope of this research to investigate the effects of using parametric distribution to represent the cumulative driving period. A clustering approach was used to try and overcome this difficulty, and the clustered group has sufficient amount of data points. However, with limited success and some loss of time resolution for certain probability distributions required for some of the Monte Carlo modelling, the main drawback of clustering was a less accurate representation of the characteristics of the original data.

2.5. References

[2.1]. Ipsos-RSL and office for National Statistics, United Kingdom Time Use Survey, 2000 [computer file]. 3rd Edition. Colchester, Essex: UK Data Archive [distributor], September 2003. SN: 4504.

[2.2]. National Statistics, Department for Transport. 'Transport statistics bulletin-national travel survey: 2008,' 9th April 2009.

[2.3]. Department for Transport, 'Focus on personal travel: 2005 Edition', National Statistics, UK Data Archive Study Number 5340, April 2005.

[2.4]. S. Shengnan, M. Pipattanasomporn, and S. Rahman, "Grid Integration of Electric Vehicles and Demand Response With

Customer Choice," *Smart Grid, IEEE Transactions on*, vol. 3, pp. 543-550, 2012.

[2.5]. J. Taylor, A. Maitra, M. Alexander, D. Brooks, and M. Duvall, "Evaluation of the impact of plug-in electric vehicle loading on distribution system operations," in *Power & Energy Society General Meeting, 2009. PES '09. IEEE*, 2009, pp. 1-6.

[2.6]. National Household Travel Survey Oakridge National Laboratory, 2001 [Online]. Available: http://nhts.ornl.gov/index.shtml

[2.7]. Lojowska, A.; Kurowicka, D.; Papaefthymiou, G.; Van der Sluis, L., "Stochastic Modeling of Power Demand Due to EVs Using Copula," *Power Systems, IEEE Transactions on* , vol.27, no.4, pp.1960,1968, Nov. 2012

[2.8]. Verzijlbergh, R.A.; Grond, M.O.W.; Lukszo, Z.; Slootweg, J.G.; Ilic, M.D., "Network Impacts and Cost Savings of Controlled EV Charging," *Smart Grid, IEEE Transactions on* , vol.3, no.3, pp.1203,1212, Sept. 2012

[2.9]. Ministry of Transport, Public Works and Water Management, "Mobiliteitsonderzoek Nederland (in Dutch)," April 2009, last visited October 2010. [Online]. Available: www.mobiliteitsonderzoeknederland.nl

[2.10]. I. Richardson, M. Thomson, D. Infield, and C. Clifford, "Domestic electricity use: A high-resolution energy demand model," *Energy and Buildings*, vol. 42, pp. 1878-1887, 10// 2010.

[2.11]. E. E. R. E. U.S. Department of Energy, *Charging Plug-In Electric Vehicles in Public*. Accessed date: 11 November 2013, Available: http://www.afdc.energy.gov/fuels/electricity_charging_public.html

[2.12]. A. Papoulis and S. U. Pillai, *Probability, Random Variables, and Stochastic Processes*: Tata McGraw-Hill, 2002.

[2.13]. W. L. Martinez, A. R. Angel, and J. L. Solka, "Finding Clusters," in *Exploratory Data Analysis with MATLAB, Second Edition*, Second Edition: CRC Press, 2010, pp. 155-203.

[2.14]. S. Huang, R. Carter, A. Cruden, and D. Infield, "Ford Connect Battery Electric Vehicle Academic Study Report," University of Strathclyde30 January 2013.

3.Chapter 3: Monte Carlo Simulation of Daily Car Driving Patterns

In Chapter 2, probability distributions of weekday car daily use have been estimated from the Time of Use Survey data. Now the task is to reproduce weekday car driving patterns based on these probability distributions so that electric vehicle charging load can be calculated. In order to achieve this, Monte Carlo method has been chosen and three models have been structured to generate random samples from these probability distributions so that synthesised daily car use can be simulated. The Monte Carlo methodology is a well-known technique for solving uncertainty problems, and the origin of the concept was developed by French scientist Georges-Louis Leclerc Comte de Buffon in 1733. In this chapter, three Monte Carlo simulation models are presented and the simulation results have been analysed to verify the results are as expected and are consistent with the statistics extracted from the TUS data.

3.1. The Concept of Monte Carlo Simulation

The basic concept of the Monte Carlo (MC) method dates back to the 18th century when the French scientist Georges-Louis Leclerc Comte de Buffon presented the famous needle throw test method to calculate π in 1733, [3.1] and [3.2]. The method is as follows. A needle of length d is thrown randomly onto a plane on which some parallel lines separated by distance, a, have been drawn, where $d < a$. It can be shown that the probability of the needle hitting a line is $p = 2d/\pi a$. Since the probability can be estimated as the ratio of the number of throws hitting a line to the total number of throws, the value of π can be obtained by $\pi = 2d/pa$. This is the earliest example of a MC method. The method can be used to solve both stochastic and deterministic problems. Monte Carlo is the general term for a stochastic simulation that makes use of random numbers (or events as in Buffon's case) and takes its name from the suburb in Monaco made famous by gambling. The name was also used as the secret code for atomic bomb work performed during World War II involving random simulation of the neutron diffusion process. MC methods have been used in many areas since that time.

In modelling city scale traffic, agent-based approach has been used, such as in [3.3]. This approach also appear ideal to study interdependencies between different human activities, [3.4]. However, Monte Carlo method has been recognised as the simplest approach to simulate household car by utilising the car use statistics calculated from the TUS data. For the interests of this research, MC simulation models for privately owned car use have been structured based on the statistics described in the previous chapter.

3.2. Monte Carlo Simulation Methodology

Monte Carlo simulation involves several stages. Random number generation is the first part of the process, in which random numbers appropriate to the problem being studied are generated. Creating samples of defined random variables (RVs), X, is the next stage. This procedure produces a sample of RV X each time it is called, and a large MC computation may spend most of its time doing this. There are several different sampling methods for the generation of random samples from a probability distribution (also known as random variates)[14] for MC simulation, such as the Inverse-Transform method, Acceptance and Rejection techniques, the Composition approach, etc., [3.5]. The inverse-transform sampling method has been used in this work for generating synthetic domestic car daily use patterns, and is explained below.

3.2.1. Inverse-Transform Method for Discrete Distribution

The basic idea of this transformation method is to generate random samples from the given target distribution[15] using the cumulative distribution function (CDF), by using random numbers created over the interval, $U \in [0,1]$, with uniform probability distribution. This approach to generating random samples for MC simulation is known as the Inverse-Transform Method (see [3.5], [3.6], and [3.7]). Let X be a discrete random variable (e.g. duration of car driving period within a round trip), with probability of X as $P(X = x_i) = p_i$, cumulative driving period $i = 1,2,3,4,5$ with $\sum_i p_i = 1$ and $x_1 < x_2 < x_3 < x_4 < x_5$. The CDF[16] F of RV X is given by $F(x) = \sum_{i:x_i \le x} p_i$, with $0 \le F(x) \le 1$ for all driving period x. For any uniformly distributed random

[14] A random variate is a particular outcome for a random variable (i.e. a particular sample from the pdf).
[15] The target distribution needs to be invertible.
[16] The CDF is an increasing function, however it is not necessarily continuous.

number generated from the interval $U \in [0,1]$, there is a range of x with $U \leq F(x)$. Thus the *generalised inverse* can be defined as $F^{-}(U)$, is equal to the smallest element of x where $F(x) \geq U$. An example cumulative distribution function is shown in Figure 3.1.

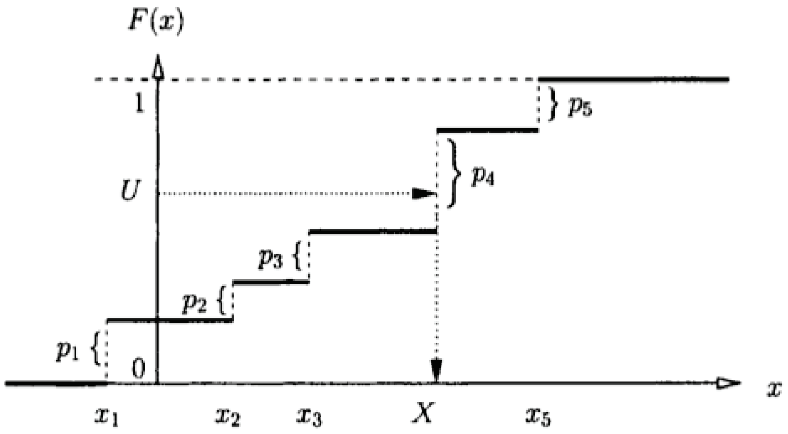

Figure 3.1 Illustration of the generating of random samples from a given CDF, [3.6].

The inverse-transform algorithm can be implemented as follows:

1. Generate random number $U \sim \mathrm{U}(0,1)$.

2. Find the smallest positive integer, k, such that $U \leq F(x_k)$ and return the sample from RV X as x_k.

Note that in general, the most time consuming process is Step 2, which makes comparisons between the random number and the given by the CDF of X. For some random variables that will be used in the MC modelling described in section 3.3 below, there are only two possible states and in this case the inverse-transform method is computationally fast. It simply comprises of a check whether the random number U is less than or greater of equal than the probability of state 1. In Chapter 2, the probability that a car departs from home at a given time, $P_{\text{departure}}(t)$, and probability that a car arriving back home, $P_{\text{arrival}}(t)$, are both time dependent probabilities and the notation used here makes this time dependence explicit. However, since all of the RVs and distributions used in the MC simulations of EVs in this work [17] are time dependent, there will be no further need to show this explicitly. The inverse-transform method is an effective tool for generating random variables sampled from a specified distribution. Their implementation requires a reliable random number generator; these are readily available in most programme environments, such as the MATLAB function 'rand' that generates uniformly distributed random numbers between 0 and 1.

Besides inverse-transform method, Markov Chain method has also been considered by utilising car transient status probabilities, such as in [3.8]. The inverse-transform method takes the advantage of the high resolution of TUS data by direct sampling from the car use probability distributions.

3.2.2. Random Number Generator

Various methods exist to generate random numbers, [3.9]. In this work, random numbers are generated using the 'RandStream' random number generation function implemented in the mathematical software, MATLAB, [3.10]. This function creates a random number stream that uses the uniform pseudo-random number generator algorithm specified by the function call. In this work the algorithm used is 'mrg32k3a', [3.11] and [3.12]; it generates a series of random numbers between 0 and 1.

[17] This is in contrast with much of the published work on EV modelling to date.

3.2.3. Convergence Criteria

Recent MC studies in the context of electrical engineering have used a fixed MC sample size; a very large number of iterations is specified to ensure convergence (usually 10 to some integer power), see for example [3.13] and [3.14]. In these fixed-sample-size procedures, a single simulation run of N_{trials} is performed, and then the computed variance obtained from the MC sample N_{trials} is used as the unbiased point estimate of the process variance, [3.15]. An experimenter using this procedure has to be content with a default value of confidence level (CL), which can be specified as a whole or half width confidence level, [3.16]. After specifying an acceptable CL half width, the experimenter usually prefers to perform the MC experiment using excessively long run lengths to avoid the possibility that the default confidence level falls below a reasonable level. By using these exceptionally long runs, such authors do not feel the need to use a more rigorous assessment of convergence. In terms of computing time, the saving, due to not estimating the process variance, may be overtaken by the extra computing time required to generate redundant MC sample points. A more sophisticated method to assess convergence is the *acceptable shifting convergence band rule* (ASCBR), [3.16]. This method defines that the simulation has converged when the sample mean of the output variable of interest falls inside the convergence band (CB) of a given width and length; otherwise, the convergence band shifts to a new sample mean outside the existing CB with a new width and length. The width of the convergence band, 2ε, is calculated from the confidence interval wanted by the modeller (e.g. 90% or 95% confidence level) and the standard deviation of the iterations results. The length of the convergence band, ζ, is self-defined value and depends on the judgement of the standard deviation of the sample mean. Let ε be the calculated half value where $\overline{x}_i$ is the MC mean, then the CB can be constructed with the upper and lower bound as follow:

$$Up(\overline{x}_i) = \overline{x}_i + \varepsilon \tag{3.1}$$

$$Lo(\overline{x}_i) = \overline{x}_i - \varepsilon \tag{3.2}$$

$$\varepsilon = Z_{\alpha/2} \frac{\sigma^i_{\text{driving}}}{\sqrt{n}} \tag{3.3}$$

$Up(\overline{x}_i)$ and $Lo(\overline{x}_i)$ are the upper and lower confidence bound, and $Z_{\alpha/2}$ is calculated from the confidence level $(1-\alpha)$. The value of $Z_{\alpha/2}$ is equal to 2.58 for a 95% and 1.96 for a 90% confidence level respectively. Figure 3.2 illustrates the concept of the ASCBR convergence criterion, [3.16].

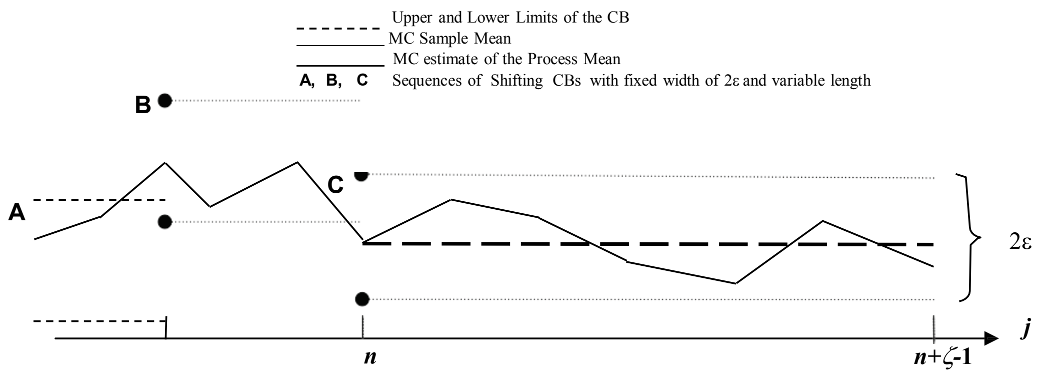

Figure 3.2 The illustration of ASCBR convergence criterion.

3.3. Monte Carlo Simulation Modelling for Privately Owned Car Daily Driving Pattern

Monte Carlo simulation models have been developed to represent daily car use. Various modelling approaches for structuring the MC simulation have been implemented and validated. Different MC methods have their strengths and weaknesses; therefore, there is no unique approach of formulating the simulation for this application. In this research, the MC model generates random samples directly from probability distributions taken from the TUS data rather than from fitted distribution functions. This sampling approach takes advantage of the high time-resolution of the TUS data.

The car location in a week day period was simulated using a discrete-time MC simulation model at each time step of ten minutes. It is assumed that for every given time, only one activity from a finite set of activities can be allocated to the simulated car. Four car location status descriptors that apply to all times, t, are used: car parking at home (S_H), car not parking at home (S_{NH}), car departs from home (S_{DH}), car arrives back home (S_{AH}); $S_L \in [S_H, S_{NH}, S_{DH}, S_{AH}]$. Time terminology will be used to reflect the ten-minute nature of the TUS data and MC trials will be made at each time step in time sequence, with car location status S_L simulated at time t represented by S_L^t. It is assumed that the initial time for simulation purposes is given by $t=1$ and this refers to 4.00am in clock time for consistency with the TUS diaries. Therefore, $S_L^{t=1}$ denotes that the initial status of a car, this can be written as S_L^1. Technically, taken together, this is a discrete-time stochastic process (given that t is finite and can be enumerated) with a finite state space, $S_L \in [S_H, S_{NH}, S_{DH}, S_{AH}]$. The purpose of the modelling is to simulate car use status for a representative weekday; although for some purposes five consecutive weekdays are considered.

3.3.1. Monte Carlo Modelling of Household Car Ownership

Before car use patterns can be simulated, household car ownership must be established for all houses included in the modelling. Each household is taken in turn. The number of cars that are owned is determined for each household.

This is done by sampling from the CDF for household car ownership (see Chapter 2 Section 2.3.1). The process of random sampling from this CDF using the inverse transform method described earlier is illustrated in Figure 3.3.

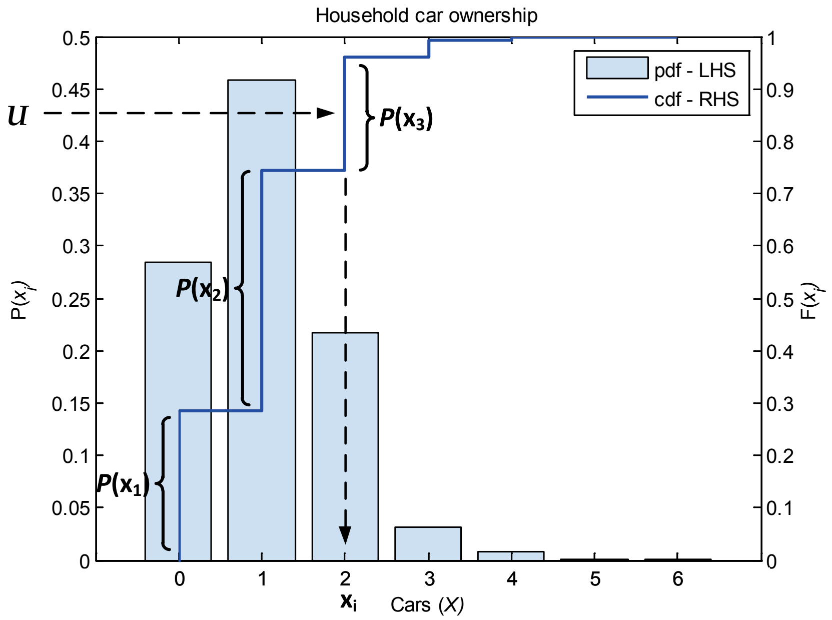

Figure 3.3 The CDF of household car ownership.

In the case of car ownership per household, the distribution is of course discrete. As already made clear, the number of cars per household, n_{cars}, does not exceed 6[18]. Sampling to give the number of cars for the household in question is very straightforward to implement. If $F(x_i)$ is the CDF of cars per household, then the number of cars owned in a given household is given by:

$$n_{\text{cars}} = x_i \tag{3.4}$$

$$\textit{if } F(x_i) = \sum_{i=1}^{i} P_{\text{cars}} < U < F(x_{i+1}) = \sum_{i=1}^{i+1} P_{\text{cars}} \text{ , } i = 1, 2, \ldots, 7$$

[18] In Chapter 2 section 2.3.1, it is stated that the maximum number of cars owned per household in TUS sample is equal to 6.

where n_{cars} is the sample value for the number of cars owned by the household. i represents the number of available sample points in the distribution (in this case 7 as there can be zero cars in a household).

As calculated in Chapter 2 section 2.3.1, the probability of a no-car household is $P_{\text{cars}}(x_1) = 0.28$, the probability of one-car household is $P_{\text{cars}}(x_2) = 0.46$, the probability of two-cars household is $P_{\text{cars}}(x_3) = 0.22$, and so on. For illustration purpose, a random number $U = 0.82$ is generated from the interval (0,1). Since this is a discrete CDF, this number is first compared with the value of the CDF corresponding to the lowest car ownership (zero), i.e. $F(x_1) = P_{\text{cars}}(x_1) = 0.28$. As result, random number generated, $U = 0.82$, is bigger than $F(x_1)$, and the model compares U with $F(x_2)$, where $F(x_2) = P_{\text{cars}}(x_1) + P_{\text{cars}}(x_2) = 0.74$. Again, the random number is greater than $F(x_2)$. The model continues comparing U with $F(x_3)$, and $F(x_3)$ is larger than U, where $F(x_2) = P_{\text{cars}}(x_1) + P_{\text{cars}}(x_2) + P_{\text{cars}}(x_3) = 0.96$. Therefore, the sample generated by the model is $F^{-}(U) = x_3$, which gives the number of cars owned by the household is $n_{\text{cars}} = 2$.

Later in this chapter, the same algorithm is applied when sampling from the CDF of the away period, parking period, and the driving period.

3.3.2. Different Approaches to Structure the Monte Carlo Model

There are different approaches that can be followed in the design of the Monte Carlo model, and these different approaches use different statistics describing domestic car use. As already mentioned, the simulation of domestic car use can be regarded as discrete event simulation, with the state of the system continuously changing to reflect domestic car status, [3.15]. In the following sub-sections, two different approaches of Monte Carlo modelling are introduced and explained in detail; the first approach focuses on household car returning activities developed specifically for home based charging; the next approach follows car locations. The return time dependent Monte Carlo model is then structured based on this modelling approach. Two variants of the second approach are developed. One is called fixed time increment MC model, which generates an appropriate random sample at every time step; it is a fixed-increment, time-advance method. The other one is called multiple time increments MC model, and it uses a next-event time-advance mechanism in which time can progress in multiples of the ten-minute time step determined by sampling from a CDF of duration (for example of car parking at home). These MC simulation models are discrete-time models as the state variables can change their values only at discrete instants of time reflecting the ten-minute sampling of the TUS data. MC modelling can be used to derive the likelihood of particular events happening given certain modelling assumptions, and so the sensitivity of the results to the input assumptions (for example the number of EVs) can easily be calculated.

3.3.2.1. Return Time Dependent Monte Carlo Model

The return time dependent MC model focuses on household activity related to car use, and generates random samples for two discrete RVs. The first is sampled from the time dependent two state PDF $P_{\text{arrival\_household}}$ for a car arriving back home at a specific household. The second is sampled from the multi-state PDF, $P(T_{\text{driving}} \mid t_{\text{arrival}})$ for cumulative car driving period dependent on car arrival time at the household. The model thus contains two sub-models as shown in Figure 3.4; the first one generates random samples for the two state

RVs representing a car arriving back home, denoted $p_{\text{arrival\_household}}$ and a second that generates random samples for the RV representing cumulative driving time prior to arrival home, denoted $p_{\text{driving}}^{t_{\text{arrival}}}$.

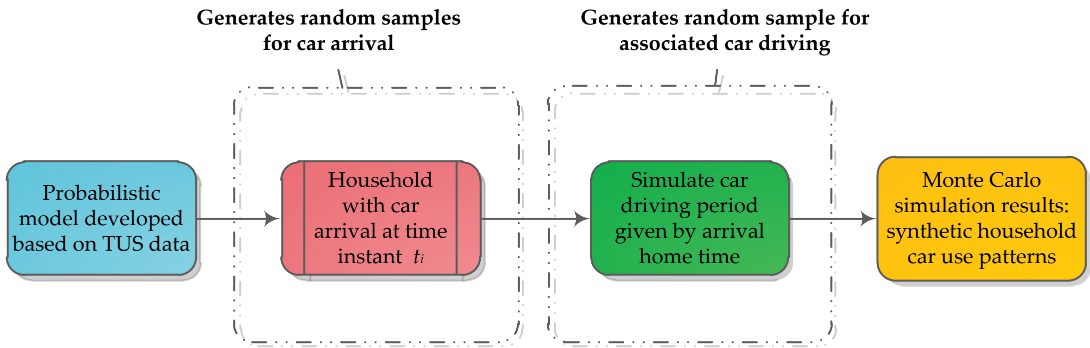

Figure 3.4 The structure of return time dependent MC model.

The simulation flowchart is presented in Figure 3.5 and it proceeds as follows. In the first sub-model, each household is taken in turn, generating random samples from probability distribution of household having a car arrival at that time, $P_{\text{arrival\_house}}$. This probability distribution represents households with a car arriving at a discrete time regardless of the number of cars that might have arrived at this household in previous time steps. For example, a household can have a car return at time *t*, and a second car returns the same household at time *t+1*. By only performing one sample at each time step, the model limits the number of cars arriving at a given time to one (i.e. household can have only one car returning at time *t*). The model generates samples by directly comparing the random number U with the probability of household with car arriving at given time $P_{\text{arrival\_household}}$. The simulation timeframe is $t \in [1, 2, ..., t_{tot}]$. When U is less than or equal to $P_{\text{arrival\_household}}$, the car location status changes to $S_L^t = S_{AH}$. Otherwise, the car location status is $S_L^t = S_{NH}$. It is possible in this model for each household that multiple cars arrive back within the same simulation timeframe since the information regarding when the car departed is not used. Because such simulation events are rare, there is no significant distortion caused by this, as will be seen later, when the model is tested for consistency with the TUS data. Again, the assumption, household can only have one car returning at a time, is reasonable as the TUS diary does not distinguish different cars in the household. In order to capture individual car use pattern, it is necessary to have sufficient diaries of covering individual car use diary.

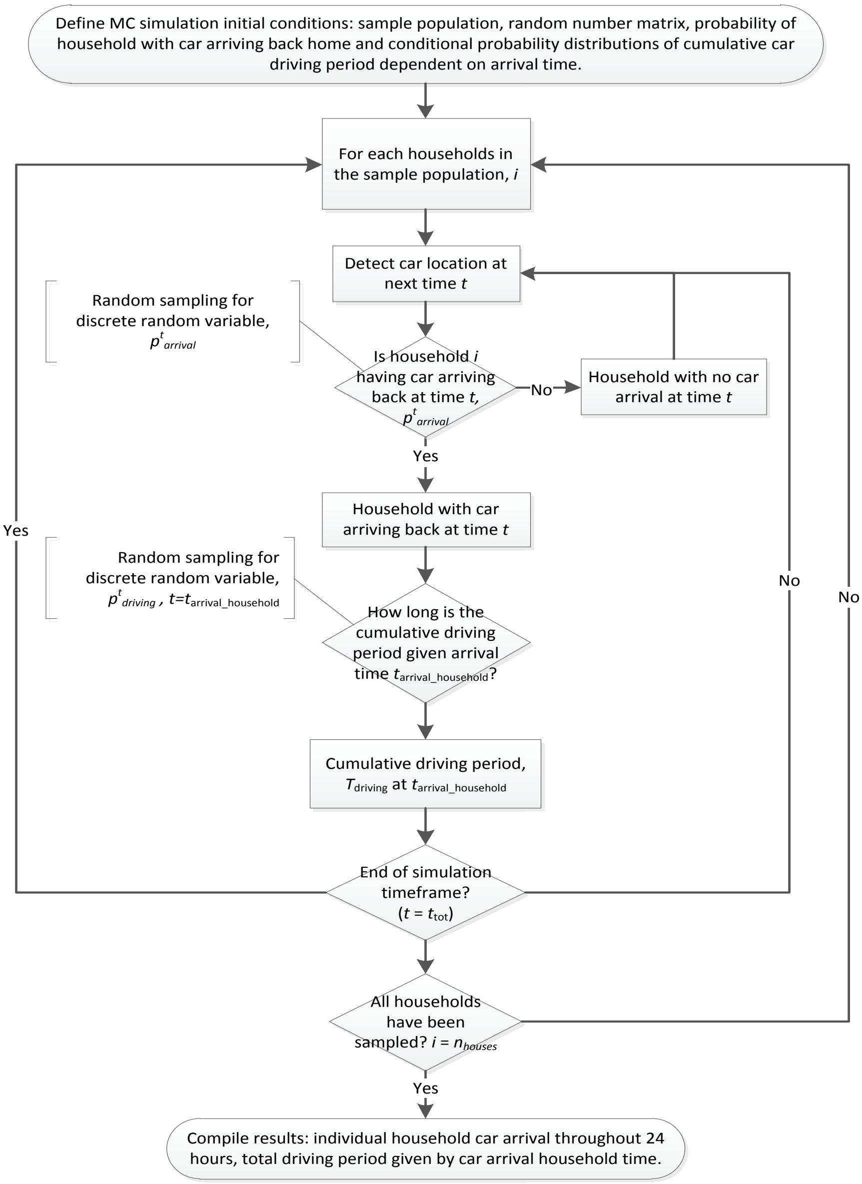

Figure 3.5 Simulation flowchart of return time dependent MC model.

The next step is to determine T_{driving}, the cumulative car driving period dependent on the car arrival time, assuming there are any, and for the car in question to calculate the total time it drives before arriving home. The model generates samples for discrete time variable $p_{\text{driving}}^{t_{\text{arrival\_household}}}$ by sampling from the PDF of cumulative driving period on cars arrival time. For each household, information regarding time of day that cars arrive home and the associated total driving period is generated by this model.

3.3.2.2. Fixed Time Increment Monte Carlo Model

The fixed time increment MC model follows the car movement and thus the MC model can generate the daily car use patterns. It determines car initial location first, and then generates car location status from two conditional probabilities of car departing from home and arriving back home. It is defined that the car away period is the time period between the car departure time and arrival time. This approach utilises the following probabilities and probability distributions for simulating car daily use:

1. probability of car parking at home at $t = 1$, P_{park}
2. conditional probability of car departing from home dependent on car at home at previous time, $P_{\text{departure}}$
3. conditional probability of car arriving back home dependent on car not at home at previous time, P_{arrival}
4. conditional probability distribution of cumulative driving period dependent on car away from home period, $P\left(T_{\text{driving}} \mid T_{\text{away}}\right)$

Model output comprises the synthesised daily car use patterns and includes car location at a given time of day, car departure and arrival time, cumulative driving period dependent on car away period, and time period that car is parking at home and car is away from home. The model consists two sub-models, where the first sub-model generates random samples from PDF of car departure and car arrival, $P_{\text{departure}}$ and P_{arrival} respectively. The second sub-model generates samples from the conditional PDF of cumulative driving period dependent on car away period, $P\left(T_{\text{driving}} \,|\, T_{\text{away}}\right)$. Figure 3.6 illustrates the structure of fixed time increment MC model.

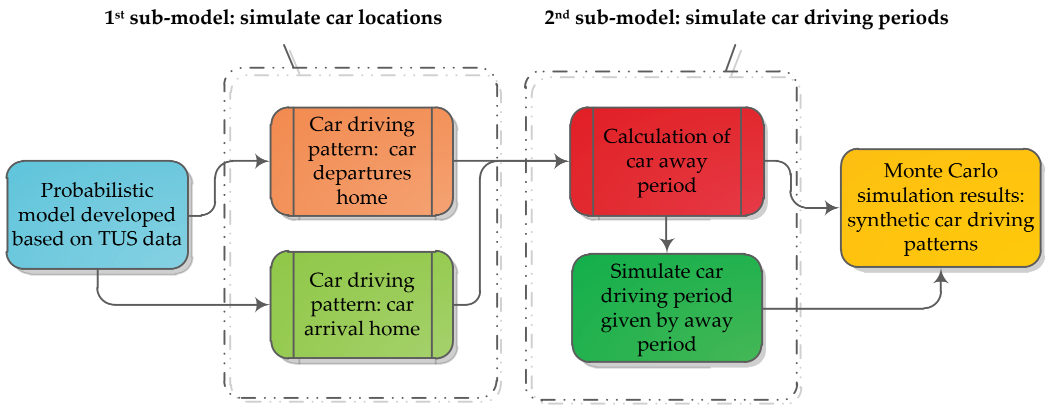

Figure 3.6 Overall structure of fixed time increment MC model.

The activities of car departure and arrival home have been treated as statistically independent in the approach implemented here, although it is possible to evaluate the correlations between these events, [3.17] and [3.18]. In [3.17], a mathematical formulation, called a copula function, was used to evaluate an approximation to the relationship between car departure and arrival home and is limited to a maximum of two home-to-home (h2h) journeys per day. No validation is presented in the paper; therefore, it is not possible to know the accuracy of the driving patterns represented in the paper. In [3.18], a curve fitting technique was applied to the hourly distribution of the last arrival time home dependent on car departure time to generate the required time dependent distribution. However, as the car arrives home, the synthetic driving cycles are randomly assigned to the temporal distribution. In fact, the driving activity is highly dependent on the car arrival time, as presented in Chapter 2 Section 2.3.6.4, and this is ignored in [3.18]. Both approaches have shown the challenges of determining the mathematical relationship between car departure from home and arrival back home. In Chapter 2 Section 2.3.6, the relationship between car departure time and subsequent car arrival time has been investigated; however, due to data limitations, it is not possible to capture the car arrival beyond the 24-hour period. The probability distributions of car departure and arrival have been calculated dependent on the previous time step car status (i.e. car being away from home or parked at home). The resulting simulation procedure follows the logical sequence of car movements. Arrival and departure events are treated as independent for simplicity; the alternative would be large number of different dependencies for each of the combinations of departure and subsequent arrival time. Despite this simplification the time dependence of the probability distributions indirectly capture much of the connection between departure and arrival times. The benefit of this modelling approach is the effectiveness and simplicity of implementation. Therefore, the fixed time increment MC model developed here treats car departure and arrival as independent events. In the multiple time increments MC model, the car departure and arrival events are linked by using car away period and car parking period probability distributions calculated from the TUS data.

The flowchart is illustrated in Figure 3.7. An initial trial is performed to identify the location status of every car at $t = 1$. The model generates random samples for the discrete RV p_{home}^{t} to determine the car's initial location, $S_L^{t=1}$ (i.e. $S_L^1 = S_H$ or $S_L^1 = S_{NH}$). Again, t is a fix-increment time-advance variable and it varies from 1 as the starting value to t_{tot} as the maximum simulation time value. At next time instant $t = 2$, the model simulates the next location (depending on the car location at time $t = 1$) by sampling from the two state probability distribution $P_{\text{departure}}$ or conversely P_{arrival}. For the RV p_{depart} (and the same for RV p_{arrival}), the car location is set to $S_L^2 = S_{DH}$, when U is less than $P_{\text{departure}}$; otherwise, the car remains parking at home, $S_L^2 = S_H$. Again, the random number is directly compared with the probability. For the next time step, the model generates another U and compares this with $P_{\text{departure}}$. Note that the simulation timeframe can be longer than 24 hours in this case, and the time index t will then be converted into a 24-hour periodic variable. This process continues until car location status is $S_L^t = S_{DH}$ signifying that the car departs from home. Therefore, the car departure time can be formulated as follow:

$$t_{\text{departure}} = t + \Delta t \tag{3.5}$$

where $t_{\text{departure}}$ is the time of day that the selected car departs from home, and Δt is the number of time steps until car status changed. Δt could be equal to 1, meaning car departs from home at the next time instant; however, Δt could also be equal to $t_{tot} - 1$, which indicates the selected car parks at home during the entire simulation timeframe. The model continues by generating samples for RV $p_{arrival}^t$ to determine next car location. This process will be repeated until the car location status is $S_L^t = S_{AH}$ signifying that the car arrives back home. The car arrival time, t_{arrival}, is then equal to $t_{\text{departure}} + \Delta t$. This Monte Carlo simulation loop terminates when time t is larger than simulation timeframe t_{tot}.

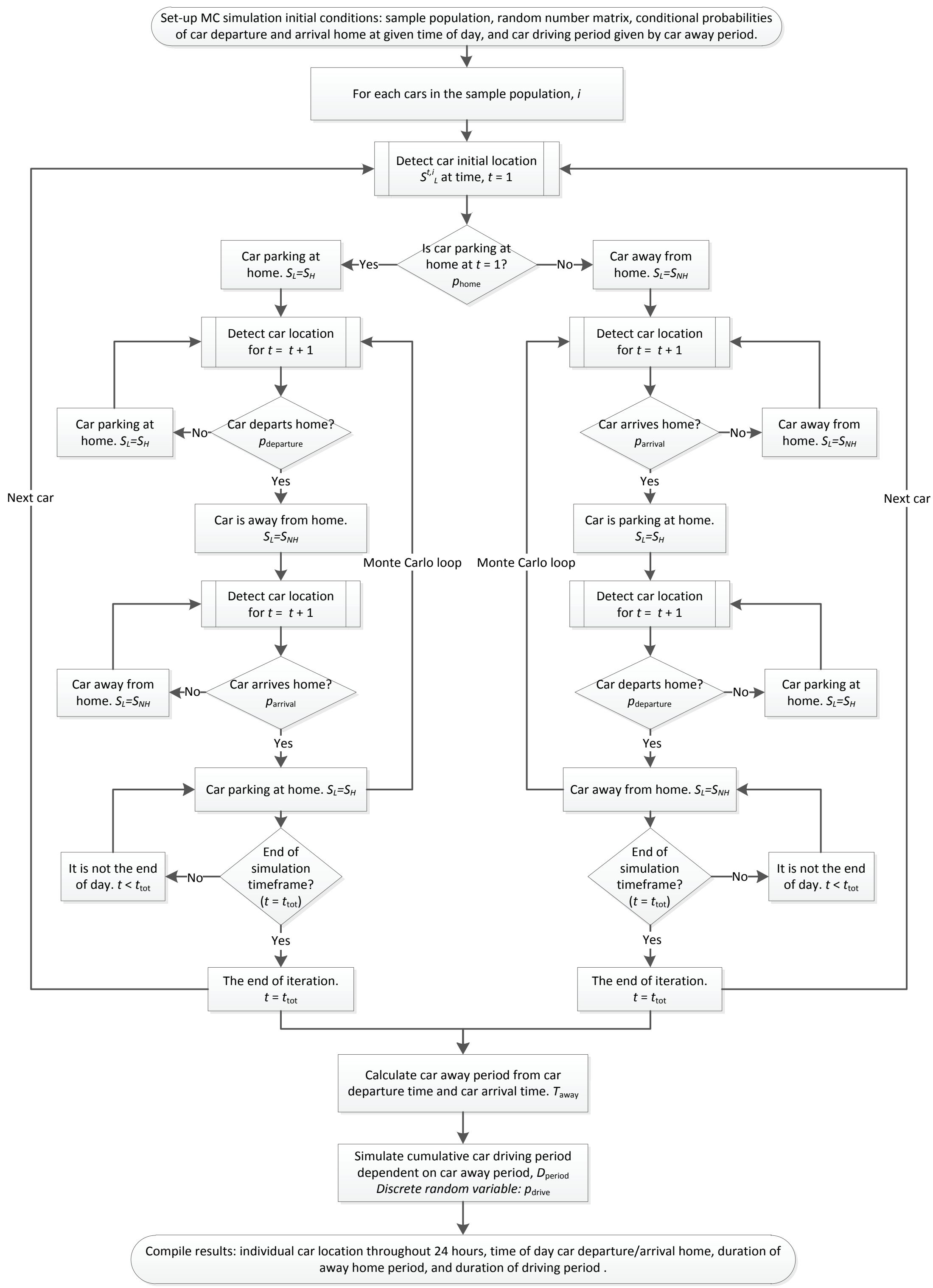

Figure 3.7 The flowchart of fixed time increment MC model.

The car away period T_{away} is calculated from:

$$T_{\text{away}} = t_{\text{arrival}} - t_{\text{departure}} \tag{3.6}$$

The car being parked at home period is then calculated from the time slots between the car arrival time and next departure time:

$$T_{\text{park}} = t_{\text{arrival}} - t_{\text{next\_departure}} \tag{3.7}$$

For each car away period calculated, the model generates random samples for cumulative car driving period dependent on car away period, as before. Sampling cumulative driving period, T_{driving} can be performed as follow. The sampling process is undertaken in a manner analogous to that described in detail in section 3.3.2.1. For RV p_{driving}, samples are generated from the PDF, $P\left(T_{\text{driving}} \mid T_{\text{away}}\right)$, at car departure time $t_{\text{departure}}$. The cumulative car driving period, T_{driving}, is the total amount of time occupied by car driving activity. The cumulative driving period cannot exceed the car away period. The analysis of the simulation results will be explained and discussed in the section 3.4.

3.3.2.3. Multiple Time Increments Monte Carlo Model

The first part of multiple time increments MC model exactly follows the fixed time increment MC model, until the point where the car changes status for the first time, i.e. $S_L^t = S_{DH}$ or $S_L^t = S_{AH}$. Depending on the car location, the model generates random samples T_{away} and T_{park} from $P\left(T_{\text{away}} \mid t_{\text{departure}}\right)$, $P\left(T_{\text{parking}} \mid t_{\text{arrival}}\right)$. The model then generates car location status from these two conditional probabilities until the simulation timeframe is reached. The final part of this model generates samples for cumulative car driving period dependent on car away period, p_{driving}. In contrast to the fixed time increment

MC model, this model only uses $P_{\text{departure}}$ and P_{arrival} for initialisation, after which the loop generating T_{away} and T_{park} is repeated as 'hopping process' shown in Figure 3.8. The 'hopping process' is defined as time index t increases dependent on the simulated car away period and car parking period. The loop will be terminated when the time index t reaches t_{tot}.

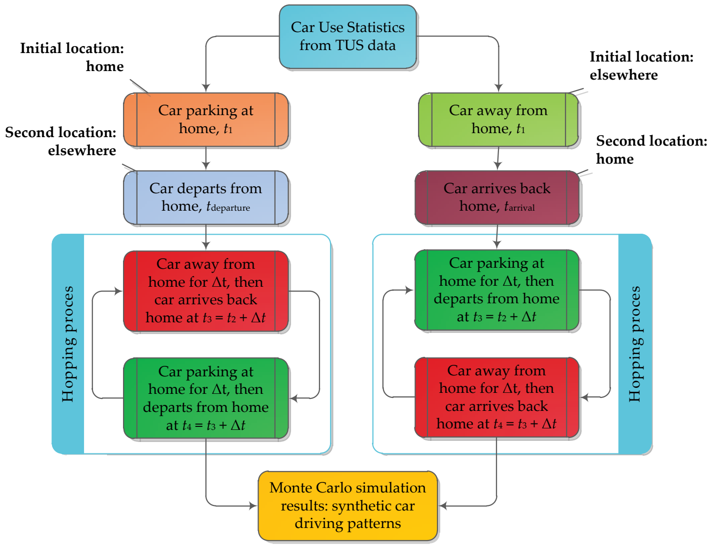

Figure 3.8 Overview of the multiple time increments MC model.

As defined and calculated in Chapter 2 Section 2.3.6.2, the away period (round-trip journey time) is the total amount of time between car departing from home and the following arrival. Therefore, the time of the car arriving back home, t_{arrival}, is equal to $t_{\text{departure}} + T_{\text{away}}$. The car parking period T_{park} is sampled from the PDF $P\left(T_{\text{park}} \mid t_{\text{arrival}}\right)$. The car next departure time equals $t_{\text{arrival}} + T_{\text{park}}$. One advantage of this approach is that the model can simulate multi-day car use patterns much more quickly. The flowchart is illustrated in Figure 3.9. The analysis of the simulation results will be explained and discussed in the section 3.4.

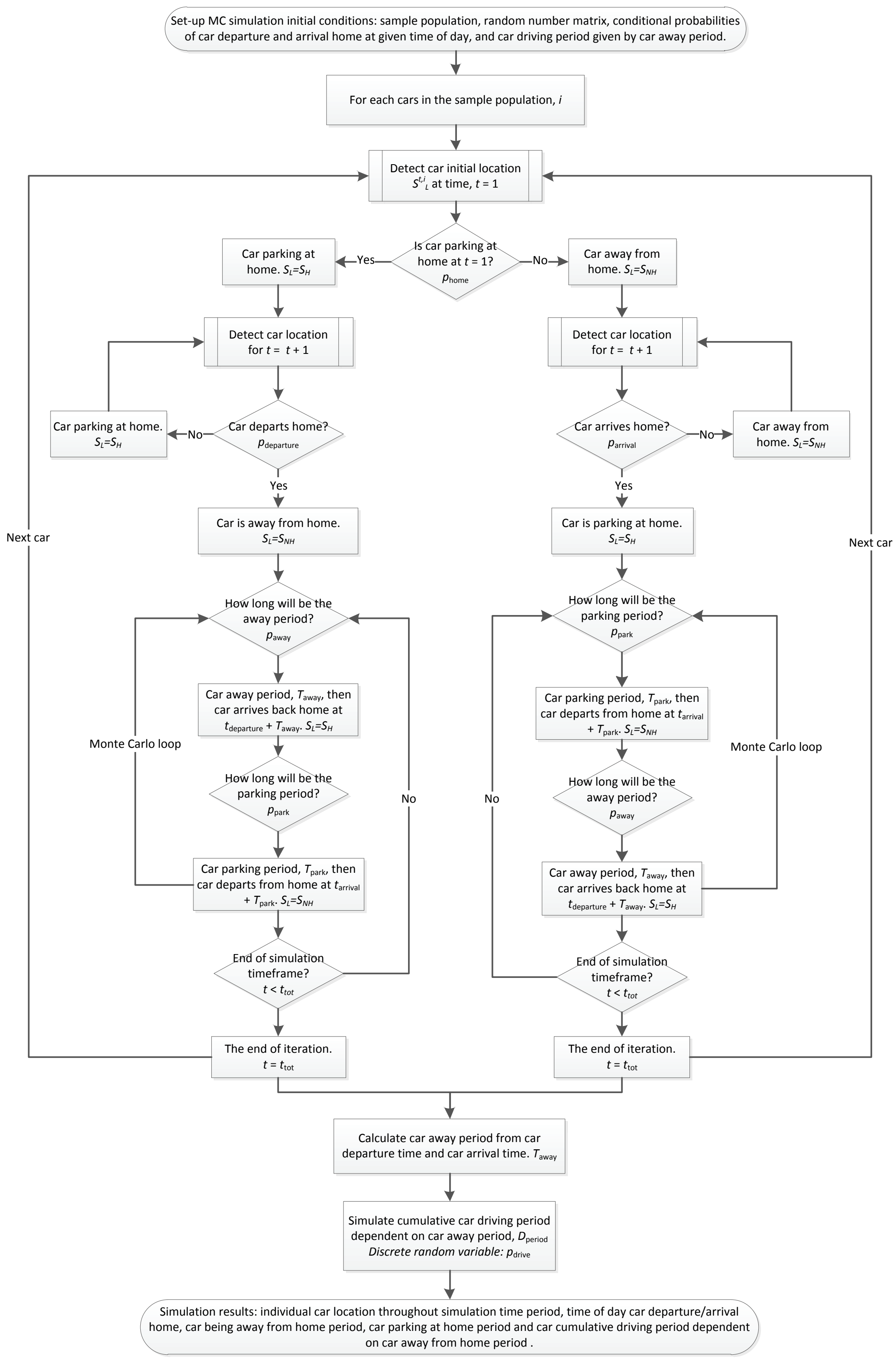

Figure 3.9 The simulation flowchart of multiple time increment MC model.

3.4. Analysis of Monte Carlo Simulation Modelling Results

To ensure structured Monte Carlo models do not significantly distort the simulation results, a careful statistical analysis of the results has been performed, comparing the driving patterns simulated with those of the original TUS data, [3.19]. Before this can be done, it is essential to ensure convergence as discussed above. A statistical consistency analysis can then be done to determine whether or not the MC simulation results reflect the original input data.

3.4.1. Diagnosing Convergence of Monte Carlo Simulation Results

The convergence of MC simulation depends on the number of trials or iterations performed. For the car modelling, convergence can be taken as convergence of the mean driving period, $E[X_{driving}]$. For the purpose of identifying convergence of three structured Monte Carlo models, iterations have been performed as shown in Table 3.1. The mean driving period is then calculated using equation 2.4 for each additional iteration and the sample mean and standard deviation are calculated. These are then input into the equations 3.1 to 3.3. The convergence criteria described in section 3.2.3 is adopted and then applied to determine the required number of iterations. Note that the higher the level of confidence, the wider the confidence band. A wider the CB allows more points fall within the acceptable convergence area.

Table 3.1 Sample population and number of trials for MC models.

Monte Carlo Model	Iterations	Days
Return time dependent	10,000	1
Fixed time increment	20,000	5
Multiple time increments	20,000	5

3.4.1.1. *Return Time Dependent Monte Carlo Model*

For the return time dependent Monte Carlo model the convergence of the mean driving period is shown in Figure 3.10. A 'burn-in' period up to $i = 2000$ is apparent so convergence is assessed beyond this point. For $i = 2000$, the mean driving period calculated as a percentage of time is $\overline{x}_i = 4.6906$ and the standard deviation is $\sigma_{\text{driving}}^{i=2000} = 0.6193$. Applying the convergence criteria described in section 3.2.3, the mean value is deemed to have converged by $i = 9051$ with a 90% confidence interval and $i = 8192$ with the 95% confidence interval. Note that for higher confidence levels, the probability of divergence of the solutions is greater, which leads to early stopping of the simulation. It is clear that sufficient iterations have been undertaken; the converged values are equal to 4.7427 and 4.7336 for confidence levels of 90% and 95% respectively. For practical purposes it can be stated that the return time dependent MC model estimates that a typical car is driving for 4.7% of the time.

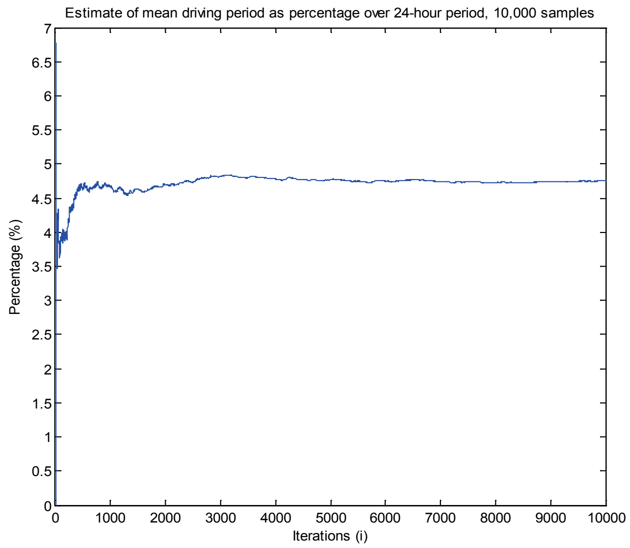

Figure 3.10 The estimated mean driving period for return time dependent MC model.

3.4.1.2. *Fixed Time Increment Monte Carlo Model*

The process above is repeated for the fixed time increment MC model. Figure 3.11 presents the estimator of mean driving period as a percentage over the 24-hour period as the outcome of up to 20,000 MC iterations. As shown in the figure, there is a 'burn-in' period of the mean value up to $i = 3000$. Therefore, the convergence check starts from $i = 3000$. For $i = 3000$, the mean driving period calculated as percentage is $\overline{x}_i = 5.6700$ and the standard deviation is $\sigma_{\text{driving}}^{i=2000} = 0.7581$. After applying the convergence criteria of section 3.2.3, the mean value converged at $i = 7356$ with the 90% confidence interval and at $i = 7463$ with the 95% confidence interval. The resulting mean driving period value are 5.6139% and 5.6121% for confidence level of 90% and 95% respectively. For practical purposes the fixed increment time MC model estimates that a typical car is driving for 5.6% of the time.

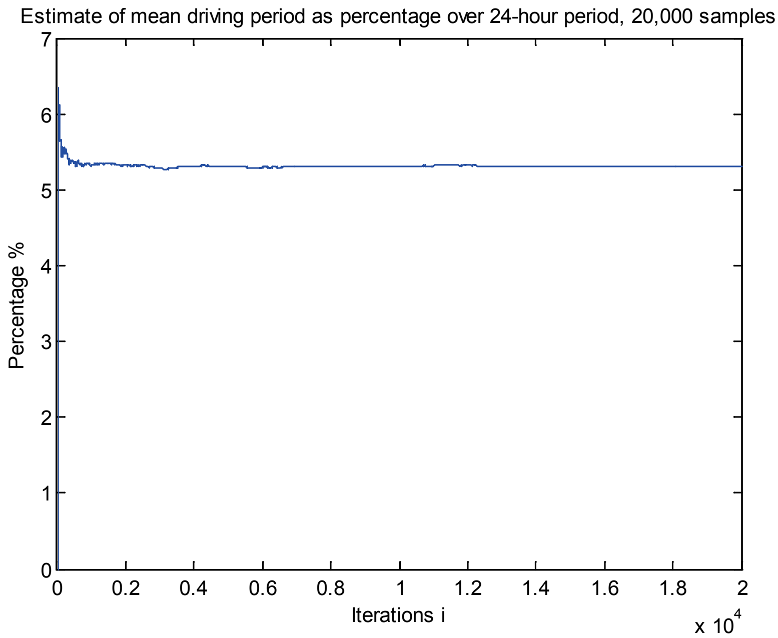

Figure 3.11 The estimated mean driving period for fixed time increment MC model.

3.4.1.3. *Multiple Time Increment Monte Carlo Model*

The convergence check process was applied to the multiple time increment MC model. Figure 3.12 presents the estimator of mean driving period as percentage over the 24-hour period as the outcome of up to 20,000 MC iterations. As shown in the figure, there is a 'burn-in' period of the mean value up to $i = 3000$. Therefore, the convergence check starts from $i = 3000$. For $i = 3000$, the mean driving period calculated as percentage is $\overline{x}_i = 5.2909$ and the standard deviation is $\sigma_{\text{driving}}^{i=2000} = 0.6458$. After applying the convergence criteria, the mean value converged at $i = 9930$ with the 90% confidence interval and at $i = 9795$ with the 95% confidence interval. The resulting the mean value equals to 5.3083 and 5.3071 for confidence level of 90% and 95% respectively. For practical purposes the multiple time increments MC model estimates that a typical car is driving for 5.3% of the time. Not surprisingly there are differences between the results from all three MC models.

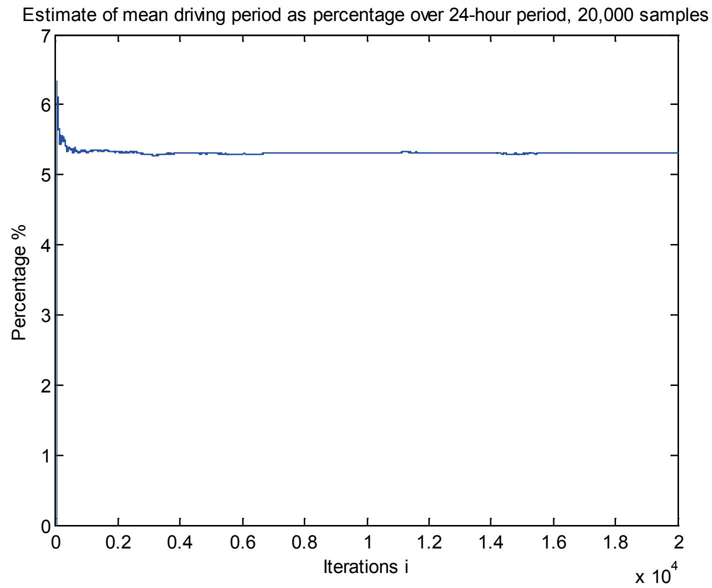

Figure 3.12 The estimated mean driving period for multiple time increment MC model.

3.4.2. Consistency Analysis of Monte Carlo Simulation Results

There are two distinct ways in which the consistency of the Monte Carlo simulation results with TUS data can be established. Where TUS data is directly used to create the Monte Carlo model, the model output can be directly compared to the input. In the second case outputs from the model can be checked against data from TUS not used as input to the Monte Carlo simulation. The purpose of the MC modelling is to produce the car use patterns based on the statistics obtained from the TUS data. The structured MC models can only utilise the empirical distribution and recover the statistics from the sampling process.

3.4.2.1. Return Time Dependent Monte Carlo Modelling Results

A key outcome of return time dependent MC model, the probability of household car arrival time, has been validated against probabilities calculated directly from the TUS weekday dataset (as described in Chapter 2 Section 2.3.6). Figure 3.13 and Figure 3.14 compare in different ways the probability that a car arrives back at the household based on 10,000 MC simulations with those based on the original TUS data. The percentage of difference between MC model results and TUS data has been calculated for both probability of a car returns to house and cumulative driving period dependent on car arrival time. The percentage error of probability of a car returns to house is 0.37%, and for cumulative driving, the percentage error is less than 1%. Therefore, the return time dependent MC model produces acceptably accurate results and recover the statistics calculated from the TUS data by sampling directly from the empirical distributions. Therefore, the return time dependent MC model produces acceptably accurate results and recover the statistics calculated from the TUS data by sampling directly from the empirical distributions.

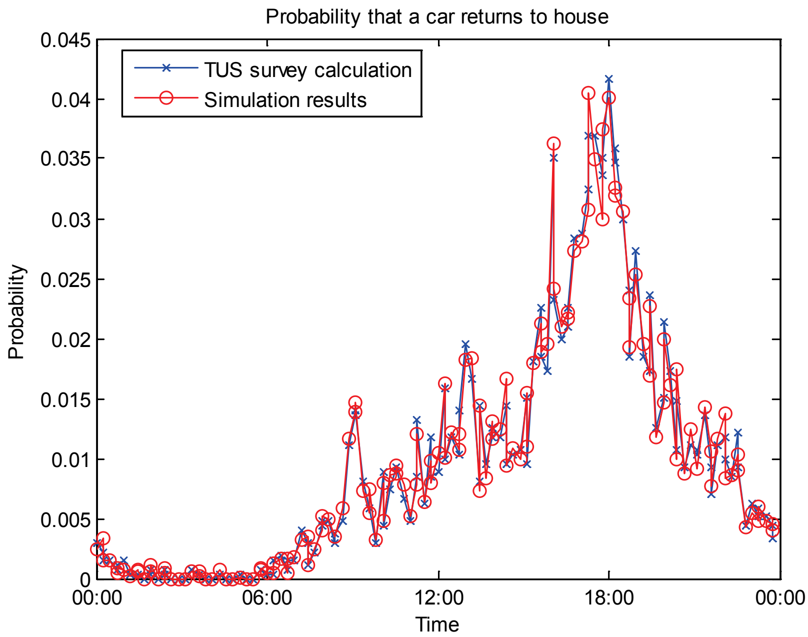

Figure 3.13 Comparison of probability of a car arriving at a household derived from return time dependent MC model results and from TUS data.

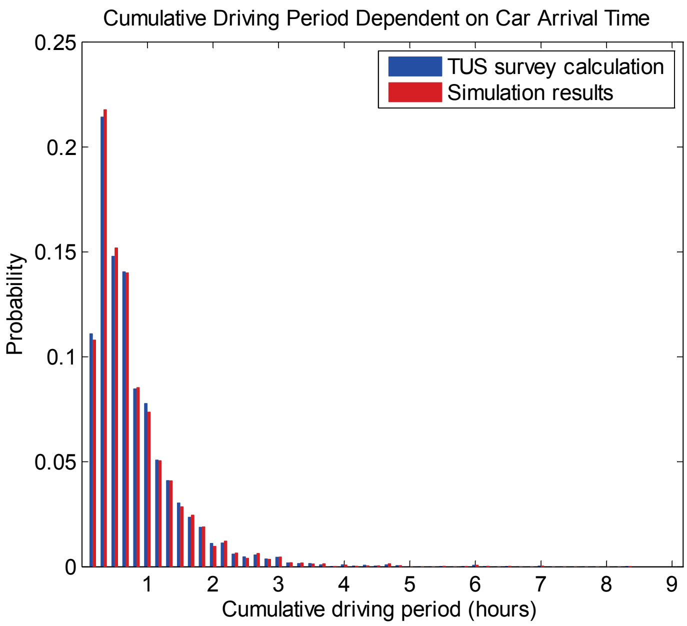

Figure 3.14 Comparison between return time dependent MC model results and TUS data calculation for marginal distribution of cumulative driving.

3.4.2.2. *Fixed Time Increment Monte Carlo Model Results*

The fixed time increment MC model uses much more information than the return time dependent MC model. In order to analyse the consistency of the MC model, and the MC simulation results, in this case from 20,000 iterations, results have been compared for the following:

1. Probability of car parking at home.
2. Probability of car departure at t dependent on car being parked at home at $t-1$.
3. Probability of car arrival at time t dependent on car being away from home at time $t-1$.
4. Probability distribution of cumulative car driving period as conditional on car away period for cars that departed at departure time, $t_{\text{departure}}$.

The car away period is calculated from car departure time and its next arrival time as described in previous section; its probability distribution as calculated by MC simulation outcome and TUS data calculation has been compared. Figure 3.15 illustrates the comparison of probabilities of car departure and arrival. The percentage error between MC model results and TUS data has been calculated for both probability of a car departure from home and probability of a car arrive back home. The percentage error of car departure is 1.63%, and 2.76% for car arrival; therefore, MC model produces acceptably accurate results.

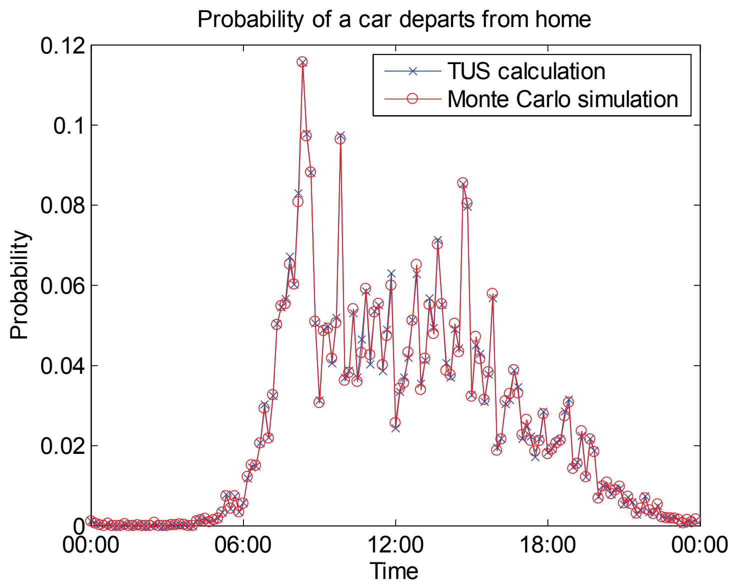

(a)

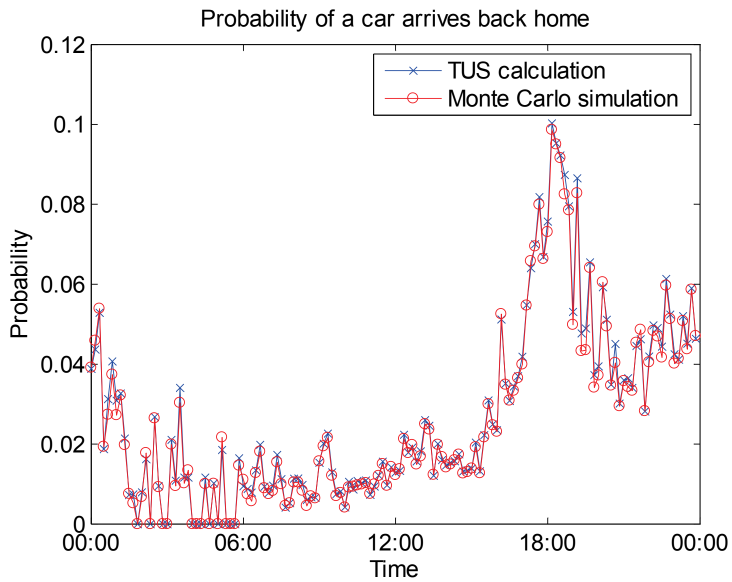

(b)

Figure 3.15 Comparison of fixed time increment MC results and TUS calculation for (a) probability of car departure; (b) probability of car arrival.

Unlike the return time dependent MC model, this MC model can also capture the car location over multiple days as in Figure 3.16[19]. The probabilities follow the same trends from 2nd day to 5th day. However, there is a significant

[19] Monte Carlo simulation starts at 4:00am, the same as the TUS data, and the axes have not been adjusted in this case.

difference between the model output and the input data for time between 8pm in the night and 8am in the morning.[20]

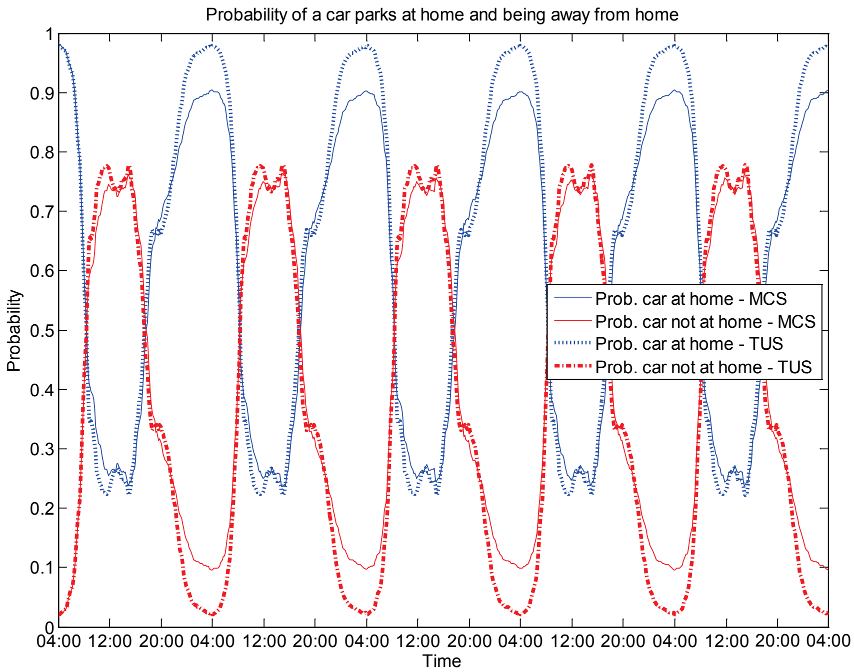

Figure 3.16 Comparison of fixed time increment MC model results and TUS calculation for probability of a car being parked at home and being away from home.

In the fixed time increment MC model, car departure and arrival events have been treated as two independent events; the result is a significant error in the simulation of the probability of an individual car away period as shown in Figure 3.17. The MC model generates fewer short away period (<2 hours) comparing to TUS data, and more medium away period (between 3 hours and 9 hours). As a result, the simulation results for the cumulative car driving period also show some, although less, error, Figure 3.18. Therefore, the fixed time increment MC model has the disadvantage when reproducing car away

[20] TUS data only has one 24-hour profile, so the following days are an exact replication of the first 24-hour profile.

home period and cumulative driving period. Consequently, this MC model is not ideal to be used to generate individual household car use patterns.

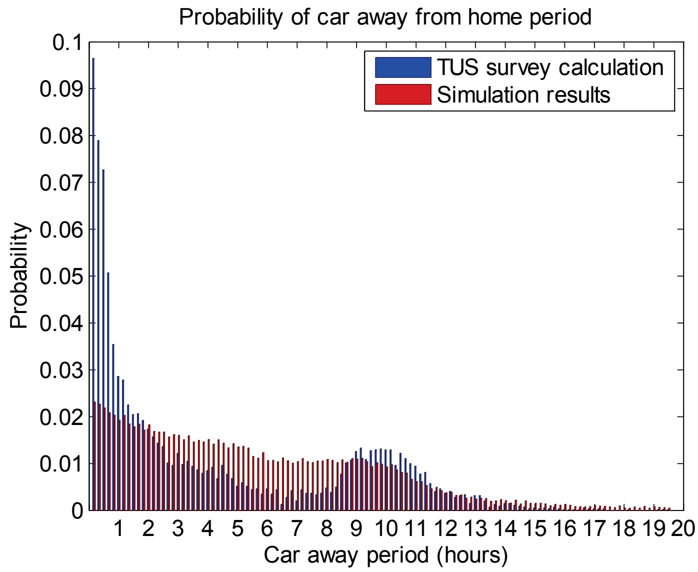

Figure 3.17 Comparison of fixed time increment MC model results and TUS data calculation for car being away from home period.

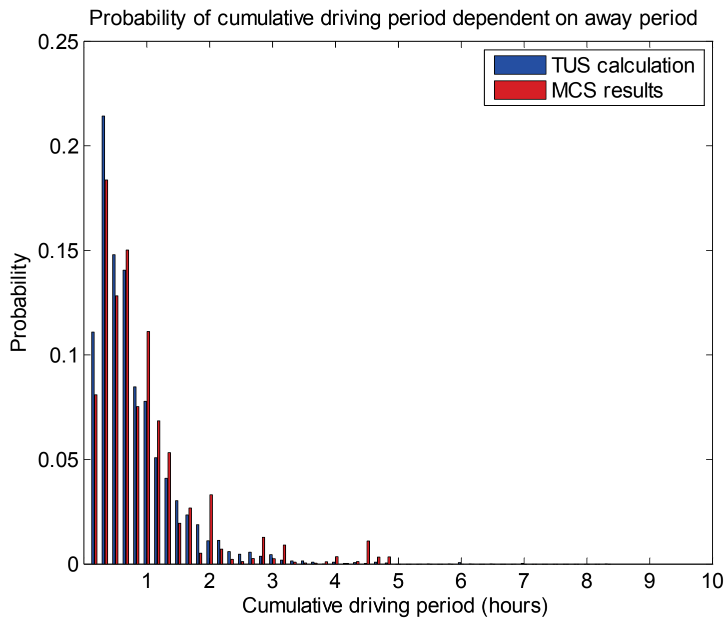

Figure 3.18 Comparison of fixed time increment MC model results and TUS data calculation for cumulative car driving period.

3.4.2.3. *Multiple Time Increments Monte Carlo Model Results*

The multiple time increments MC model uses more car use statistics than the fixed time increment MC model. As before, 20,000 iterations are used. Results are shown for:

- Probability of car parking at home.
- Probability of car departure at t dependent on car being parked at home at $t-1$.
- Probability of car arrival at t dependent on car being away from home at $t-1$.
- Probability distribution of car away period at $t_{\text{departure}}$
- Probability distribution of car parking period at t_{arrival}
- Probability distribution of cumulative car driving period as conditional of car away period at departure time, $t_{\text{departure}}$.

In contrast to fixed time increment model, the car away period is directly sampled from the relevant probability distribution, as is the car parking period. The probability distributions of car away period and car parking period have been compared that shown as quantile-quantile plot in Figure 3.19 and Figure 3.20. The cumulative car driving period is sampled as conditional on car away period. The probability distribution of cumulative car driving period provides good correlation with the TUS data that shown as quantile-quantile plot in Figure 3.21. This demonstrates the effectiveness of the multiple time increments MC modelling method in replicating relevant statistical characteristics of the original TUS data. Multiple time increments MC model can also reproduce multi day car location as shown in Figure 3.22. The probability of car being parked at home has almost the same trends from 2nd day to 5th day, as is the probability of car being away from home. It can be seen that significant modelling error occurs for car location during two time periods. The first period is between 8am and 6pm. Second period is between 7pm and midnight.

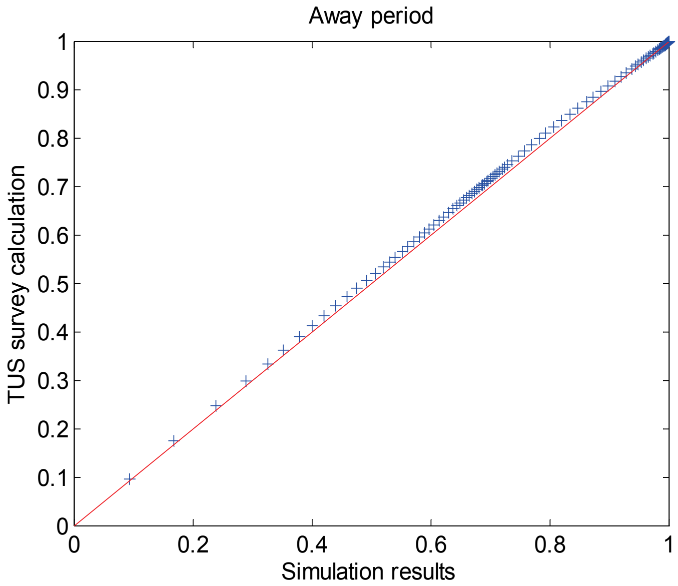

Figure 3.19 Comparison of multiple time increments MC model results and TUS data calculation for car away period.

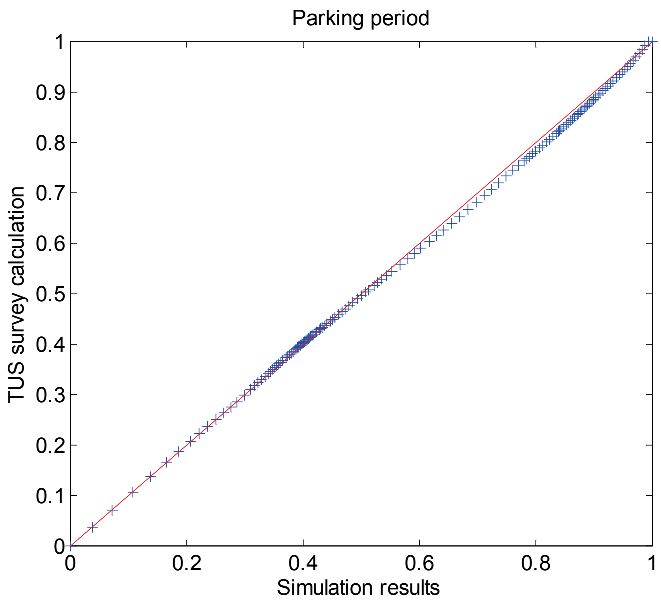

Figure 3.20 Comparison of multiple time increments MC model results and TUS data calculation for car parking period.

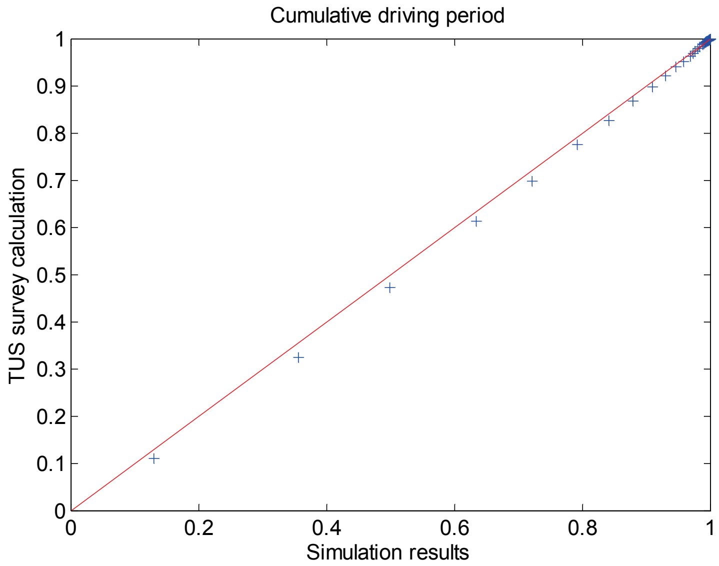

Figure 3.21 Comparison of multiple time increments MC simulation results and TUS data calculation for cumulative car driving period.

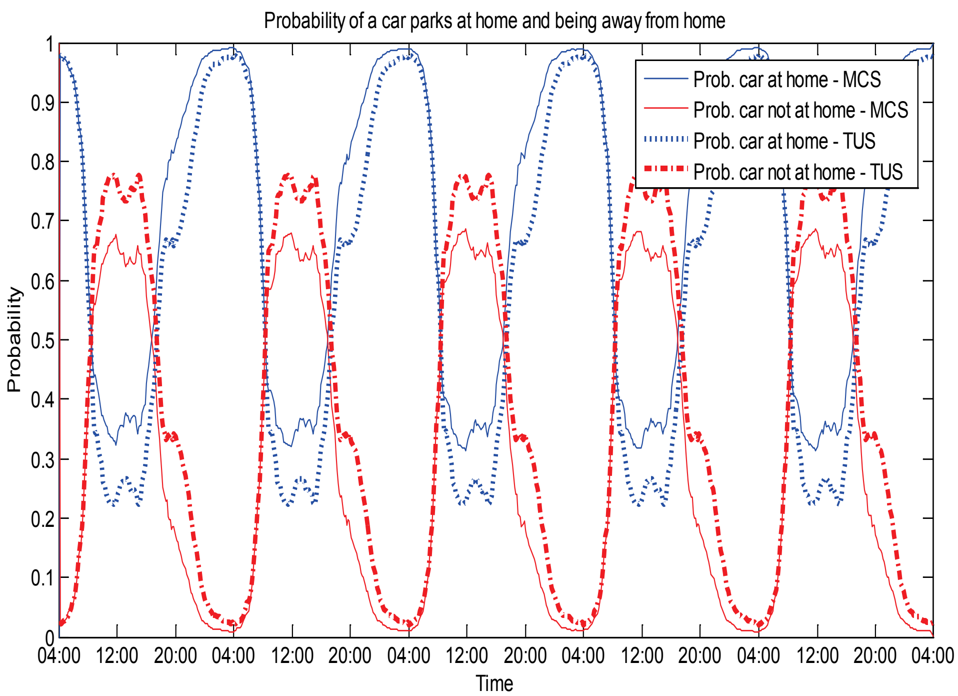

Figure 3.22 Comparison of multiple time increments MC model results and TUS calculation for probability of car being parked at home and being away from home.

The probability of car departure and arrival can be calculated by using equations 2.11, 2.12, 2.13, 2.14, and are shown in Figure 3.23. The probability of car departure has been plot against the TUS calculation in Figure 3.23a. The percentage error of car departs from home is only 1.4% between MC model results and TUS data. In Figure 3.23b, the probability of car arrives back home has been plot against the TUS calculation. However, the probability of car arrival is poorly modelled as seen from the figure, especially around 5pm in the afternoon and 4am in the morning. The simulation results has been further analysed in order to explain the discrepancy.

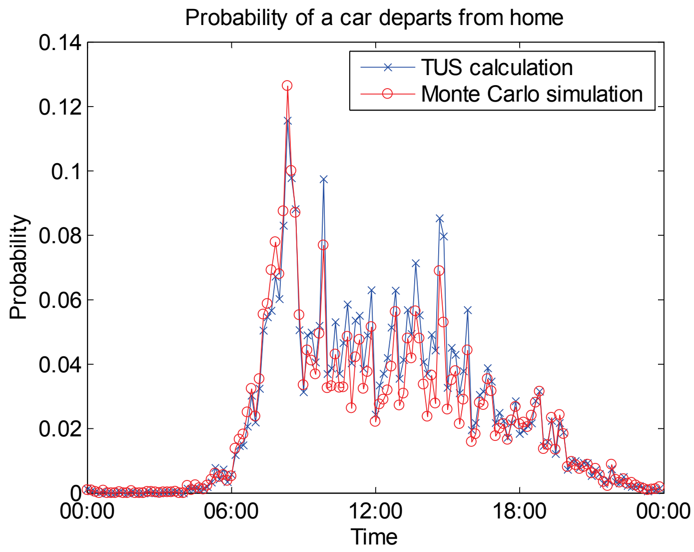

(a)

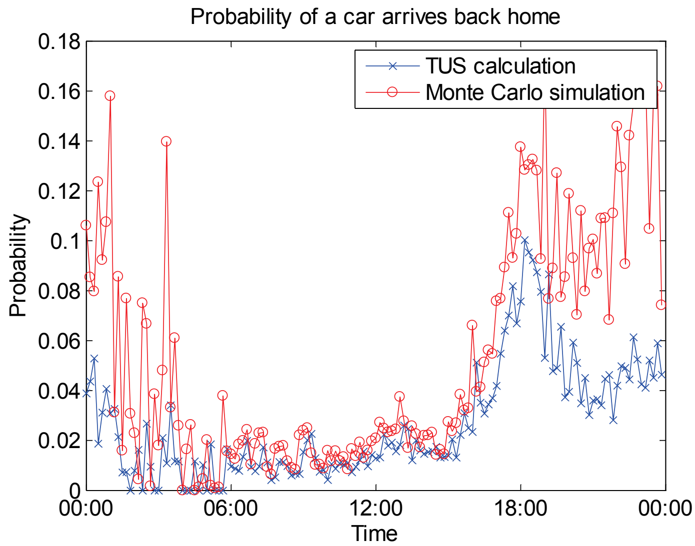

(b)

Figure 3.23 Comparison of multiple time increments MC results and TUS calculation. (a) Probability of car departure; (b) Probability of car arrival.

As stated in Chapter 2, the probability of car arrival is calculated from the number of cars arriving back home at time t divided by the number of cars away from home at the previous time step $t-1$. The car arriving back home events depend on the car being away from home at previous time step. The difference for the probability of a car being away from home has been calculated as percentage between simulation results and TUS data, and is shown in Figure 3.24. There is a marked correlation between the periods when there is large error modelling the car arrival and when the percentage of error in the probability that a car is away from home is large. From Chapter 2 section 2.3.5.3, it is known that the majority of journeys happened between 7am in the morning and 4pm in the afternoon as illustrated in Figure 2.22. The absolute difference between the MC results and TUS data is below 20% for this time period, as shown in Figure 3.24. As a result, the simulated car arrivals during the important part of the day should be reliable. The bias in the simulation of car arrival is caused by the error of car away from home. To resolve this error, a different Monte Carlo simulation method might be helpful; however, this is beyond the scope of this research and is left for future research.

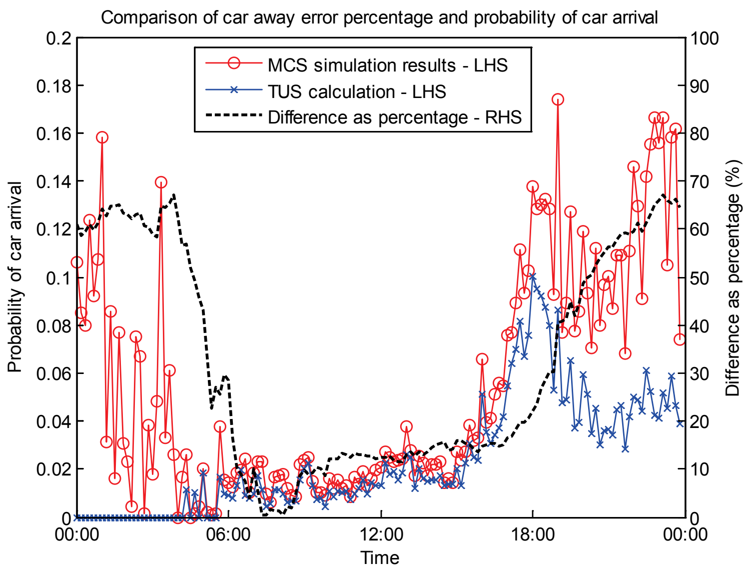

Figure 3.24 Comparison of car away error percentage and probability of car arrival home.

Additionally, the percentage of cars arriving back home over a day has been calculated as follow:

$$Percentage\left(n_{\text{arrival}}\right) = \frac{n_{\text{arrival}}\left(t\right)}{\sum_{t=1}^{t=t_{tot}} n_{\text{arrival}}}, t = 1, 2, 3, \ldots, t_{tot} \tag{3.8}$$

where n_{arrival} is the number of cars arriving back home. The percentage of cars arriving back home correlate well with the TUS calculation, as shown in Figure 3.25. The percentage error calculated for car arrival home distribution is less than 1%. This also explains the effectiveness of the multiple time increments MC model in replicating the statistical nature of the original TUS data where the emphasis is on the car driving period.

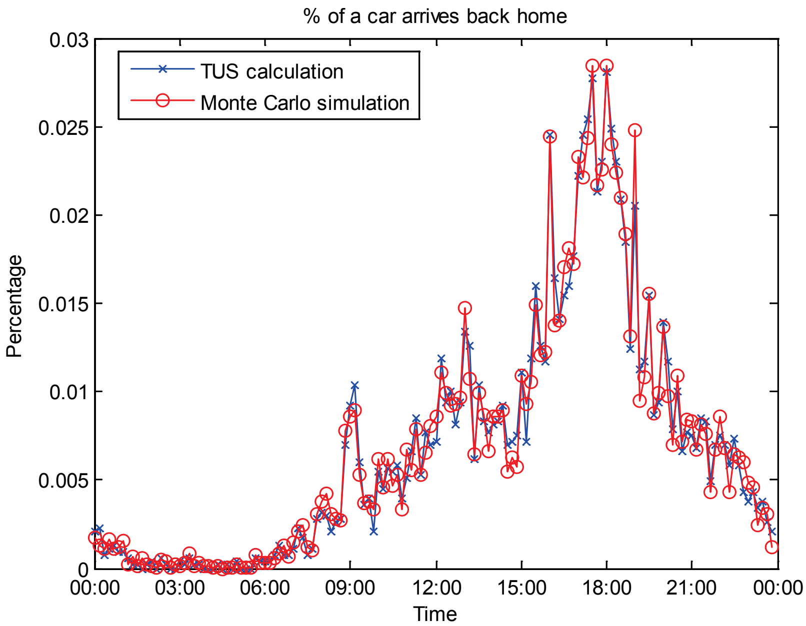

Figure 3.25 Comparison of multiple time increments MC model results and TUS data calculation for car arriving back home as percentage.

3.4.2.4. *Average Daily Driving Period*

The estimate of mean driving period has been calculated as percentage over the 24-hour period from the three MC model simulation results. This mean value should provide a good approximation to the expectation calculated from the TUS data. Note that the estimate of mean driving period (75 minutes) can be directly calculated from the weekday TUS dataset as illustrated in Figure 2.23, (Chapter 2 section 2.3.6.3). Furthermore, all three MC models can only generate the cumulative driving period between departure from home and subsequent return. Individual journeys that might contribute to this driving period have not been resolved in this analysis of the TUS data. It is thus reasonable to use the mean cumulative driving period as the modelling consistency check criteria. The method of calculating the percentage of overall driving period as a proportion of single day is given by the following formula:

$$\overline{T}_{\text{driving}} = \frac{1}{N_{\text{iterations}}} \times \frac{1}{t_{tot}} \times \frac{1}{N_{\text{days}}} \times \sum_{i=1}^{i=N_{iterations}} \sum_{t=1}^{t=t_{tot}} T_{driving}\left(t_i\right) \tag{3.9}$$

where $N_{\text{iterations}}$ denotes the number of iterations performed by MC models, N_{days} is number of days performed by MC models, t_{tot} means the number of time slots for 24-hour period. i is the diary index and $T_{\text{driving}}\left(t_i\right)$ is the individual driving period in each individual diary. The value obtained directly from the TUS weekday data used to determine the probability used in the Monte Carlo simulation is 5.2%. For the return time dependent MC model, the mean driving period as percentage is 4.7%, which has a fractional error of 0.096. The fixed time increment and multiple time increments MC models produced 5.6% and 5.3% respectively. The fractional errors are 0.077 and 0.019 for these two models. In the context of the imprecision resulting from the use of limited data, all these results are viewed as acceptable. Clearly, for this important measure of performance, the return time increment MC model produced less accurate results. However, in the view of its simplicity, it remains attractive. Comparing Figure 3.14, Figure 3.18 and Figure 3.21, it can be seen that the return time increment MC model actually reproduces the driving period PDF more accurately.

3.5. Discussion and Summary

In this chapter, Monte Carlo simulation has been explained and regarded as the effective approach to generate synthetic individual car use patterns. Based on the Inverse-transform method, three different Monte Carlo simulation models have been described. For each MC model, analysis has been performed on the simulation results to demonstrate convergence and also to check consistency with the TUS input data. The purpose of the MC modelling is to produce the car use patterns based on the statistics obtained from the TUS data. As discussed previously, it is possible to fitting parametric distribution to certain car use probability distributions; however, the concern is that MC modelling results might not reflects the statistics calculated from the TUS data. In this case, the structured MC model can only utilise the empirical distribution and recover the statistics from the sampling process.

The advantage of the return time dependent MC model is that it utilises only two car use statistics: the probability of a car arriving back at a household; and the probability distribution of cumulative driving period dependent on car arrival time. The return time dependent MC model allows simulation results to converge with less iterations as illustrated, which means less computational time compared to both fixed time increment and multiple time increments MC modelling approaches considered. This model can only generates car arrival activities and its associated cumulative driving period; however it produces accurate estimation and time distribution of car arrival time and cumulative driving period, which is the main objective of the MC models. Both fixed time increment and multiple time increment MC models can generate car parking locations and departure and arrival events by sampling from different statistical distributions. For example, the fixed time increment MC model only needs probabilities of car departure and arrival to generate car parking location information. The multiple time increments MC model uses probability distributions of car parking period and away period to generating car parking location information. Additionally, both fixed time increment and multiple time increments MC models can provide information about the next car departure, which could be helpful in the study of demand side management applied to EV charging.

Cumulative driving period, when car arrives back home, determines the amount of energy required for vehicle charging calculations. All three structured MC models produced a mean driving period within ±5% of TUS data statistics, with the multiple time increments MC model being most accurate in this regard.

Both fixed time increment and multiple time increments MC models follow the car movement. The fixed time increment MC model assumed independent car departure and arrival. The benefit of this modelling approach is the effectiveness and simplicity of implementation. However, the calculated car away period and the cumulative car driving period have significant differences from those calculated from the TUS data. On contrast, the multiple time increments MC model can accurately reproduce frequency distributions of car away and parking period, the number of cars arriving back home at any time, and also the probability of car departure. However, there is significant error in calculating the probability of car arrival with the multiple time increments MC model, which is caused by errors in modelling the time of day that the car returns home. These two models have different strengths and weaknesses. Nevertheless, both MC models can accurately simulate two most critical parameters: car arrival home probabilities and cumulative driving period on arrival home. A different modelling approach might provide a more complete model able to reproduce all the relevant statistics, and this is suggested as future work.

3.6. References

[3.1] Weisstein, Eric W."Buffon's Needle Problem." From *MathWorld*--A Wolfram Web Resource. http://mathworld.wolfram.com/BuffonsNeedleProblem.html

[3.2] H. Solomon, “BUFFON NEEDLE PROBLEM, EXTENSIONS, AND ESTIMATION OF π,” in *Geometric Probability*, 1st ed. Philadelphia. City of Publisher: Society for Industrial and Applied Mathematics, 1978, ch. 1, pp. 1-5.

[3.3] Abedin, Z.U. and R.A. Waraich (2014) Modelling Inductive Charging of Battery Electric Vehicles using an Agent-Based Approach, *Journal of Sustainable Development of Energy, Water and Environment Systems*, **2** (3), 219-233.

[3.4] K. H. van Dam, I. Nikolic, and Z. Lukszo, *Agent-Based Modelling of Socio-Technical Systems*: Springer, 2012.

[3.5] S. M. Ross, *Simulation*: Elsevier Science, 2012.

[3.6] R. Y. Rubinstein and D. P. Kroese, *Simulation and the Monte Carlo Method*: Wiley, 2011.

[3.7] Whiteley, N. (2010) *Monte Carlo Methods*. [Lecture Notes] Department of Mathematics, University of Bristol.

[3.8] F. Soares, J. P. Lopes, P. R. Almeida, C. Moreira, and L. Seca, "A stochastic model to simulate electric vehicles motion and quantify the energy required from the grid," *PSCC, Stockholm, Sweden*, 2011.

[3.9] C. B. Moler, *Numerical Computing with MATLAB*: Society for Industrial and Applied Mathematics (SIAM, 3600 Market Street, Floor 6, Philadelphia, PA 19104), 2008.

[3.10] MATLAB and Statistics Toolbox Release 2012b, The MathWorks, Inc., Natick, Massachusetts, United States.

[3.11] RandStream constructor, MATLAB, http://www.mathworks.co.uk/help/matlab/ref/randstream.randstream.html

[3.12] Creating and Controlling a Random Number Stream, MATLAB, http://www.mathworks.co.uk/help/matlab/math/creating-and-controlling-a-random-number-stream.html#brvku_2

[3.13] Grahn, P. (2013) *Electric Vehicle Charging Impact on Load Profile*. PhD thesis. School of Electrical Engineering, Royal Institute of Technology, Stockholm, Sweden.

[3.14] Papadopoulos, P. (2012) *Integration of Electric Vehicles into Distribution Networks*. PhD thesis. Institute of Energy, School of Engineering, Cardiff University.

[3.15] W. L. Winston and J. B. Goldberg, Chapter 21 – Simulation, *Operations research: applications and algorithms*: Thomson Brooks/Cole, 2004.

[3.16] Mustafa Y. Ata, A convergence criterion for the Monte Carlo estimates, Simulation Modelling Practice and Theory, Volume 15, Issue 3, March 2007, Pages 237-246, ISSN 1569-190X, http://dx.doi.org/10.1016/j.simpat.2006.12.002.

[3.17] Lojowska, A.; Kurowicka, D.; Papaefthymiou, G.; Van der Sluis, L., "Stochastic Modeling of Power Demand Due to EVs Using Copula," *Power Systems, IEEE Transactions on* , vol.27, no.4, pp.1960,1968, Nov. 2012

[3.18] Tae-Kyung Lee; Bareket, Z.; Gordon, T.; Filipi, Z.S., "Stochastic Modeling for Studies of Real-World PHEV Usage: Driving Schedule and Daily Temporal Distributions," *Vehicular Technology, IEEE Transactions on* , vol.61, no.4, pp.1493,1502, May 2012

[3.19] M. Guizani, A. Rayes, B. Khan, and A. Al-Fuqaha, *Network Modeling and Simulation: A Practical Perspective*: Wiley, 2010.

4. Chapter 4: Impact Assessment of Electric Vehicle Charging on UK Low Voltage Distribution Network

The driving patterns of electric vehicles are expected to follow the conventional or internal combustion engine car use statistics for all but the longest journeys. The return time dependent Monte Carlo model developed in the previous chapter allows an accurate representing of the likely domestic car journeys. The electrification of these journeys places additional electricity loads on the distribution system that dependent on the different scenarios of EV take-up. In addition, the multiple time increments MC model developed in the previous chapter has been extended to incorporate a household electricity load model so that house by house total load profiles (including EV charging) can be generated for use in distribution system load flow studies as part of power distribution system impact assessment. The uncertainty associated with these charging loads can also be estimated, which is important for network expansion and contingency planning. Simple 'plug and charge' strategies are shown to significantly add demand at the times of existing peak domestic load, potentially causing problems for distribution network operators.

4.1. Case Study 1: Impact on Substation Transformer

Before assessing in detail the impact of vehicle charging on the low voltage network secondary transformer (400V/230V) including line flows and voltages, it is useful to present an assessment of the aggregate impact of EV charging on the 11kV primary substation transformers. As described in Chapter 3, the return time dependent Monte Carlo model simulates household car arrival time and the associated cumulative driving period. Knowing the cumulative driving period and thus the degree of battery discharge at the time of arrival home is all that is required to calculate the vehicle charging for a simple 'plug and charge' strategy. The 'plug and charge' strategy regards home as the only location for charging and allows vehicle charging to begin as soon as the EV arrives back home. When these charge durations are overlaid for the population of households under consideration the result is the additional electricity load for the population of houses.

The residential network data is provided by Scottish Power, comprising one 33/11kV 7.5 MVA primary substation transformer, and six 11kV secondary substation transformers with a mix of 300kVA and 500kVA capacities. Census data provides the total number of household in the area is 1,885, [4.1]. It is assumed that the LV networks considered supplies predominantly domestic housing. On average, each distribution transformer in this system supplies 259 houses. Initially all households supplied by the primary transformer are considered together so as to examine the additional charging load on the substation transformer. With Monte Carlo simulation, it is important to determine how many independent trials using different random number seeds are required to achieve reasonable convergence to the required distribution or characteristic of interest. Here the concern is with the aggregate EV charging load and how this varies through the day. This approach provides accurate forecasting of the additional electricity loads placed on the 11kV distribution system for different assumed scenarios of EV take-up.

4.1.1. Electric Vehicle Deployment in the Residential Area

The TUS household car ownership distribution has been adapted to allow households with at least one car to have one EV. Number of cars owned per household is simulated from the distribution calculated from TUS data, see Figure 2.6a. The maximum number of cars for each household is six. It is recognised, certainly for a modest overall take-up rates, that it is unlikely that any household would have more than one EV. For simplicity, and because of lack of more detailed data, it has been assumed that EVs are distributed evenly across all the households having cars. Before calculating the EV charging load, the MC model (see Chapter 3 section 3.3.1) simulates the number of cars owned by each household. After sampling for 1,885 households supplied by the same primary transformer, there are 1,966 cars owned by these households in the district. As a result, there are 1.042 cars per household. For the 215 households supplied by the same secondary transformer, the MC model gives 205 cars as the outcome of one simulation calculation. Among these 215 households, there are 68 households (32%) without a car. It is higher than the statistics presented in the Chapter 2. However, it is reasonable that these results are the outcome of single Monte Carlo simulation. The deployment level of EVs among car owning households, defined as the proportion of cars owning households with an EV, has been assumed to vary from 0% to 100% with 10% increments.

4.1.2. Electric Vehicle Charging Modelling

Once the round trip total driving times have been established (see Chapter 3 section 3.3.2.1), it is possible to calculate the corresponding degree of battery discharge for each returning vehicle based on reasonable assumptions of average driving speed and energy consumption. The average driving speed used in this study is 33 mph and is based on the results reported in [4.2] for measurements of urban driving. Calculation of the total energy consumed also requires knowledge of the vehicle performance in terms of the energy consumed per unit time at this average speed. The energy consumption value for a typical urban driving cycle is taken from the BMW i3, which is 0.21 kWh/mile[21], [4.3]. This vehicle has a practical range limit of 90 miles (a 19kWh lithium-ion battery), so that cumulative driving journeys, simulated by the MC model, must be equal to or less than this limit. Longer journeys simulated by the MC model are ignored for recharging calculations. The total energy used E_{drive} for a particular driving journey of duration T_{drive} is calculated as follows:

$$E_{\text{drive}} = T_{\text{drive}} * v_{\text{speed}} * k \tag{4.1}$$

where v_{speed} is the average driving speed (33 mph) and k is the energy consumption (0.21 kWh/mile). For example, if an EV drives for period of time of 10 minutes (1/6 hours), it will consume 1.16 kWh according to these assumptions. Since all re-charging is assumed to start immediately on return to the house, and is assumed to be at a fixed rate until the battery is fully charged, it is straightforward to calculate the charging duration T_{charge} (in hours) from:

[21] Units have been converted from km to miles for the each BMW i3 specifications.

$$T_{\text{charge}} = \frac{E_{\text{drive}}}{P_{charging\_rate} * \eta_{\text{charging}}} \tag{4.2}$$

where $P_{\text{charging\_rate}}$ is the rating of domestic charger, which can be set for either single phase standard charging or fast charging [22], [4.3]. The charging efficiency η_{charging} is assumed to be 0.90, [4.4]. Table 4.1 shows the charging characteristics for standard and fast single phase charging. In the next stage of system impact evaluation, both low and high charging profiles have been considered in order to assess the impact on the substation transformer.

Table 4.1 Domestic charging characteristics for BMW i3.

	Standard charging	**Fast charging**
Charging rate	AC Type 2/ Mode 2 charging/ Up to 2.4kW/10Amps	AC Type 2/ Mode 3 charging/ 7.4kW/32Amps
Time period (h)	< 7 for 0-80% State of Charge	< 3 for 0-80% State of Charge

4.1.3. Impact on Primary Substation

Initially all 1,885 households are considered together so as to examine the additional charging load on the primary substation transformer. Since at this stage we are interested in aggregate charging loads at substations and distribution transformers, there is no need to model the house by house variations in non-EV loads. The worst case scenario of UK winter electricity profiles is used to understanding the impact of EV charging on the distribution network substation loading. In case study 2 to examine the charging impact on LV network flows and voltages, these house by house loads have been modelled. Here the concern is with the aggregate EV charging load and how

[22] The model does not consider 'ramp up' or 'ramp down' charging, and charging rate is constant.

this varies through the day. The power factor is defined as the ratio of true power in kW to apparent power in kVA, [4.5]. It can be measured by a power factor meter, which determines the cosine value of the angle between the voltage and current. Unity power factor has been assumed for this case, therefore all units are presented in kW instead of kVA. Good convergence has been achieved for only 100 trials; this is not unexpected given the large number of independent households modelled in each of the trials. Of the 1,885 households supplied by the primary substation, 10% of these are initially assumed to be EVs. Figure 4.1 gives the calculated additional EV charging load as a function of time of day for a take-up rate of 10%[23]. It is clear that fast charging creates a higher peak load than standard charging; however, the duration of fast charging is shorter than standard charging. As a result, fast charging profile has greater impact overnight under the 'plug and charge' strategy.

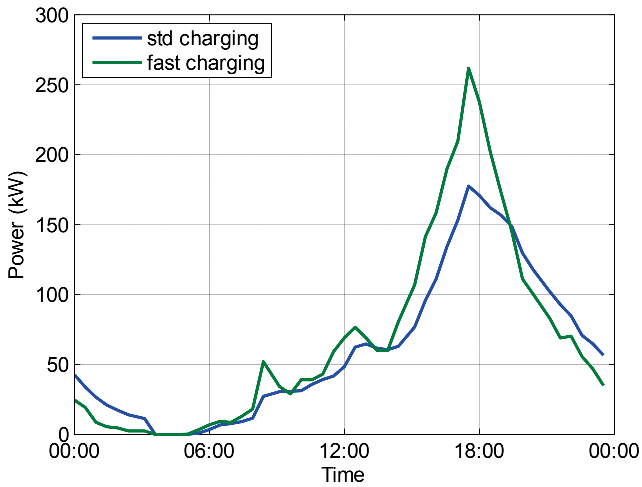

Figure 4.1. 10% EV charging load without base load.

Figure 4.2 shows EV charging (fast charging only) together with a typical UK domestic daily load taken from United Kingdom Energy Research Council (UKERC) winter weekday profile, [4.6], but suitably scaled to the number of

[23] A 10% take-up signifies that one in ten of households owning cars are assumed to have one EV.

houses supplied. The mean load for a single household according to the UKERC profile is 580 Watts; this is close to the figure of 536 Watts available from DUKES for 2009, [4.7]. It should be noted that the load information has a time resolution of 30 minutes, reflecting the UK market arrangements. For comparison purposes only, the 10 minute Monte Carlo results have been averaged up in 30 minute blocks. It is apparent that for this UK example the charging load occurs very much at the time of the existing peak load at 18:00. This is unsurprising but the magnitude of the new peak (increased by 14%) is considerable, even for the modest EV ownership assumed for this case. Figure 4.3 shows the impact of different levels of EV charging on the primary substation loading. It is clear that with higher EV penetration, the peak load of the substation will be considerably increased by as much as three times.

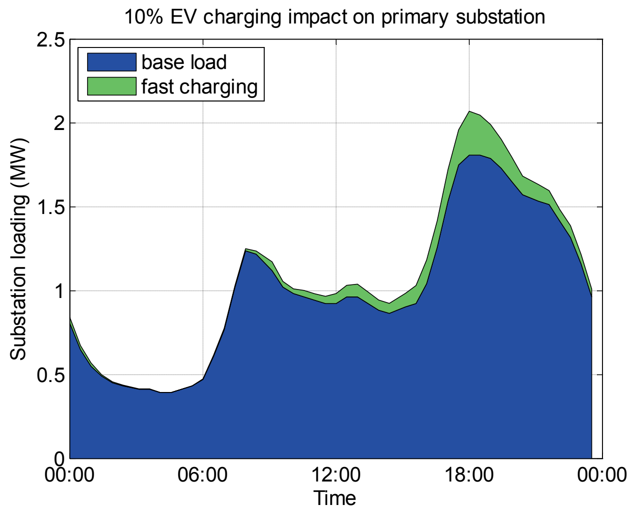

Figure 4.2. 10% EV charging impact on primary substation loading.

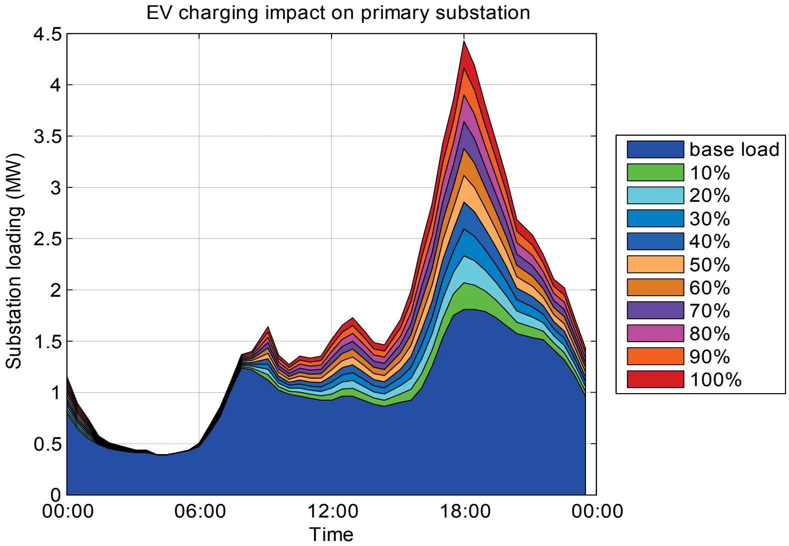

Figure 4.3 EV charging impact on primary substation loading.

4.1.4. Impact on Secondary Substation

As mentioned above, Figure 4.2 was the result of 100 Monte Carlo trials to calculate the additional electricity demand from domestic EVs. Attention is now focused on a single group of 215 houses supplied by a single 300kVA distribution transformer and with an EV take-up, as before, of 10%. With this smaller sample size there is expected to be greater variation between individual simulation trials. As for larger group of houses, the model needs to be re-run until convergence has been achieved. As well as the mean behaviour importantly this will quantify the uncertainties associated with the additional load. Good convergence was achieved with 200 simulation trials[24]; this is more than for 1,885 houses, reflecting the reduced number of houses. A total of 21 EVs was used, consistent with the car ownership statistics already presented. Figure 4.4 shows the mean of 200 EV charging simulation trials (fast charging profiles only) with 95% confidence interval as function of time. [4.8]. The 30 minutes time resolution has been maintained here. The simplest

[24] Sample population of 215 houses has been used in the MC simulation. Therefore, there is total of 43,000 trials (215 houses * 200 trials) performed.

measure of the uncertainty associated with these values is provided by the standard deviation. These have been calculated from the 200 trials, again as a function of time of day.

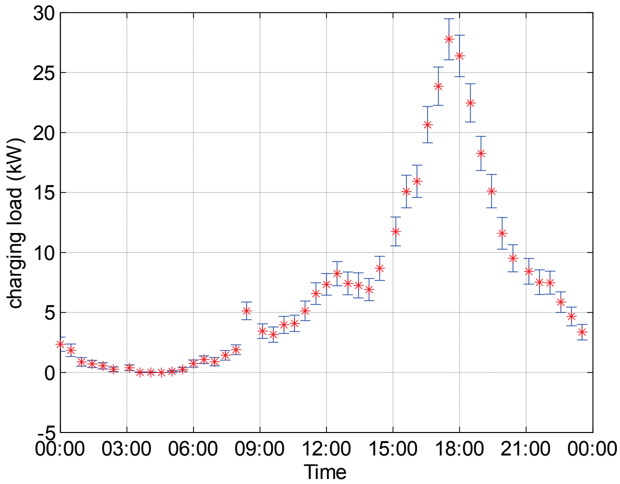

Figure 4.4. Expected mean EV charging with 95% confidence level.

For the sample of 215 houses, the peak mean charging load occurred at 17:30 hours and was 27.8kW, with a standard deviation of 12.3. Assuming as usual that the error distribution is Gaussian, the peak charging load will lie in the range from 26.07kW to 29.49kW with 95% confidence. So to take a simple example, this distribution transformer would need to be sized (for 95% confidence) to be 29.49kW larger than at present to account for this likelihood of additional EV charging load. This is approximately 15% of the existing domestic peak load (197.8kW) and thus not insignificant. However, the worst case scenario is the unexpected high vehicle charging load that was calculated from these 200 MC simulation results. It is shown as the maximum likely vehicle charging impact on the domestic load profile. Figure 4.5 brings together the expected electricity load profile for a typical weekday with the expected mean and maximum value of EV charging from the 200 trials. This shows that the maximum likely EV charging load will cause the domestic peak load to increase from 197.8 kW to 295.8 kW at the relatively low EV penetration of 10%. It is important to reiterate that this is for the simple 'plug and charge' strategy in which the vehicle battery is recharged immediately on return to the home.

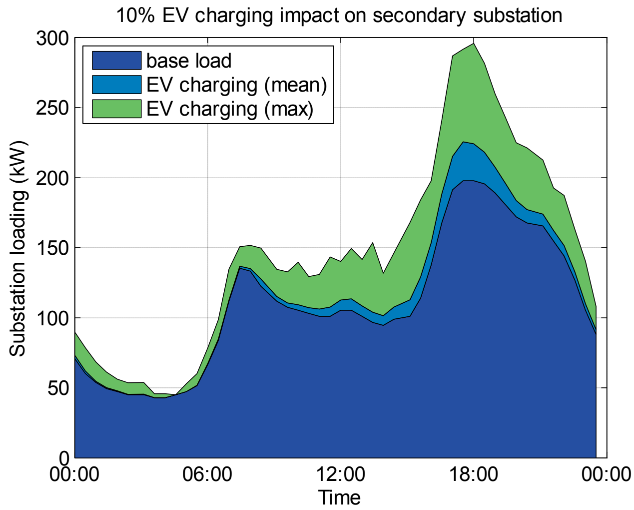

Figure 4.5. 10% EV charging impact on secondary substation.

4.2. Case Study 2: Impact on Low Voltage Network

In order to assess the potential impact of EV charging on power distribution network, especially on 400/230V low voltage (LV) part, a case study has been undertaken for a hypothetical residential community but using real network parameters. This case study illustrates the modelling approach which integrates the Monte Carlo model for household car use with an LV network power flow model. A worst case scenario (UK winter electricity profile) is used to understand the impact of EV charging on the substation feeder loading. Voltage variation due to EV charging has been calculated at the monitored house at the end of single phase service cable. Again, for simplicity, only the simple 'plug and charge' strategy has been considered for the power flow simulation.

4.2.1. Overview Modelling Structure

In this section, the integrated model is explained in detail and the various sub-models developed for the vehicle charging impact assessment. The integrated model consists of the MC household car model, a household electricity model that depends on occupancy, and an LV network model. There are three stages to the analysis: generation of house by house electricity profiles, power flow performance; and analysis of results (as shown in Figure 4.6).

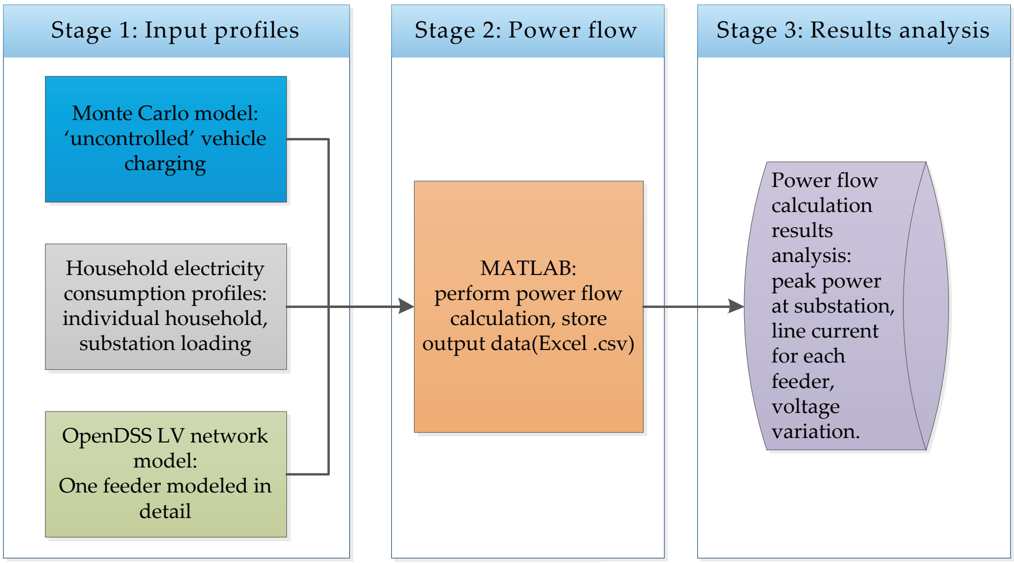

Figure 4.6 Overview modelling structure.

The multiple time increments Monte Carlo model for household car use generates synthetic vehicle charging patterns. Household electricity consumption profiles are created using the CREST model developed by Richardson, which generates individual household electricity load based on active occupancies[25], [4.9]. EV charging load profiles are added on top of the household load profiles in order to create the new household electricity consumption profiles. The LV network model has been structured in Open Distribution System Simulator software (OpenDSS) based on network

[25] The active occupancy has been modified for the consideration of EV use.

parameters for one feeder, including number of households, cable types, length, and thermal limits, [4.10]. Monitoring data was available for peak load, and feeder voltage/current values. To assess the potential impacts of electric vehicle charging on LV network, power flow calculation[26] has been performed based on the penetration level of electric vehicle and household electricity consumption. Both the distribution of the EVs on the network and their charging profiles were generated anew with each run of the simulation. Figure 4.7 shows the detailed programme flow for the study.

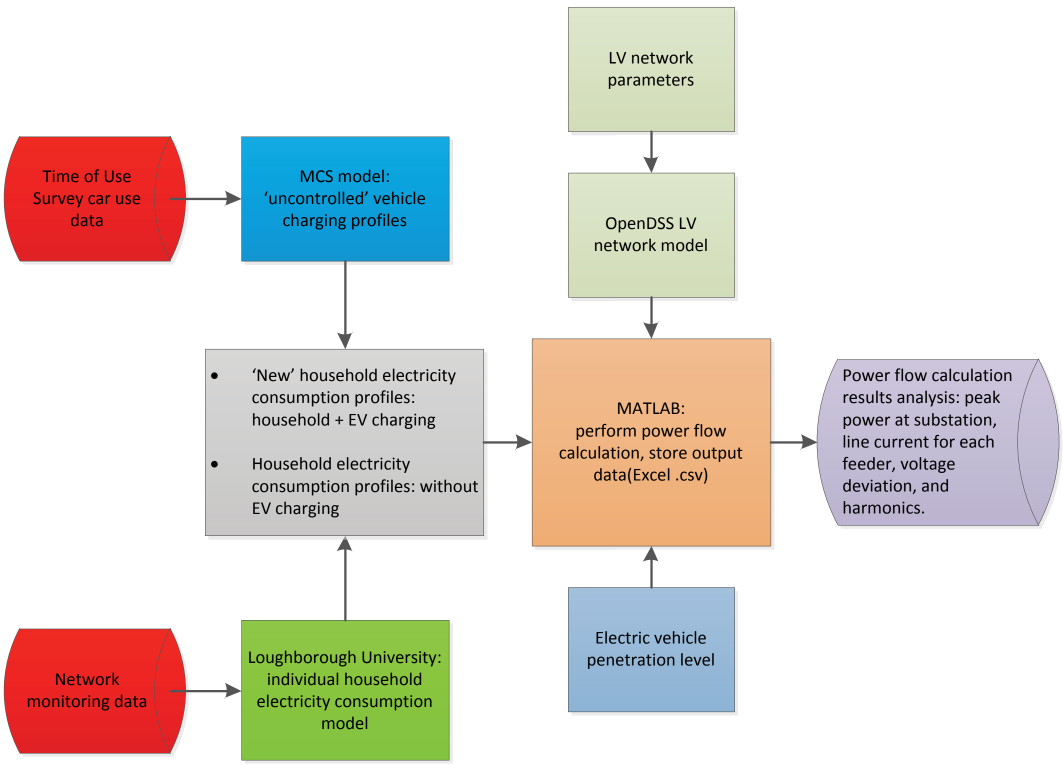

Figure 4.7. Programme flow.

Note that time resolution varies for different models. For example, MC EV charging profiles are in ten minutes resolution because of the format of Time of Use survey data. For household load profiles, the CREST model produces one minute resolution data. When adding EV charging load on top of

[26] The power-flow calculation (sometimes called load flow) is the basic tool for investigating system impact due to system load or generation variation.

household load, EV charging load has been converted into one minute basis data as same resolution as the CREST model outputs. Therefore, 'new' household electricity load profiles are in one minute resolution.

4.2.2. Simulation Software

The Open Distribution System Simulator (OpenDSS) is a comprehensive electrical system simulation tool for electric utility distribution systems. It is an open source developed by the Electric Power Research Institute, [4.10]. The basic user interface is a text scripting standalone user interface which is sufficient for most of the analysis. The COM interface can be used to design and execute custom solution modes and features of the simulator from any third party analysis programs such as MATLAB, VBA, and Python.

4.2.3. Distribution Power Flow Algorithm

As the design of distribution system in UK, the system commonly serves unequal single phase loads; hence the loading of the system becomes inherently unbalanced. The non-equilateral conductor spacing introduces an additional unbalance for three-phase overhead and underground cable segments. The cable in a distribution network have higher (R/X) ratios. Therefore, the conventional power flow or short circuit methods are not adequate for the radial characteristics of the distribution system; additionally these methods display poor convergence characteristics, [4.11]. The non-linear and iterative methods for load flow algorithm have been developed and employed [4.12] and [4.13]. It is imperative that the distribution feeder is modelled as accurately to perform accurate power-flow and short-circuit studies by utilizing the three-phase models of the major components.

4.2.4. Low Voltage Distribution Network Modelling

The residential network data was provided by Scottish Power, comprising one 33/11kV 7.5 MVA primary substation transformer, and six 11kV secondary substation transformers with a mix of 300kVA and 500kVA capacities. All associated LV (400/230 V) networks, providing power to some 1,554 connected customers, has been used as a guide to a distribution system supplying predominantly domestic housing. On average, each distribution transformer in this system supplies 259 houses. One substation (11kV/400V 300kVA transformer) supplying 215 households with five feeders has been modelled with one feeder for 42 households modelled in detail, while the remaining four feeders represented as lumped loads. For low voltage network modelling, many factors must be determined including transformer settings, cable parameters, and household phase connections. This information has been obtained from the low voltage network data for cable parameters and the phase allocation of the individual houses, supplied in a geographic information system (GIS) data (see Appendix B). Table 4.2 lists the modelled LV network feeder parameters.

Table 4.2 Number of premises supported by LV network feeder.

Premises	**43**
3-phase cable (m)	171
Single phase cable (m)	396

4.2.4.1. *Substation Transformer*

The modelled 11/0.4kV 300kVA secondary distribution transformer supplies five LV feeders with the impedance percentage of 4.75%. The transformer tap changer is adapted from [4.14]. Taps should be able to step from -5% to +5% in 1.25% intervals, and it is an off-load tap changer[27].

4.2.4.2. *Low Voltage Cables*

The network uses of two types of cables; one is the main 3-phase cable, and second type is the service single phase cable, [4.15]. Details of cable parameters are listed in Table 4.3.

Table 4.3 LV network cable parameters.

Cable	Type	Rphase (Ohm/km)	Xphase (Ohm/km)
3 phase cable	95mm AL	0.379	0.069
Single phase Mural cable	0.0225in Cu	1.477	0.0865

4.2.4.3. *Network Voltage Limits*

Distribution network operators are obliged to supply their customers at a voltage within specified limits. In the UK, these limits are +10% and -6% from the nominal single phase voltage of 230V, according to the Electricity Safety, Quality and Continuity Regulations [4.16].

4.2.4.4. *Phase Information*

The service cables stored in the DNO's current GIS database are often assumed, and even where they are not there is no information to indicate what phase single-phase cables or consumers are on. Thus a phase allocation strategy is required as the load flow calculations are carried out on a phase by phase basis

[27] A tap changer is a connection point selection mechanism along a power transformer winding that allows a variable number of turns to be selected in discrete steps. A transformer with a variable turns ratio is produced, enabling stepped voltage regulation of the output. The tap selection may be made via only manual tap changer mechanism.

and this follows, [4.17]. From the available monitoring data[28], the phase allocation for each household has been defined (see Appendix B for more details). The household phase information is shown as a single line diagram in Figure 4.8. The red line, Phase A, supplies 13 premises, the yellow line, Phase B, is connected to 19 premises, and the blue line, Phase C, is connected to 12 premises. This modelled feeder is clearly unbalanced.

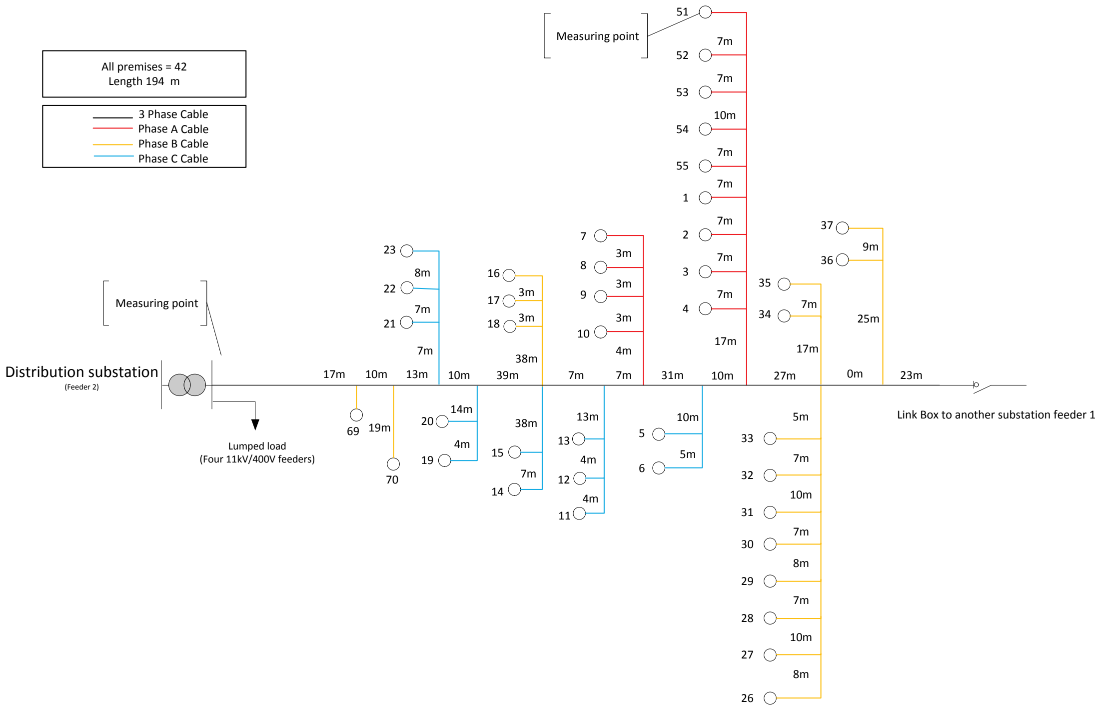

Figure 4.8 The single-line diagram of the modelled feeder.

4.2.5. Household Electricity Load Modelling

For the modelled feeder, individual household electricity load is generated by the CREST model. The other feeders use the UKERC winter load profile as in section 4.1.3. The CREST model is an open source tool that generates individual household daily electricity consumption and it allows user to set the model input parameters (e.g. number of people, day of week, month of the

[28] There are two sets of monitoring data provided by Scottish Power. One set is for one feeder measured at the substation, and the other is measured at the specific household/premise. Both sets provide information on phase voltage values.

year). The model is based on daily active occupancies[29] within the household that extracted from the United Kingdom Time of Use Survey 2000. In the Chapter 3 section 3.3.2.3, the multiple time increments MC model simulates household daily car use patterns, such as car departure, car arrival, car driving period, etc. As stated in the TUS technical report, a driving activity is defined when the person drives the car as the main driver. Therefore, when the car departs from home or arrives back home, it also indicates that a person sets off or returns home at that specific time. These changes of personal location results changes of active occupancies within the house as shown in Figure 4.9 and changes in household electricity use. Consequently, the household electricity profile generated by the CREST model is adapted to reflect the changes of active occupancies associated with the car use.

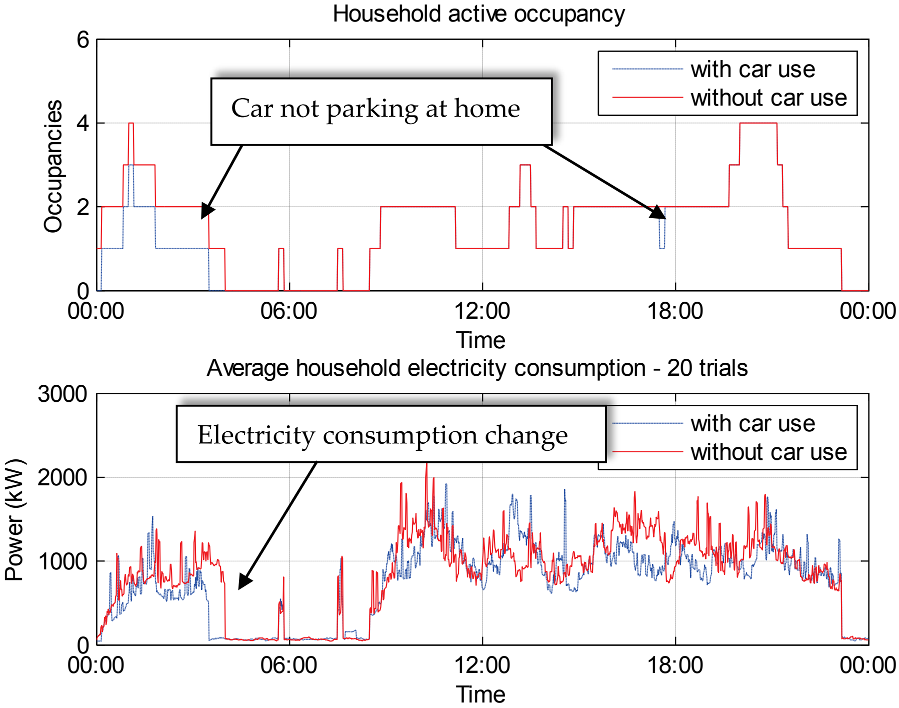

Figure 4.9 Household active occupancies and electricity consumption change due to car use.

[29] "active occupancy" (that is, when occupants are within a dwelling and not asleep).

The person's driving activity can consequently affect the household electricity consumption, although most researchers neglect this, for example [4.18] - [4.20]. In [4.21], a household electricity model takes into account the vehicle use, which is structured based on active residential patterns. The integration of the Monte Carlo model with CREST electricity model in this way can more accurately predict household electricity consumption in the context of vehicle use. This modified CREST model should enable DNOs to improve their existing household After Diversity Maximum Demand (ADMD) profiles when considering domestic EV take-up in the future. However, there are other approaches to establish a household electricity model by using smart meter data. In [4.22] to [4.24], researchers identify that the household electricity consumption has behavioural patterns and less diversity than expected. The CREST model is one approach to generate household electricity consumption profiles. Appendix C explains in more detail the process of integrating MC model with the CREST model.

Individual housing occupancy is available from the Census data as shown in Figure 4.10. In this particular area, the largest group of housing is for two people (31%), followed by equal proportions of three and four people households (19% each). Five and six people households share a total 14%, and one person household accounts for the rest 17%. Note that a two people household could mean one adult and one child. The CREST model only requires number of residents in the house; therefore, the housing occupancy statistics from Census data has been directly used to generate household electricity load.

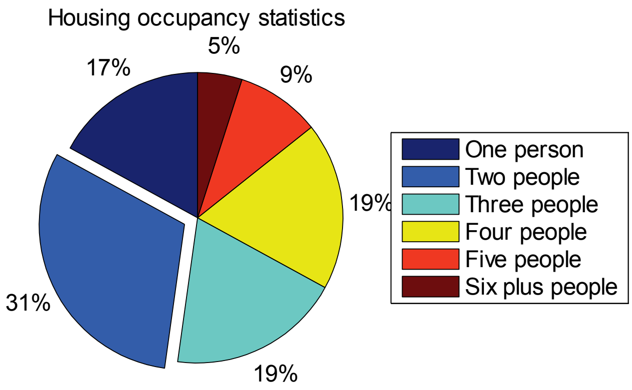

Figure 4.10 Housing occupancy for modelled feeder.

For the modelled feeder, car ownership has been calculated by the MC model described in Chapter 3 section 3.3.1. As the outcome of the MC simulation, there are 13 households without cars, as shown in Table 4.4. Households are restricted to at most one EV. The maximum penetration of EV in the system is 29 and only fast charging is considered. The EV charging demand is calculated as described in section 4.1.2.

Table 4.4 Car ownership for 42 households.

Cars	Households
0	13
1	19
2	8
3+	2

Figure 4.11 shows an example of a single 3 people household in January with and without EV fast charging load. The existing peak load of this particular household is 11.66kW and occurred at 07:26 without EV fast charging. After adding EV charging on top of the household load, there is an additional peak load (11.65kW) occurring at 19:59.

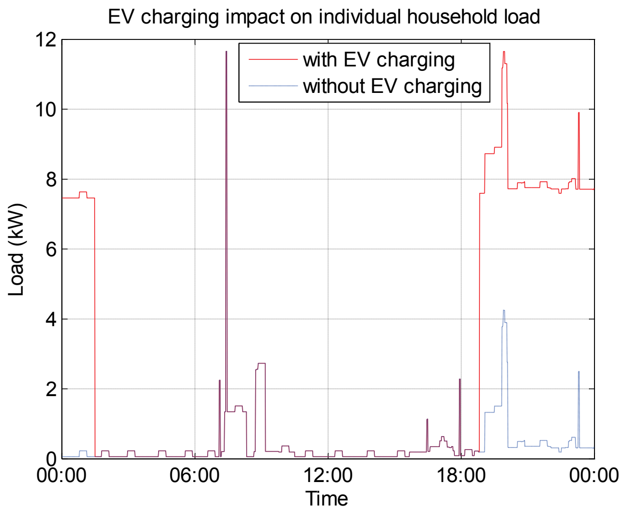

Figure 4.11 EV charging impact on single household loading.

4.2.6. Impact Assessment

In order to assess the 32A EV charging impact on the LV system, 24 hours household load profiles generated in section 4.2.5 have been assigned to the modelled feeder. Penetration of EVs in the system has been assumed from 0% to 100% with 10% increments. Initial power flow has been performed without any EV charging in order to setup the initial system status. This LV network looks at the feeder loading at the substation and the voltage levels at the monitored household as shown in Figure 4.8. The analysed results are for 462 runs (42 houses * 11 levels of EV penetration) as one run for one level of EV penetration, for each one minute time step of a week day (24 hours period), including maximum, minimum and average substation power; maximum, average and minimum voltages, minimum load voltages for those loads that were monitored, and maximum line currents for those lines that were monitored. In the following subsections, vehicle charging impact on substation feeder loading and voltage variation at the monitored household are analysed and discussed in details.

4.2.6.1. *Feeder Loading*

The load profiles for the feeder with increasing EV penetration level are shown in Figure 4.12. The peak load at the feeder of 90.4 kVA occurs at 19:00 when EV penetration level reaches 100%. There is also a local peak occurring just prior to 12:00 that results from a specific EV that starts charging at a household at that time (see Appendix D). It is known that the feeder rating is 60kVA. The simple 'plug and charge' strategy increases the peak load and exceeds the existing feeder rating with only a 30% of EV penetration for 32A charging, as shown in Figure 4.13. Note that the peak load calculated from power flow results is the highest value throughout the 24 hours period. For such a small group of households, the range of times when EVs start charging will be large. As a consequence, the peak load remains the same for 10 per cent and 20 per cent EV penetration levels (see Appendix D). Therefore, this particular LV feeder can cope with a maximum of 20% EV penetration (e.g. 6 households with an EV). More details of the feeder loading results can be found in Appendix D.

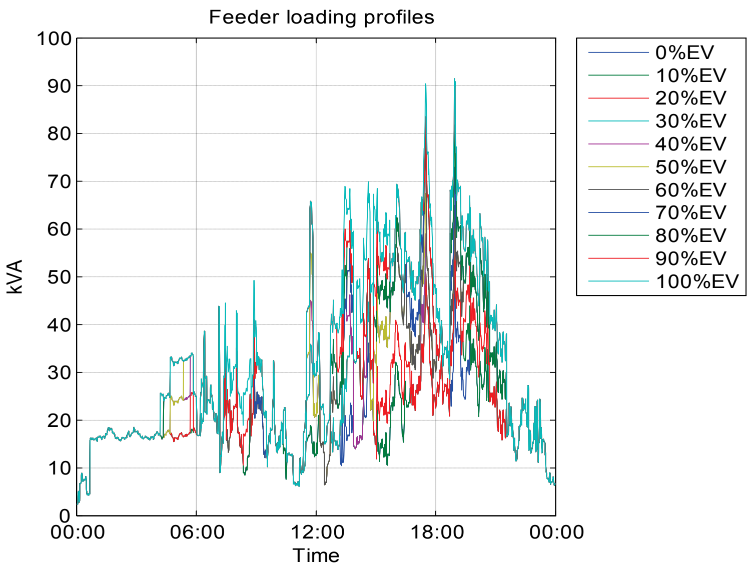

Figure 4.12 Feeder loading profiles for EV penetration from 0% to 100%.

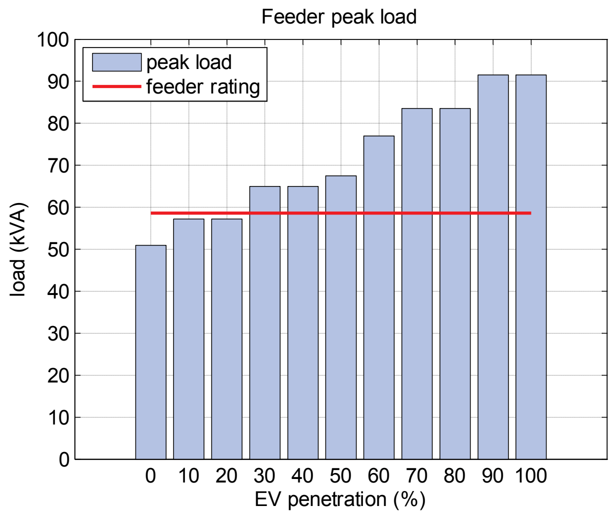

Figure 4.13 Peak load exceeds feeder rating as 30% EV penetration.

4.2.6.2. *Voltage Profiles at House 51*

The voltages at House 51, found at the end of a service cable supplying 9 households (see Figure 4.8), were monitored for each level of EV penetration. Figure 4.14 illustrates the voltage profiles of House 51 for increasing levels of EV penetration. It is seen that the voltage profiles at House 51 dipped significantly between 12:00 and 22:00 while EV penetration level increases. More details of the House 51 voltage results can be found in Appendix D.

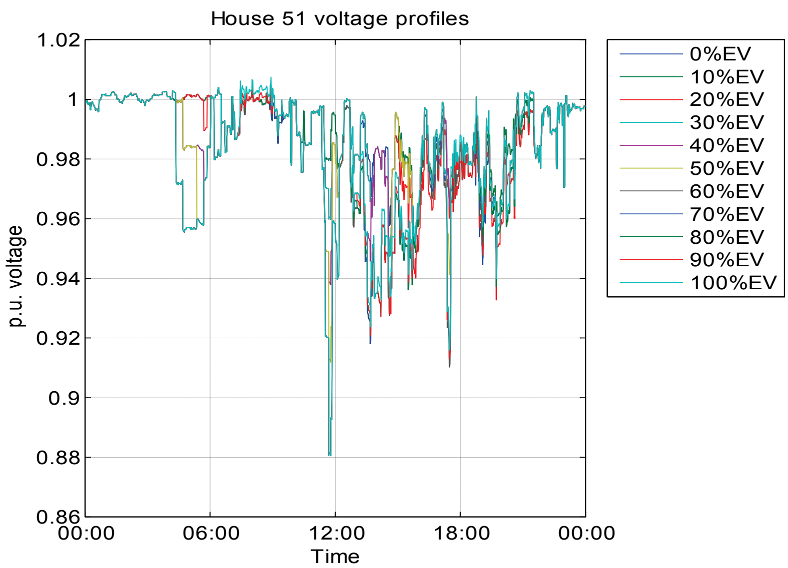

Figure 4.14 House 51 voltage profiles for EV penetration from 0% to 100%.

The lowest voltage at House 51 is 0.88 p.u., which is well below the network voltage limits (0.94 p.u.), as shown in Figure 4.15. It is obvious that House 51 suffers from a relatively low voltage level even with no EVs in the system due to its location at the end of a long service cable. When EV penetration level reaches 20%, the voltage dips below the network limits. Voltage continues dropping as EV penetration levels increase. This is due to households located up-stream of House 51 having EV charging. When EV penetration level reaches 60%, House 51 is assigned an EV. As a result, all the households on Phase A (red line in Figure 4.8) have EV charging activity during the 24-hour period, and as a result the voltage value dips to 0.88 p.u. Voltage value at House 51 remain the same while EV penetration level down-stream of House 51 increase from 60% to 100% (Phase B yellow line in Figure 4.8). Because of this peculiarity, a 20% EV penetration results in an unacceptable voltage at House 51. Thus from the standpoint of voltage, the highest allowable EV penetration is 10%.

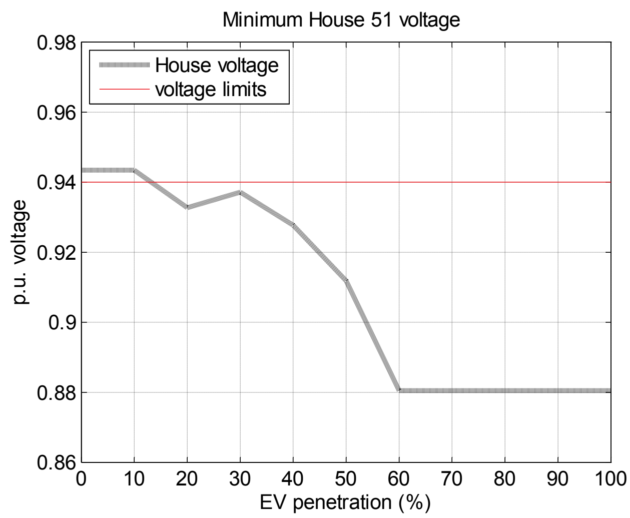

Figure 4.15. Minimum House 51 voltage profiles.

4.3. Discussion and Summary

In this chapter, two case studies have been presented in order to assess the impact on electric vehicle charging on typical parts of the UK distribution network. In case study 1, the impact on primary and secondary substation transformers has been assessed for a residential area. The return time dependent Monte Carlo methodology has been used to model EV charging loads. This approach makes use of two statistical characteristics of domestic car use: the probabilities of cars returning home (as a function of time of day) and the distribution of driving time whist away from the home. This simplification is appropriate when, as in this analysis, the assumption is that charging takes place only at home. Winter weekday household load profiles from the UKERC have been be used with residential Census data to provide representative substation and distribution system loads so that the potential impacts on the distribution network of different penetrations of EVs could be investigated. As the key outcome of the impact analysis, even a modest 10% EV take-up can results in a considerable increase in peak load at primary substation transformers. Again, the simple 'plug and charge' strategy has been applied. For the secondary substation transformer, mean EV charging increased the existing peak load by 15%; with possible peaks up 48%. For higher EV penetrations, charging impact on the substation loading significantly increases the peak load as much as three times. Thus appropriate charging strategy need to be implemented as EV developed in a residential area.

In case study 2, EV charging impacts on the LV network have been assessed on a section of real distribution network as provided by Scottish Power. There are some challenges in modelling the substation feeder accurately. One of the most difficult tasks is to acquire all the necessary network data, such as transformer capacity, cable type, length, household phase allocation. Feeder GIS maps provides most of the needed network data. Distribution network modelling tool, OpenDSS, provides the capability of performing power flow analysis via MATLAB. Individual household load on the distribution system are created by CREST model with the consideration of household occupancy change due to car use. The main advantage of integrating the multiple time increments MC model with the CREST model is to produce a more realistic household electricity consumption profile when considering EV charging. The power flow calculation results show that for the modelled secondary substation feeder, 32A fast charging undoubtedly increases the existing peak load. The feeder rating was found to allow up to 20% EV deployment. Voltage profiles at one particular house at the end of a service cable has been investigated for EV penetration level varying from 0% to 100%. Due to the configuration of the LV network, this house suffers relatively low voltage when no EV. Power flow calculation showed that for this house, the minimum voltage drops below the UK LV network standard when EV penetration level exceeds 10%. This indicates that voltage limit violation at an individual house occurs before the substation feeder reaches its thermal rating. Applications of the power flow results shows that distribution transformers, and also of course the associated distribution lines, will need substantial upgrading if any significant use of EVs develops. This LV network load flow model provides a useful tool for DNOs to gain a better understand of the potential EV charging impact so that appropriate demand side management scheme needs to be implemented.

4.4. References

[4.1] Office of National Statistics (2001). Census: Standard Area Statistics (England and Wales). Available: http://www.ons.gov.uk/ons/rel/census/census-2001-key-statistics/urban-areas-in-england-and-wales/index.html

[4.2] Department for Transport (DfT), Transport Statistics: Great Britain - 2009 Edition 35th Edition ed.: TSO (The Stationery Office), 2009.

[4.3] BMW i3 technical data, available: http://www.bmw.co.uk/en_GB/new-vehicles/bmw-i/i3/2013/technicaldata.html accessed on 14.04.2014.

[4.4] Taylor, J. and Maitra, A., "Evaluation of the impact of plug-in electric vehicle loading on distribution system operations," in Power & Energy Society General Meeting, 2009. PES '09. IEEE, 2009, pp. 1-6.

[4.5] J. Duncan Glover, *et al*., "Chapter 2 Fundamentals" in *Power System Analysis and Design*, 4th international student ed. Canada: Thomson Learning, 2008, ch. 2, sec. 2.2, pp.47.

[4.6] UK Energy Research Centre (UKERC), Energy Data Centre, "Electricity user load profiles by profile class", [Online]: Available at: http://data.ukedc.rl.ac.uk/cgi-bin/dataset_catalogue/view.cgi.py?id=6, [Accessed 26 September 2011].

[4.7] BERR, DUKES 2009, available online at: http://www.decc.gov.uk/en/content/cms/statistics/publications/dukes/dukes.aspx

[4.8] W. L. Winston and J. B. Goldberg, Chapter 21 – Simulation, *Operations research: applications and algorithms*: Thomson Brooks/Cole, 2004.

[4.9] I. Richardson, "Integrated high-resolution modelling of domestic electricity demand and low voltage electricity distribution networks," PhD A doctoral thesis, School of Electronic, Electrical and Systems

Engineering, University of Loughborough, Leics, UK, LE11 3TU, 2011.

[4.10] Open DSS Manual, Electric Power Research Institute, July 2010. Available: http://sourceforge.net/projects/electricdss/

[4.11] Zimmerman R.D. *Comprehensive distribution power flow: modelling, formulation, solution algorithms and analysis*. PhD thesis. Cornell University; 1995.

[4.12] Khushalani, S., Schulz, N., N., "Unbalanced distribution power flow with distributed generation," *Proceedings of the IEEE Transmission and Distribution Conference*, Dallas, TX, May 2006.

[4.13] Vaidyanath R. *Modeling of utility distribution feeder in OpenDSS with Steady State Impact Analysis of Distributed Generation*. PhD thesis. West Virginia University; 2011.

[4.14] S. Huang, et al, *Battery Electric Vehicle Academic Study Report*, internal tech. report, University of Strathclyde, 2014.

[4.15] Scottish Power. (April 2012) *ScottishPower Distribution Cables & Equipment Metal Theft*. Available: http://www.spenergynetworks.co.uk/userfiles/file/ScottishPower_cables_equipment_metal_theft.pdf

[4.16] Department of Trade and Industry (DTI), "The electricity safety, quality and continuity regulations", Stationary Office, October 2002, London, UK.

[4.17] Steels, A., MacLeman, D., *LCNF Tier 1 Close Down Report – Low voltage Network Modelling and Analysis Environment*, Scottish and Southern Energy, Project ref. SSEPDT1005.

[4.18] Grahn, P. (2013) *Electric Vehicle Charging Impact on Load Profile*. PhD Thesis. Royal Institute of Technology, Sweden.

[4.19] Papadopoulos, P. (2012) Integration of Electric Vehicles into Distribution Networks. PhD thesis. University of Cardiff.

[4.20] Paevere, P., Higgins, A., Ren, Z., Grozev, G., Horn, M., McNamara, C., Khoo, Y-B., and Elgindy, T., *Spatial Modelling of Electric Vehicle Charging Demand and Impacts on Peak Household Electrical Load in Victoria, Australia*. Australian Commonwealth Scientific and Industrial Research Organisation (CSIRO) June 2012.

[4.21] P. Grahn, J. Munkhammar, J. Widen, K. Alvehag, and L. Soder, "PHEV Home-Charging Model Based on Residential Activity Patterns," *Power Systems, IEEE Transactions on,* vol. 28, pp. 2507-2515, 2013.

[4.22] S. Haben, M. Rowe, D. V. Greetham, P. Grindrod, W. Holderbaum, B. Potter, *et al.*, "Mathematical solutions for electricity networks in a low carbon future," in *Electricity Distribution (CIRED 2013), 22nd International Conference and Exhibition on*, 2013, pp. 1-4.

[4.23] B. Stephen, A. J. Mutanen, S. Galloway, G. Burt, and P. Jarventausta, "Enhanced Load Profiling for Residential Network Customers," *Power Delivery, IEEE Transactions on,* vol. 29, pp. 88-96, 2014.

[4.24] B. Stephen and S. J. Galloway, "Domestic Load Characterization Through Smart Meter Advance Stratification," *Smart Grid, IEEE Transactions on,* vol. 3, pp. 1571-1572, 2012.

5.Chapter 5: Demand Side Management for Electric Vehicle Charging

With wider deployment of the plug-in electric vehicle, a power distribution network operator would expect increasing domestic demand due to large numbers of vehicles charging. This could lead potentially to overloading of power system assets unless appropriate demand side management is in place. In this chapter, several improved charging strategies, utilising forms of demand side management, are presented that can significantly ameliorate the demands on the power system and in particular utilise surplus wind generation in the distribution system. Such proposed charging approaches have far less impact on the distribution system, indeed it is shown in the chapter that such DSM strategies are capable of smoothing the domestic load profile at key points in the distribution system thus facilitating an improvement in distribution system operation, and also operation of the power system as a whole. Additionally, the potential of utilising electric vehicles to absorb renewable generation has been investigated considering constraints on car parking period. Wind generation has been selected for demonstration purposes, and the developed charging algorithm can also be applied to absorb other types of renewable generation, such as photovoltaic, wave and tidal generation.

5.1. Opportunities for Electric Vehicle to Participating in Future Smart Grid

By the year 2020 the Department of Energy and Climate Change (DECC) has forecast that smart meters will be installed in every house in the UK enabled by a £500 million incentive plan created by Ofgem, the UK electricity and gas market regulator, to support smart grid trials carried out by DNOs, [5.1]. Mass rollout of smart meters will be the foundation of future smart grid networks and the anticipated outcomes are benefits for both energy consumers as well as DNOs. In the context of smart grid, privately owned electric vehicles have opportunities to participate as responsive demand; or even distributed energy resources with the help of bi-directional power flow, known as vehicle-to-grid (V2G). V2G technology represents a means by which power generation capacity available from parked EVs can be used to supply electricity to the power grid, [5.2]. In technical terms, there are no barriers to V2G technology. For each electric vehicle, three elements are required: a connection to the grid for electrical energy flow; suitable communication with the power network operator (perhaps via real time price signals), power flow controls and metering either off or on-board the vehicle. In the early stages of V2G implementation, systems are expected to focus on power delivery of time-critical power market services due to the associated high value/rewards. In effect, such V2G technology makes available bi-directional energy storage that can be used to ease the integration of wind energy. V2G implementation is of value only if the appropriate match occurs between electric vehicle availability and times of high electricity cost within the power market, [5.3]. There is a cost associated with V2G resulting from the increased cycling of the battery and consequent reduced lifetime, but this cost is expected to be more than covered by the high value of electricity at peak times. Simple using the batteries as responsive load (i.e. no discharging for power generation purposes) is not anticipated to reduce the battery lifetime.

Several studies have been published on vehicle charging strategies developed to meet system constraints, reduce EV charging costs, or help absorb renewable generation in the distribution system, [5.4]. In paper [5.5], load scheduling and dispatch for vehicle charging are adjusted to reduce EV charging costs based on an electricity price signal. Deilami *et al.*, [5.6], proposed a novel load management solution for coordinating the charging of EV fleets. By identifying three prioritised time zones, vehicle charging can be shifted to times of day with less intensive system loading in order to manage system distribution system constraints and reduce costs. However, this modelling approach has the weakness of using fixed and generalised household demand profiles; therefore, the change of the household demand profiles would lead to different prioritised time zones for vehicle charging. There is also a growing interest in using the EV batteries as an alternative energy source of generation to help meet peak demands. This is often referred to as Vehicle to Grid, or V2G for short; see for example references [5.7] to [5.13]. It would be possible to apply the model developed here to V2G applications and this is currently being considered for future research alongside investigation of more sophisticated demand side management opportunities associated with vehicle battery charging than are examined here.

5.2. Cast Study 1: Electric Vehicle Charging Strategies at Substation Level

In order to reduce the adverse impact of vehicle charging on the peak load at the primary distribution transformer, it is expected that some sort of charging control or demand side management (DSM) of charging will be applied, [5.5] and [5.6]. A simple 'plug and charge' strategy has been developed and applied to vehicle charging in order to assess the impact on the substation loading profiles (see Chapter 4 section 4.1.3). The assessment shows that this simple charging strategy increases the existing domestic peak load and therefore improved charging control strategies need to be developed and applied to mitigate the impacts. The first charging strategy allows users to charge their vehicles as soon as they arrive home, but only at the standard charging rate during defined 'peak' domestic load period of 4pm to 8pm with high charging only allowed during 'off-peak' period from9pm to 3am. As shown in Figure 5.1, the peak demand of domestic plus EV profile is reduced by 4.21% and 11.41% compared with uncontrolled vehicle charging with low and high rate charging respectively.

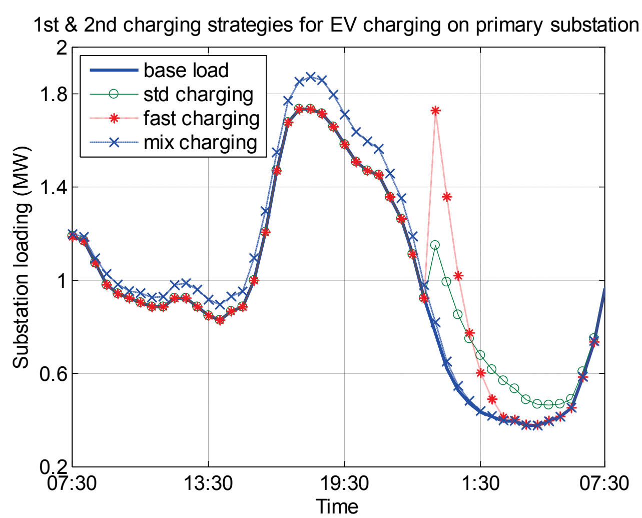

Figure 5.1. 1st and 2nd DSM schemes for managing vehicle charging.

The second method investigated is simply to delay all vehicles charging until a designated time. This was selected as 11:30 pm, since the conventional domestic load is generally low at this time of night. It is also the time used in an EV user trial undertaken by the Ultra Low Carbon Vehicle project, [5.14]. In this scenario all EVs start charging from 11:30 pm with low or high charging rates as appropriate. As would be expected, this approach creates a new peak load due to fast vehicle charging, as illustrated in Figure 5.1. Although this new peak occurs at a period of otherwise low demand, its magnitude even with only a 10% EV penetration is unacceptable in the case of fast charging since the total load then exceeds the previous peak value. In contrast, using the standard charging rates (see Chapter 4 section 4.1.2), vehicle charging has been spread out over a longer period peak load value. These simplified charge regimes do not entirely solve the problem of accommodating EV charging loads as the penetration level of EVs increases. For this reason, a progressive 'smarter' technique has been introduced to smooth out the impact of vehicle charging. The approach is to delay a proportion of vehicle charging by a random time subsequent to 11:30 pm. The delay period is determined by sampling from a truncated Gaussian distribution as illustrated in Figure 5.2. The delay period is between 0 and 7 hours. Before the EV charging starts at mid-night, a random time delay has been sampled from this truncated Gaussian distribution, and then assigned to the charging activity. For instance, the random time delay, sampled from the distribution, equals to 3 hours (180 minutes); thus, the EV charging will start at 3am instead of mid-night.

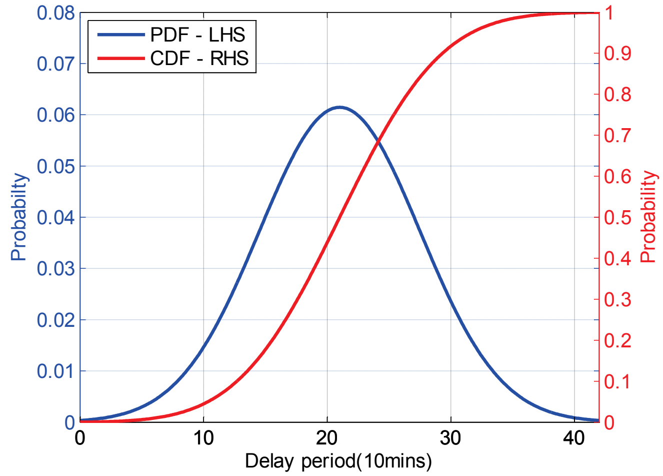

Figure 5.2. The Gaussian distribution of delay period.

This approach effectively solves the problem of creating a new night-time peak load due to EV charging, even with the high charging rate, as illustrated in Figure 5.3 below. With the standard rate charging, the resulting profile has a higher morning peak than the domestic demand profile without vehicle charging. It is also seen from the figure that the 'new' morning peak load is relatively lower than the evening peak load; therefore, this 'Smarter' charging strategy has effectively resolved the uncertainty issue of increasing peak load due to EV charging.

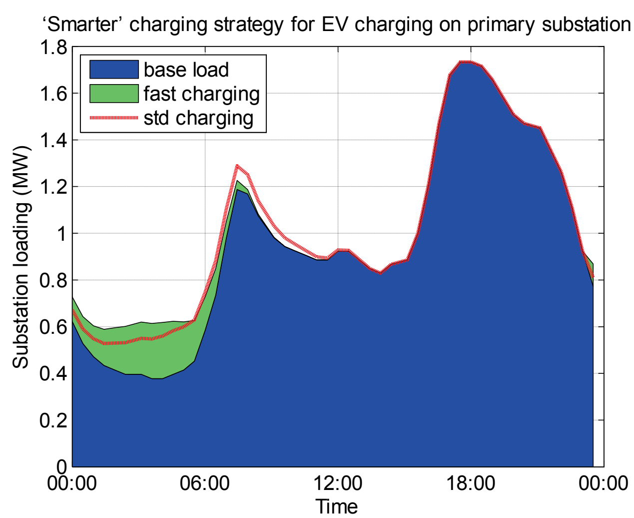

Figure 5.3. 'Smarter' charging strategy for EV charging on primary substation.

5.3. Case Study 2: Electric Vehicle as Responsive Load to Absorb Surplus Wind Generation in Power Distribution System

In this section, the potential opportunities are presented from using domestic owned electric vehicles to support the operation of regional power distribution networks in the context of a high penetration of wind generation. Unlike photovoltaic modules can only produce electricity during daytime, wind turbines can generate electricity whenever the wind is available. The main charging location in this research is assumed to be in the residential neighbourhood; therefore, it is reasonable to explore the potential of utilising EV to absorb surplus wind generation in the system. In [5.4], Bashash et al discuss how a sliding mode control strategy for grid-connected vehicles was designed to be robust to uncertainties in renewable energy generation. Vlachogiannis presented a new formulation and solution of probabilistic constrained load flow problems, which includes renewable generation, in [5.15]. Results of the load flow calculation established the first benchmark for the optimal integration of wind power generation with EV integration into the power systems, which is considered within this section. In the following section, wind power profiles are presented and a proposed smart charging strategy for these EVs is illustrated. A specific aim of this strategy is to shift the timing of EV charging in order to absorb the excessive wind generation in the power system and also to minimise the charging cost for the EV owners' perspective. The penetration level of wind generation has been assumed to be 15% for a typical day in April for illustration purposes.

The wind farm data has been taken from an operational Scottish Power owned site consisting of 26 Bonus 600kW stall regulated turbines producing a total installed (rated) capacity of approximately 15MW [5.16]. The instantaneous penetration of the wind generation in the system has been scaled down to represent approximately 2.3MW of locally installed wind capacity. Figure 5.4 shows the wind generation profiles obtained from April 2005. Most of the turbines produced electricity in one day of April during daytime and the total energy produced is 33.92MWh.

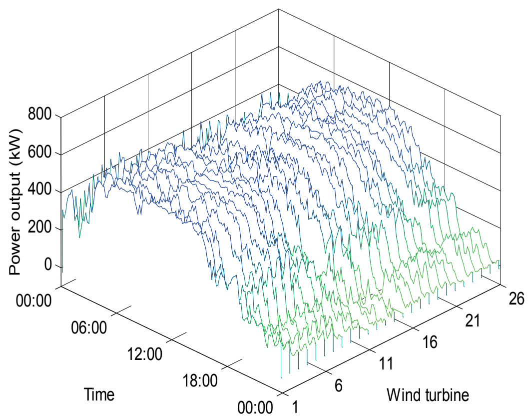

(a)

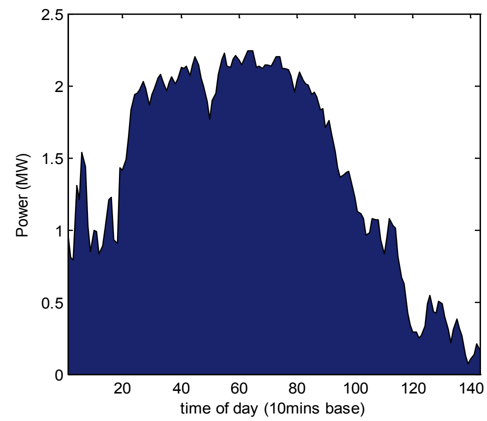

(b)

Figure 5.4. Wind farm turbines output power for one day in April. (a) individual wind turbine power generation; (b) local wind power output.

It has been assumed that there is significant local wind penetration (2.3 MW), so that not all this power is absorbed locally by domestic load, or can be exported due to network constraints. Thus at times of high surplus the local electricity cost will be driven towards zero. It is assumed that a local electricity price signal is available to EV owners and that they individually seek to minimise the their EV charging costs consistent with their daily EV use pattern, and in particular the time parked at home when charging can take place. It is assumed that the EV owners have been informed about the surplus wind tariffs for the day ahead and the power output from this wind farm is forecast perfectly for the day ahead. The actual wind farm power output is used to calculate the surplus wind generation in the system, although there are established methodologies to predict wind farm power output, such as in [5.17]. Note that the emphasis of the developed algorithm is on the framework rather than the accuracy of the wind forecasting; therefore the assumption of perfect wind forecasting is not an issue. As EV charging scheduling depends on surplus wind generation forecast, and wind forecasts are inherently uncertain, it is crucial to consider the level of confidence of the forecast wind generation, [5.18]. The wind power surplus has been calculated by deducting the local (non-EV) domestic load for 1,885 households. The EV charging profiles have been presented in Chapter 4 section 4.1.3. The objective of the system as a whole is to enable, as far as possible, for the aggregated electric vehicle charging demand to track the desired wind power surplus trajectory, in this case the measured wind power generation.

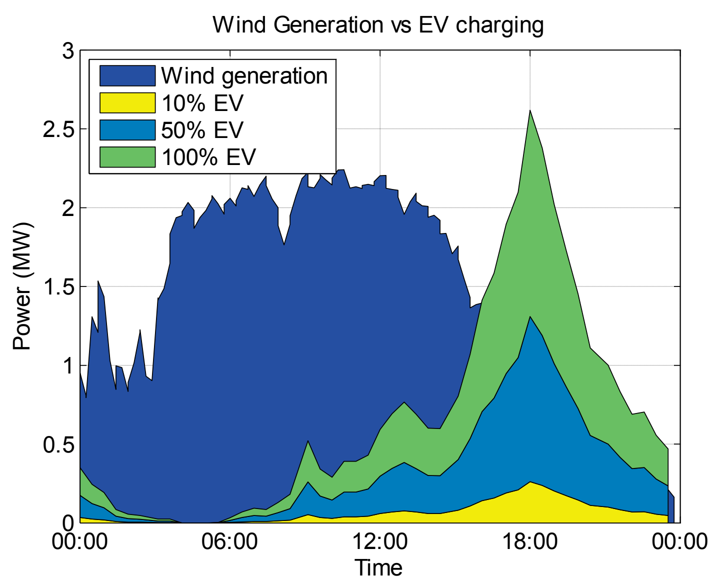

Figure 5.5. The time difference between EV charging and wind generation.

Figure 5.5 shows the vehicle charging demand profiles simulated from the MCS model with 10%, 50% and 100% penetration levels[30]. The amounts of energy required for charging these EVs are 1.26MWh, 6.27MWh and 12.56MWh for the three penetrations respectively. The amount of wind generation in the system is sufficient to charge these EVs; however, the time difference between the high wind power and electric vehicle charging peaks are the biggest challenges for distribution network operator as illustrated in Figure 5.5. However, electric vehicle users can change their recharging behaviour as long as their vehicles are ready for their next day journeys. As shown in Figure 5.6, a charging event shows as colour changes from cold to warm colours that reflect the SOC varying from low to high values. For example, a charging event takes place for two and half hours (from 17:40 to 20:10) for EV 28 and its SOC increases from 0.4 to 1 (full capacity). EV 28 user has the opportunity to delay the charging until its next departure.

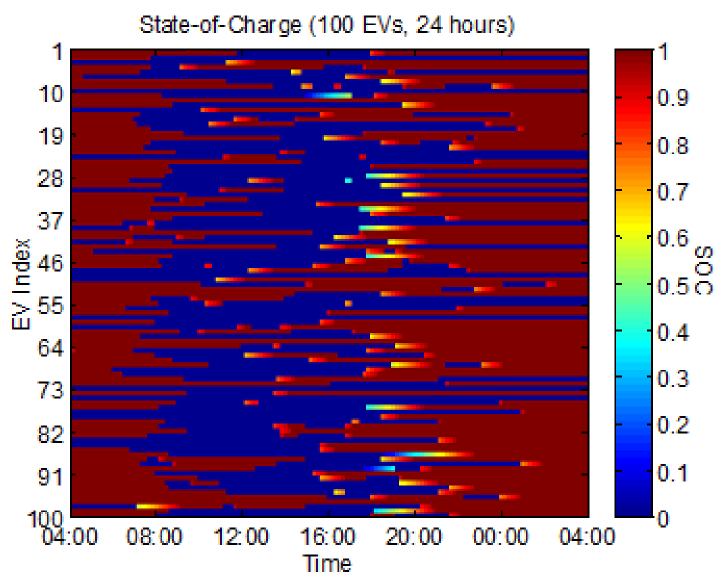

Figure 5.6. State-of-charge of 100 EVs shown as examples.

[30] Charging in the uncontrolled case is assumed to start as soon as the vehicles arrive home.

In this case study, it is assumed that EV owners schedule their charging according to the electricity tariff of surplus wind generation. Before modifying the EV load to absorb the surplus wind power, some constraints must be considered which limit the clustering and shifting the EV loads. The charging time, T_{charging}, of an EV cannot be longer than its parking period T_{parking}. A simple linear electricity price function, $C\left(P_{\text{wind}}\right)$, is assumed that gives the cost of vehicle charging in pence/kWh as a function of the surplus wind power in the local power system.

$$C\left(P_{\text{wind}}\right)=\begin{cases} 0 & P_{\text{wind}} \geq 1 \\ -13.84 * P_{\text{wind}} + 13.84, & 0 < P_{\text{wind}} < 1 \\ 13.84 & P_{\text{wind}} \leq 0 \end{cases} \tag{5.1}$$

where P_{wind} in MW is the surplus wind in the system, 13.84 is the electricity price at the standard charge rate as domestic consumers, [5.19]. A 1 MW surplus wind generation limit has been chosen to reflect assumed power export constraints in the system. For example, if the surplus wind is 0.6MW representing a discount of electricity tariff, the EV charging tariff will then be 13.84 * (1-0.6) = 55.36 pence/kWh. When the wind surplus exceeds 1 MW, the cost of local electricity is assumed to be zero. In these cases, vehicle users can charge their EVs at no cost; however, when there is no surplus wind locally, the electricity price is fixed at the standard charge rate for domestic consumers. The charging cost varies linearly for users only when there is less than 1 MW surplus wind in the system.

The model takes one EV at a time and utilises the cheapest tariffs first to undertake the required EV charging. Depending on the duration of vehicle charging, a previous continuous charging event will now potentially be broken down into several small charging events in order to achieve the most cost effective way to charging the vehicle as well as to satisfy vehicle user's next journey requirement. As a result of the cost model used, the cost of charging is free as long as the surplus wind power is greater than 1 MW. After each individual vehicle charging calculation, the absorbed surplus wind and electricity price is recalculated and made available to the remaining households. Figure 5.7 illustrates the price-driven EV charging load to absorb surplus wind generation a result of this strategy. Results indicate that for the example day, EV charging absorbed 42% of surplus wind and the average charging cost per house for the day analysed reduces from 13.84 pence per unit down to 2.08 pence per unit.

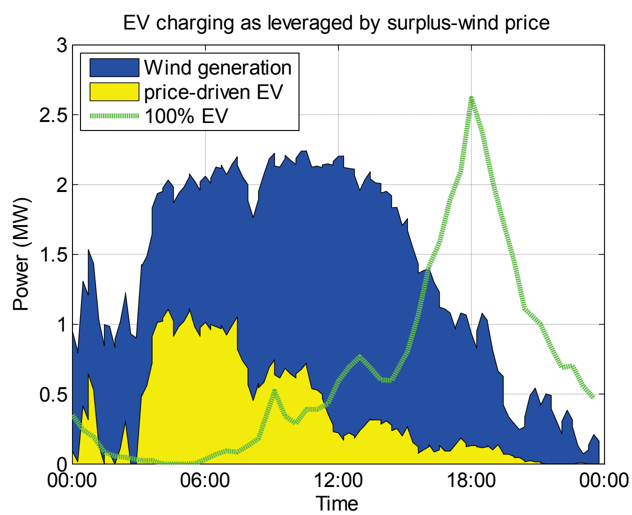

Figure 5.7. Applied strategy for electric vehicle charging as leveraged by surplus-wind price.

5.4. Discussion and Summary

In this chapter, the potential for demand side management inherent in EV charging has been explored with various charging strategies. Strategy 1 presents the simple delay technique to avoid increasing existing domestic peak load; however, the delayed EV charging creates an unwanted additional peak load at the beginning of charging time zone with 32A fast charging. Strategy 2 allows mixed rate charging throughout the day, and the outcome of this technique to only mitigate the peak load rather than completely solve the problem of additional EV charging. These two EV charging strategies, the time delay charging and mix rate of charging, successfully manipulate EV charging load to avoid increasing existing domestic peak load comparing the simple 'plug and charge' strategy. Strategy 3 applies a further random delay to EV charging based on Strategy 1. Such controlled charging approach resolves issue of impact on the domestic peak load, indeed it has been shown that such DSM strategy is capable of smoothing the domestic load profile at key points in the distribution system and thus facilitating an improvement in distribution system operation, as well as operation of the power system as a whole.

Case study 2 presents the capability of utilising electric vehicle charging to regulate surplus wind power by implementing an electricity price function. Real-world wind farm power output monitoring data are used to create a realistic example daily electricity cost function for a locality. For users charging their electric vehicles at minimum cost, the cost function shifts charging to the cheapest electricity time consistent with the EV being parked at home, and thus absorbs as much surplus wind as possible. This enables the wind farm owner to benefit from reduced curtailment of wind generation and financial rewards from electricity supplier when EV users pay for charging. The DNO will benefit from saving on infrastructure reinforcement costs as the proposed DSM scheme shifts EV charging to the off-peak period. For the users, identifies the cheapest way to charge vehicle batteries. In this example day, the cost savings to the consumer associated with EV charging are considerable.

5.5. References

[5.1] H. Davey, J. Hayes, B. Verma, "Maintaining UK energy security – Future electricity networks", 22 January 2013. Access online: https://www.gov.uk/government/policies/maintaining-uk-energy-security--2/supporting-pages/future-electricity-networks

[5.2] S. Huang, D. Infield, The Potential of Domestic Electric Vehicles to Contribute to Power System Operation through Vehicle to Grid Technology, *Proceedings of the 44th International Universities Power Engineering Conference (UPEC)*, Glasgow, 2009.

[5.3] X. Zhong, A. Cruden, D. Infield, S. Huang, Assessment of Vehicle to Grid Power as Power System Support, *Proceedings of the 44th International Universities Power Engineering Conference (UPEC)*, Glasgow, 2009.

[5.4] Bashash, S.; Fathy, H.K., "Robust demand-side plug-in electric vehicle load control for renewable energy management," *American Control Conference (ACC), 2011* , vol., no., pp.929,934, June 29 2011-July 1 2011.

[5.5] W. Di, D. C. Aliprantis, and Y. Lei, "Load Scheduling and Dispatch for Aggregators of Plug-In Electric Vehicles," *Smart Grid, IEEE Transactions on,* vol. 3, pp. 368-376, 2012.

[5.6] S. Deilami, A. S. Masoum, P. S. Moses, and M. A. S. Masoum, "Real-Time Coordination of Plug-In Electric Vehicle Charging in Smart Grids to Minimize Power Losses and Improve Voltage Profile," *Smart Grid, IEEE Transactions on,* vol. 2, pp. 456-467, 2011.

[5.7] Pecas Lopes, J. A., Almeida, P. M. R. and Soares, F. J., "Using vehicle-to-grid to maximize the integration of intermittent renewable energy resources in islanded electric grids," in Clean Electrical Power, 2009 International Conference on, 2009, pp. 290-295.

[5.8] Kempton, W. and Tomic, J., "Vehicle-to-grid power fundamentals: calculating capacity and net revenue," Journal of Power Sources, vol. 144, pp. 268-79, 2005.

[5.9] Kempton, W. and Tomic, J., "Vehicle-to-grid power implementation: From stabilizing the grid to supporting large-scale renewable energy," Journal of Power Sources, vol. 144, pp. 280-94, 2005.

[5.10] Tomic, J. and Kempton, W., "Using fleets of electric-drive vehicles for grid support," Journal of Power Sources, vol. 168, pp. 459-68, 2007.

[5.11] Mitra, P. and Venayagamoorthy, G. K., "Wide area control for improving stability of a power system with plug-in electric vehicles," Generation, Transmission & Distribution, IET, vol. 4, pp. 1151-1163, 2010.

[5.12] Ma, Y., Houghton, T., Cruden, A., and Infield, D., "Modeling the Benefits of Vehicle-to-Grid Technology to a Power System," Power Systems, IEEE Transactions on, vol. 27, pp. 1012-1020, 2012.

[5.13] Ma, Y., Cruden, A., and Infield, D., "A Matlab simulator for electric drive vehicle to grid implementation," in Industrial Technology (ICIT), 2010 IEEE International Conference on, 2010, pp. 1097-1101.

[5.14] R. Carter, A. Cruden, D. Densley, and T. Nicklin, "Timed Charging Points for Electric Vehicles: User Behaviour and Potential Impacts to Low Voltage Networks," in *European Electric Vehicle Congress*, Brussels, Belgium, 2011, p. 7.

[5.15] J. G. Vlachogiannis, "Probabilistic Constrained Load Flow Considering Integration of Wind Power Generation and Electric Vehicles," Power Systems, IEEE Transactions on, vol. 24, pp. 1808-1817, 2009.

[5.16] Zaher A.S., McArthur S.D.J, "A Multi-Agent Fault Detection System for Wind Turbine Defect Recognition and Diagnosis", Power Tech 2007IEEE Lausanne, 1-5 July 2007, pages 22-27.

[5.17] J. Dowell, S. Weiss, D. Hill, and D. Infield, "Short-term spatio-temporal prediction of wind speed and direction," *Wind Energy*, [online], 2013.

[5.18] S. Gill, G. W. Ault, and I. Kockar, "Using dynamic optimal power flow to inform the design and operation of active network management schemes," in *Electricity Distribution (CIRED 2013), 22nd International Conference and Exhibition on*, 2013, pp. 1-4.

[5.19] Scottish and Southern Energy, *'Prices & Tariff Information – Price Fix 7'* [online]: https://www.sse.co.uk/ourprices/historic/?ekfxmensel=1045_1050_1050&postcode=g40%201dr (Accessed 27 June 2013)

6.Chapter 6: Conclusions and Future Work

This chapter presents the conclusions of the thesis. These have been divided into three parts: key findings from domestic car use statistics, lessons learnt from the specification and development of the Monte Carlo models; and key results from the case studies for impact assessment as well as control strategies for demand response. This chapter also summaries the main original contributions of this thesis, and proposes future work for the improvement and further development of the models presented.

This thesis has presented new approach to modelling future electric vehicle charging with high time resolution, and thus quantify the impact on the power distribution network. In additional, a number of control strategies for EV charging have been presented that can mitigate the impact on the distribution system. Case study results demonstrate the capabilities of the various models developed throughout the research. The work presented in this thesis can be used to enable distribution network operators to quantify the potential electric vehicle charging impact on the network.

6.1. Key Findings from Domestic Car Use Statistics

Detailed analysis of privately owned car use in the UK has been presented in Chapter 2 based on the United Kingdom Time of Use Survey 2000 data. The reasons for choosing TUS data as the main data source for this research was explained, in particular the much higher time resolution than other UK sources such as the United Kingdom National Travel Survey. Preliminary analysis shows that majority of households in the survey has only one car. Privately owned cars are utilised only 5.2% of the time for transportation, thus making them, in principal, available for the remaining 94.8% of time to provide ancillary services to the power system. The focus is on car use during the working week as this is when most power network problems are anticipated. Probabilistic characterisation of car usage during weekdays has been undertaken that covers time of use, and duration of use dependent on the time that a car arrives home, and also as dependent on the round trip duration, and both of these as a function of the time of day. For example, during weekdays, over 90% of cars park at home between mid-night and 06:00 in the morning. More than 50% of cars are used to travel to workplaces in the morning and late afternoon. Another important statistical feature is that the highest probability of a car returning home during weekdays occurs around 18:00 hour, reflecting in the main return from work. Various challenges were encountered in the search for good quality data on the use of privately owned cars and also the derivation of car use statistics. For example, due to the daily nature of survey diaries, it is not possible to know exactly the time car returns home if it departs late in the diary day.

6.2. Lessons Learnt in Monte Carlo Modelling

Monte Carlo simulation is widely regarded as the best approach to generate synthetic individual car use patterns, as has been explained in Chapter 3. In order to utilise the statistics calculated in Chapter 2, the inverse-transform method has been used to structure three different MC models. The return time dependent MC model had the advantage of only needing two car use statistics and was found to converge with relatively less iteration than fixed time increment and multiple time increments MC models, which means reduced computational time. This approach can only partially capture car use patterns, but it gives a reasonable estimate and includes the distribution of car driving time (the main objective of the MC models). Both fixed time increment and multiple time increments MC models can generate car parking locations and departure and arrival events by sampling from different statistical distributions. The outcome of the multiple time increments MC model has been used to calculate the modification of individual household electricity consumption caused by EV charging (Chapter 4). For each MC model, detailed analysis has been performed on the simulation results to check convergence and also to check consistency with the TUS input data. Cumulative driving period is the most critical parameter for vehicle charging calculations. Both time increment MC models and the return time dependent MC model produced a mean driving period within an acceptable range, with the multiple time increments MC model being most accurate in this regard. Both time increment MC models produced some errors in car use patterns. Significant error occurred in car away from home period in the fixed time increment MC model. As a consequence, the calculated cumulative car driving periods were in poor agreement with the TUS data. The multiple time increments

MC model produced significant error in the estimation of the probability of car arrival. The bias in the simulation of car arrival is caused by the modelling error in the calculation of the probability of the car being away from home. To resolve this error, a different Monte Carlo simulation method might be helpful; however, this is beyond the scope of this research and is left for future research.

6.3. Key Results from the Case Studies

The results from the case studies are presented and discussed in the Chapter 4 and 5. Although the results from the case studies are related to the specific household population and network typology, some general conclusions were identified. Key findings are highlighted here. The first case study discussed the impact on the primary and secondary distribution transformer for a residential area (Chapter 4). The worst case scenario is that vehicle charging takes place on a typical winter weekday. As the key outcome of the impact analysis for this specific network typology, even a modest 10% EV take-up with simple 'plug and charge' charging strategy can result in a considerable increase in peak load at primary substation transformers. For the secondary substation transformer, mean EV charging increased the existing peak load by 15%; with possible peaks up approximately 50%. Note that same charging strategy has been applied. For higher EV penetrations, charging impact on the substation loading significantly increases the peak load as much as three times. The second case study focuses on the vehicle charging impact on the LV network (Chapter 4). Despite the specific network configuration, the power flow calculation results show that unacceptable household voltage drops occur before the feeder thermal rating is exceeded. As a result, appropriate demand side management scheme needs to be implemented so that vehicle charging impact can be mitigated. Chapter 5 presents the development of several control strategies for vehicle charging for two case studies. Strategies 1 to 3, for case study 1, aim to mitigate the impact of vehicle charging on the primary substation transformer loading. In case study 2, the control strategy utilises electric vehicle charging to help absorb otherwise surplus wind power by implementing an electricity price function. It has been assumed that the EV owner is informed about the surplus wind tariffs for the day ahead and this in turn assumes that the power output from the wind capacity is forecast perfectly for the day ahead. As the outcome of this case study, for the example day, EV charging absorbed 42% of the surplus wind and the average charging cost per house for the day analysed reduces from 13.84 pence per unit down to 2.08 pence per unit. This demonstrates the potential of power distribution network operators to benefit from the reduced curtailment of wind and for the users, to reduce the cost of charging their vehicle batteries.

6.4. The Contribution to the Knowledge

The following contributions of this thesis have been identified as novel and important:

1. **It analyses car use in detail from the United Kingdom Time of Use Survey 2000 (Chapter 2).** Key statistics for weekday car usage have been identified and from these, key probabilities and probability distributions of weekday car usage, such as departure time, arrival time, cumulative driving period dependent on arrival time, etc. have been estimated.

2. **It presents different approaches to modelling domestic car use (Chapter 3).** Chapter 3 presents three high time resolution time-series Monte Carlo simulation models. A return time dependent MC model focuses on the car

arrival time and the associated cumulative driving period. Two time increment MC models follow weekday car movements. A comprehensive analysis has been performed to check the modelling results against the TUS statistics.

3. **It presents a model of individual household electricity consumption that takes in account domestic car use (Chapter 4).** In Chapter 4, an individual household electricity consumption model has been modified to include the electricity consumption changes due to car use through associated changes in household active occupancy.

4. **It presents an assessment of electric vehicle charging impact on power distribution network (Chapter 4).** Electric vehicle charging load has been calculated based on the simulation results of return time dependent MC model in Chapter 3. Chapter 4 presents the potential impact of future electric vehicle charging by performing assessment on primary and secondary substation transformers. The impact on the LV network of EV charging has been studied by performing power flow analysis.

5. **It illustrates the development of control strategies to mitigate the impact of electric vehicle charging (Chapter 5).** Chapter 5 illustrates 'time-shifting' charging strategies to utilise EV charging as responsive load in the power distribution system. EVs charging has also been scheduled to absorb local surplus wind generation, taking into account the numbers of EVs parked at home and available for charging at any time of day.

6.5. Future Work

Further work for the improvement and extension of the Monte Carlo models developed and the analysis technique applied in this thesis has been identified. Three main avenues of research are suggested. One is related to the further development of the multiple time increments Monte Carlo model to include workplace charging. The second one is to develop a Markov Chain Monte Carlo model for privately owned car use. The third one is to perform probabilistic power flow analysis for electric vehicle charging impact on the distribution network.

6.5.1. Further Development of the Multiple Time Increments Monte Carlo Model

In this thesis, the home has been regarded as the primary location for electric vehicle charging, although other locations can offer vehicle charging, such as the workplace, supermarket, public car parking, etc. In recent electric vehicle trials, such as in [6.1], vehicle owners have the opportunities to charging their vehicles at their workplace without paying for the electricity. It is common that workplace charging offers high charging rates and even 3-phase charging. With the further deployment of electric vehicles, workplace charging will become more popular for vehicle owners. UK Time of Use Survey 2000 has recorded the information regarding people travel to workplace by car as presented in Chapter 2 section 2.3.4. Furthermore, in Chapter 3 section 3.3.2.3, Multiple Time Increments Monte Carlo model for domestic car use has been structured following the logical sequence through the day; for example, time of day car departs from home, time of day car returns home. It is reasonably feasible to incorporate the statistics of people who travel to the workplace by car with the Multiple Time Increments MC model. Furthermore, the driving styles, such as driving velocity and acceleration, need to be considered in order to produce more accurate battery energy consumption figure, which is assumed as constant in this thesis. The driving style has effects on the battery state of charge as well as state of health; therefore, it is necessary to obtain relevant statistics.

6.5.2. Develop Markov Chain Monte Carlo Model for Privately Owned Car Use

In Chapter 3, section 3.3.2.2, the fixed time increment Monte Carlo model utilise two-state probability distributions of car departs from home and probability distributions of car returns home. However, car departure and arrival home have been treated as two independent events, which results some error. A rather different modelling approach has been presented that implemented a Markov Chain methodology in modelling domestic car daily driving patterns, [6.2]. Domestic car daily driving patterns are simulated based on the transition probability matrices, which presents states of car activity at each time step. The Markov Chain Monte Carlo (MCMC) model still follows the logical sequence through the day. The transition probability matrices can be easily calculated from the processed Time of Use data that presented in Chapter 2. In such a modelling approach, the relationship between various car activities can be simulated with the multi-state transition probability matrices. It will be interesting to see whether the simulation results of the MCMC model are consistent with the calculated TUS statistics.

6.5.3. Perform Probabilistic Power Flow Analysis for Electric Vehicle Charging Impact on Distribution Network

Case study 2 in Chapter 4 section 4.2, presents impact assessments of electric vehicle charging on the LV network; however, only one set of electric vehicle charging profiles are used in the power flow analysis. In order to obtain the statistical variation of EV charging impact, probabilistic and long period time-series load flow techniques are being increasingly used to provide the kind of analysis necessary to capture the stochastic nature of LV customer load profiles and distributed energy resources behaviour, such as in [6.3]. Probabilistic power flow can be undertaken using MC simulation, and in that case the approach would not significantly differ from the power flow analysis of Chapter 4. However there are faster closed form approaches to probabilistic power flow that could be undertaken using probability distributions for EV charging. This could be an interesting exercise, but it is unclear how the time of day dependence would then best be captured.

6.6. Reference

[6.1] S. Huang, et al, *Battery Electric Vehicle Academic Study Report*, tech. report, University of Strathclyde, 2014.

[6.2] Grahn, P. (2013) *Electric Vehicle Charging Impact on Load Profile*. PhD Thesis. Royal Institute of Technology, Sweden.

[6.3] D. Frame, G. Ault, "A Framework for Probabilistic Planning and Analysis of Low Carbon Technology Integration into LV Networks," internal technical report, University of Strathclyde, 2014.

Appendix A: United Kingdom Time of Use Survey 2000 Data Processing

A.1 Data Extraction

A programming script has been coded in Microsoft Visual C# 2008. The function of C# script is to extract the selected columns in the original database in order to form a new database, which containing 'Location and mode of transport' and 'Travel by Purpose' information. The function of the C# code is to locate the required variable label and extract the whole variable value for each diary entry. Extracted data contain 'Location and mode of transport' and 'TRAVEL BY PURPOSE' information. The coded information provides considerable detail level of domestic car use at each specific time slot, where the database is on ten-minute basis. Inputs file is in 'tab' formation and outputs file has been formed in Excel readable formation.

A.2 Diary Code Dictionary

In 'Location and mode of transport' database, domestic car parking location codes indicate where these cars parked. At the same time, the database shows how people travelling by mode of transport. Specific code, '15' in 'Location and mode of transport', express people travelling by passenger car as the driver. This valuable information allows us to track each household car use, which contributes to probabilistic model of domestic car use. Other codes state the car location as shown in the table below. Table A-1 and Table A-2 lists the variable value and its related information, which used to calculate the car use statistics of the TUS data.

Table A-1. Diary location code explanation.

Location	Information
2	Home
3	Second home or weekend house
4	Working place or school
5	Other people's home
15	Travelling by passenger car as the driver

Table A-2. Diary activity code explanation.

Activity	Information
110	Sleep
9130	Travel to work from home and back only

A.3 Loop-back Technique

In this section, the loop-back technique is explained and applied to calculate the car away from home period and car parking at home period for the UKTUS 2000 data. The loop-back technique goes back to the beginning of the diary as it calculates either away period of time or parking period of time. The main advantage is that it solves the issue of 24-hour time limitation of the original data format and it is saving process time for matching correct diaries. The disadvantage of this technique is that the results are not as precise as the calculation method for continuous diaries and could create significant errors. Figure A.1 shows the histogram of car away from home that calculated from the TUS data. It is clear that the longest away period does not exceed the diary day time limits (24 hours from 04:00 hour to 03:50 hour next day). Results that applied with loop-back technique agrees well with the calculation without the loop-back technique. This indicates that the loop-back technique does not affect the car away period calculation.

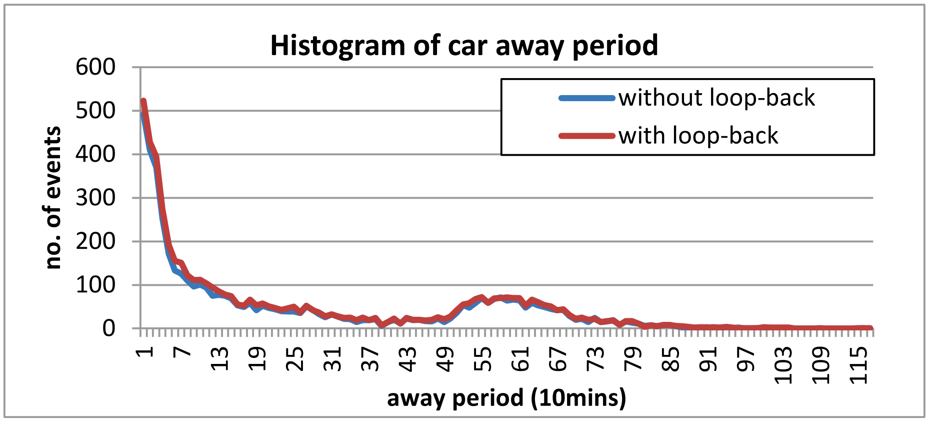

Figure A.1. The frequency distributions that car away from home.

Figure A.2 illustrates the calculation results for car parking at home period. It is obvious that the loop-back technique has huge impact on the parking period calculation. In fact, it causes almost half of the differences between the calculation methods.

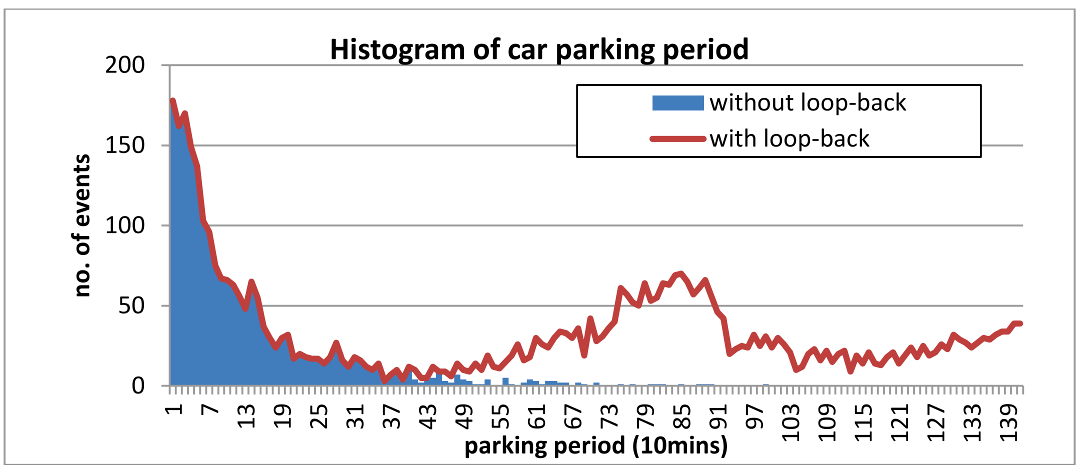

Figure A.2. The frequency distributions that car parking at home period.

A.4 Probability of each individual driving period.

Table A-3 provides the corresponding data for journey durations calculated from the TUS data, the longest journey recorded is 420 minutes (7 hours).

Table A-3. Probability of each individual driving period.

Driving period (10 mins)	Counts	Probability	Driving period (10 mins)	Counts	Probability
1	4076	0.38	22	2	$0.02*10^{-2}$
2	2502	0.23	23	4	$0.04*10^{-2}$
3	1811	0.17	24	3	$0.03*10^{-2}$
4	899	0.08	25	1	$0.09*10^{-3}$
5	506	0.05	26	2	$0.02*10^{-2}$
6	335	0.03	27	0	0
7	160	0.01	28	2	$0.02*10^{-2}$
8	114	0.01	29	1	$0.09*10^{-3}$
9	86	0.01	30	0	0
10	44	$0.04*10^{-1}$	31	0	0
11	25	$0.02*10^{-1}$	32	0	0
12	25	$0.02*10^{-1}$	33	0	0
13	19	$0.01*10^{-1}$	34	0	0
14	10	$0.09*10^{-2}$	35	0	0
15	9	$0.08*10^{-2}$	36	1	$0.09*10^{-3}$
16	9	$0.08*10^{-2}$	37	0	0
17	6	$0.05*10^{-2}$	38	0	0
18	12	$0.01*10^{-1}$	39	0	0
19	2	$0.02*10^{-2}$	40	0	0
20	2	$0.02*10^{-2}$	41	1	$0.09*10^{-3}$
21	2	$0.02*10^{-2}$	42	1	$0.09*10^{-3}$

Appendix B: Low Voltage Network Data

B.1 Distribution Network GIS information

The GIS map shows the single phase premises supports by the common service cable and then connects to the 3-phase main wire in Figure B.1. The type of the single phase connection is known as 'Mural cabling'; however, it is understood as non-standard service type. The definition of mural cabling can be explained in the context as for the terraced housing, there is a common service cable cleated to the front of the premises. This type of wiring is used in the past to save on the overall length of cable.

[1] Mural cabling is defined as cables clipped along the wall from an underground or overhead span joint position. This specific type of LV network configuration has a rather long single phase service cable to support a series of households, and can potentially lead to voltage issues when there is EV charging at the end of the cable as discussed in Chapter 4. More details is available at: E.On Central Networks, *Notes of guidance for service alterations*, http://www.eon-uk.com/images/13715_Service_Alteration_Guidance_AW.pdf

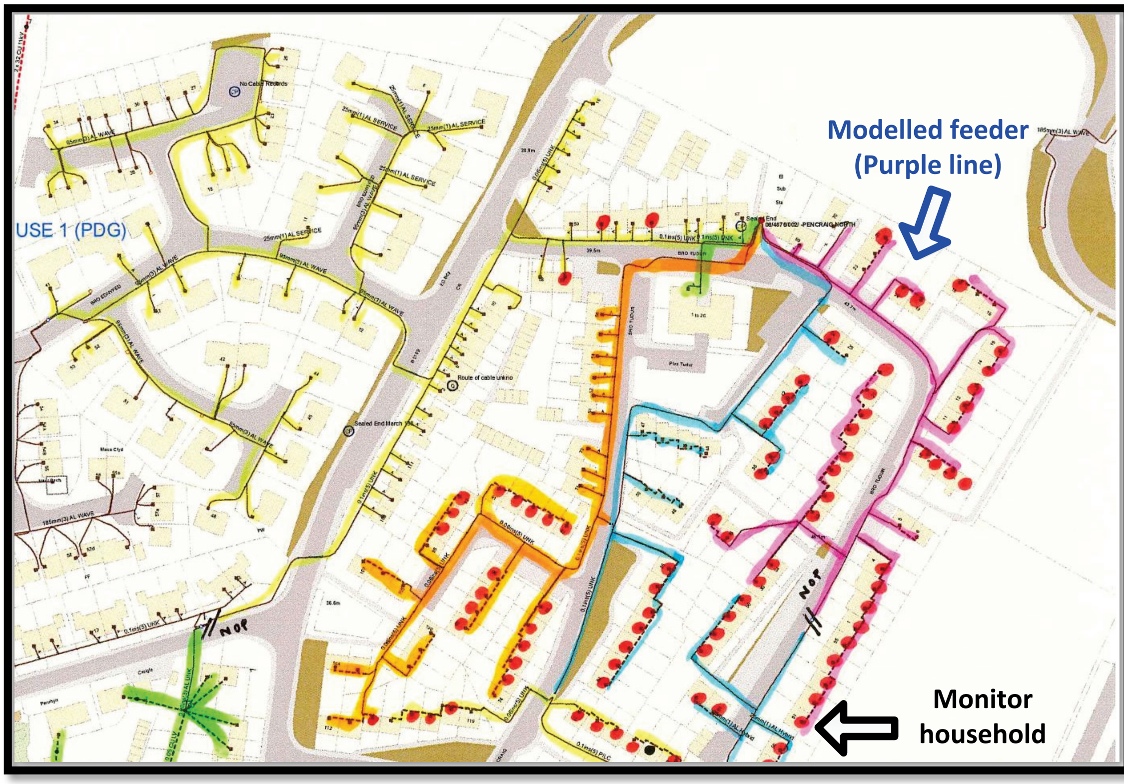

Figure B.1 GIS map for the modelled distribution network.

B.2 Premises Phase Allocation

The single premise phase allocation information is not available from substation monitoring data. The methodology of allocating the single premise phase on the 3-phase connection has been developed and will be discussed in the following section.

In order to determine the premise phase allocation information, one-week period of substation feeder monitoring data was selected for the analysis. The selected one week data starts 9th May 2011 and ends 15th May 2011, which includes the information of voltage, current and real power of each phase. Figure B.2a, b and c show the 3-phase real power profile of the one-week monitoring data.

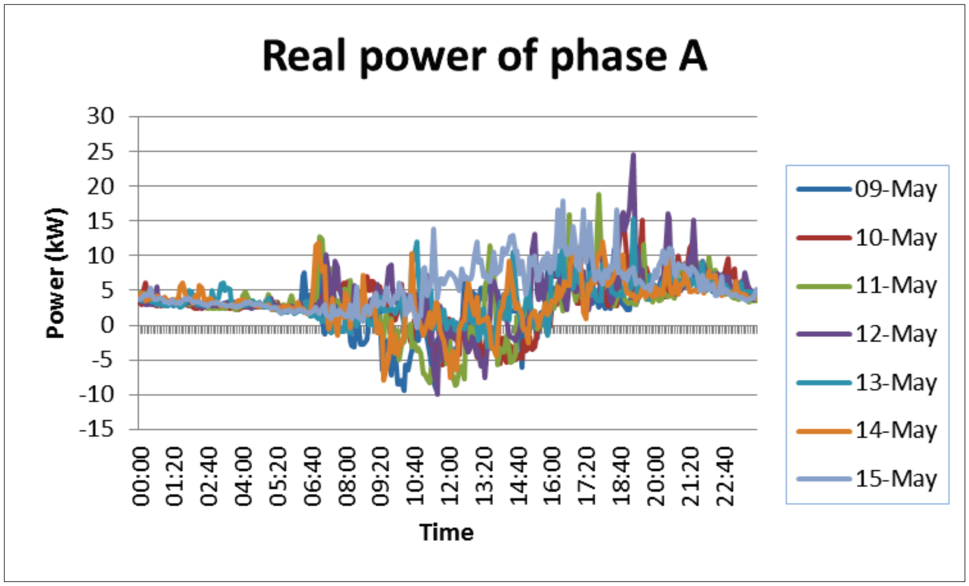
Real power of phase A
Power (kW)
Time
30
25
20
15
10
5
0
-5
-10
-15
00:00
01:20
02:40
04:00
05:20
06:40
08:00
09:20
10:40
12:00
13:20
14:40
16:00
17:20
18:40
20:00
21:20
22:40
09-May
10-May
11-May
12-May
13-May
14-May
15-May

(a)

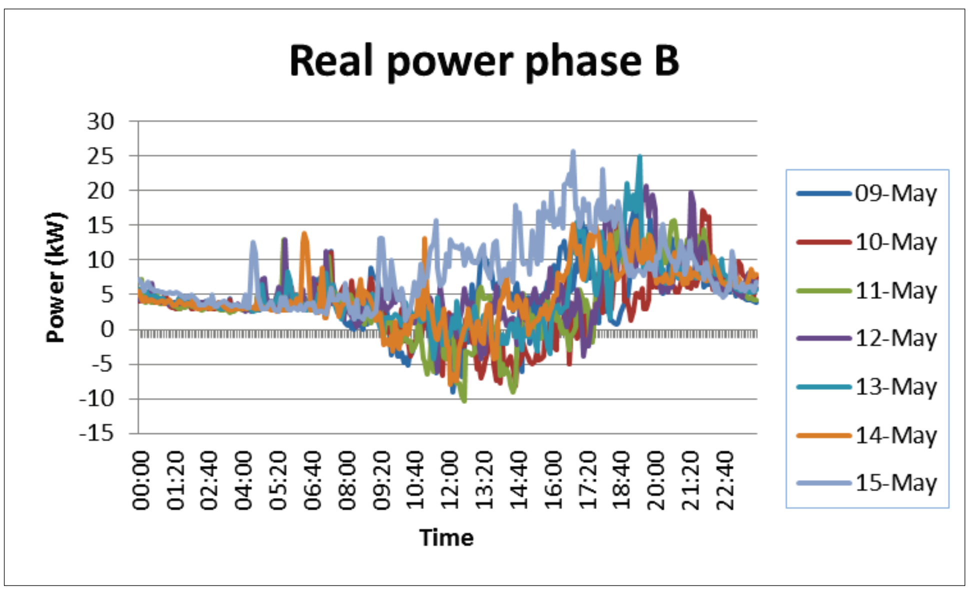
Real power phase B
Power (kW)
Time
30
25
20
15
10
5
0
-5
-10
-15
00:00
01:20
02:40
04:00
05:20
06:40
08:00
09:20
10:40
12:00
13:20
14:40
16:00
17:20
18:40
20:00
21:20
22:40
09-May
10-May
11-May
12-May
13-May
14-May
15-May

(b)

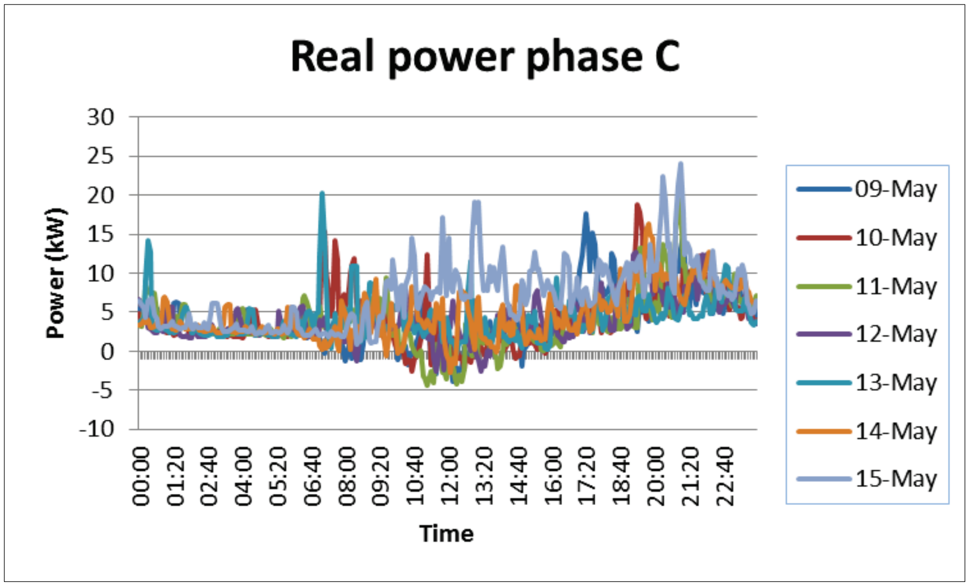

(c)

Figure B.2. The real power measurement data for the feeder. (a) phase A. (b) phase B. (c). phase C.

The one-week real power monitoring data has been aggregated into a 24-hour profile in order to determine the loading on each phase as illustrated in Figure. B.3. The purpose of the aggregation is to avoid the load deviation between different days and improves the determination of the average loading profile on each phase. The measurement data contains the electricity generated from the PV module installed at the monitor household. The PV module produces zero power during night time; therefore, it is reasonable to use the real power profile between 1:50 am and 3:50 am in order to determine the proportion load on each phase as shown in Figure. B.4.

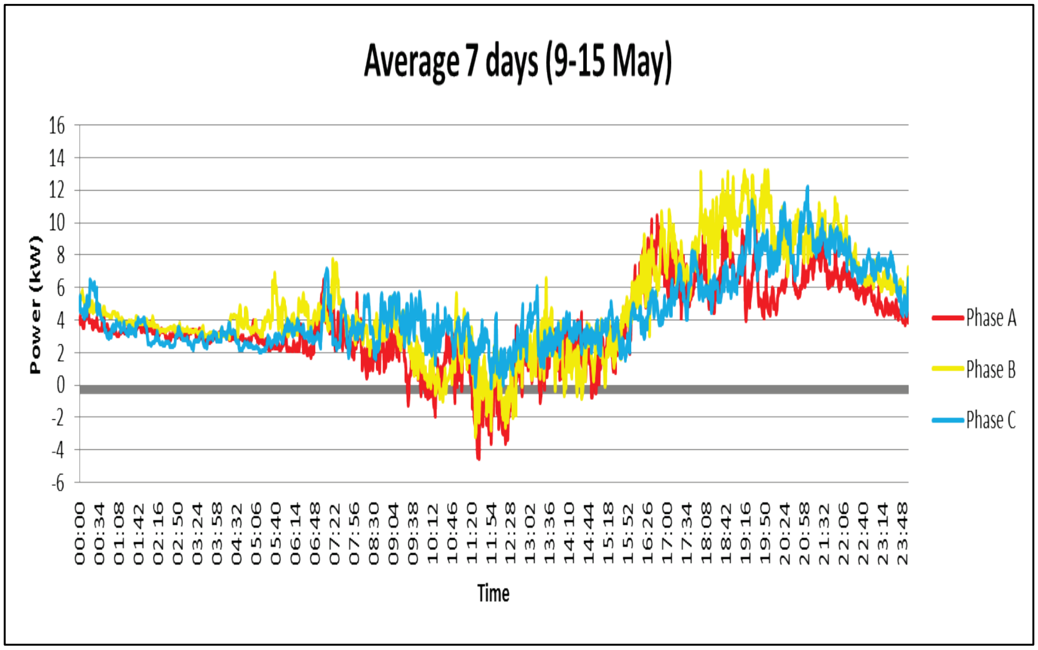

Figure B.3 The aggregated 7-day profile of real power data.

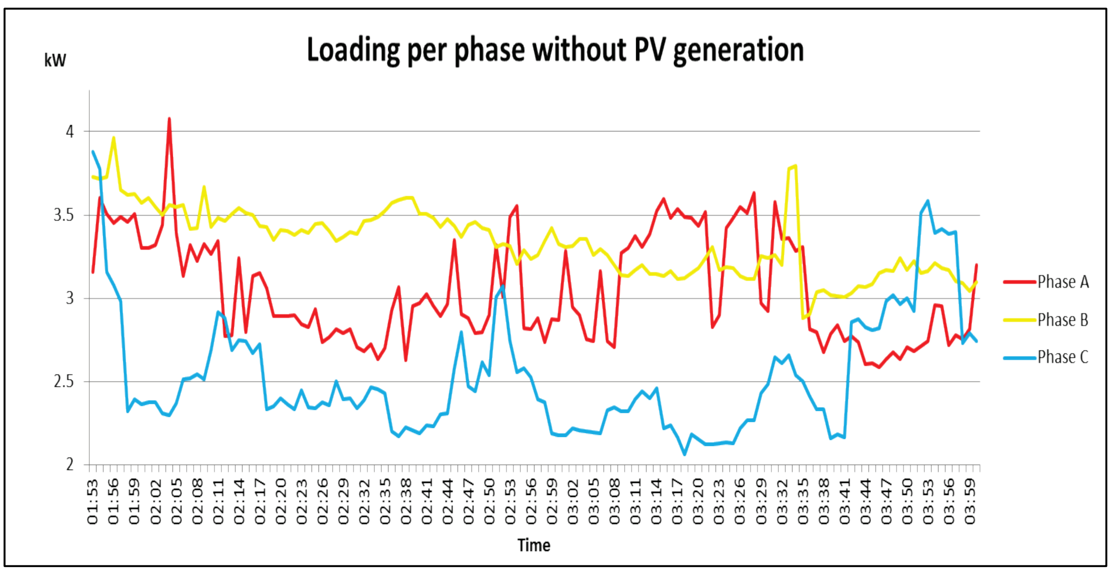

Figure B.4 The 3-phase loading on each phase between 1:50am and 3:50am of the aggregation profile.

By summing up the loads on each phase, the proportion of load on each phase can be calculated as the following:

$$\% \, phase \, load = \frac{total \, phase \, load}{total \, 3 \, phase \, laod}$$

As a result, the proportion of loading on each phase is fairly balanced with Phase B having few percentages more than other two phases. The percentages of loading on each phase are 32.85% for Phase A, 36.76% for Phase B and 30.39% for Phase C. The number of premises allocated on each phase is listed in Table B-1. Figure B.5 shows the percentage of loading on each phase based on the 7-day aggregation load profile from 9th May 2011 to 15th May 2011.

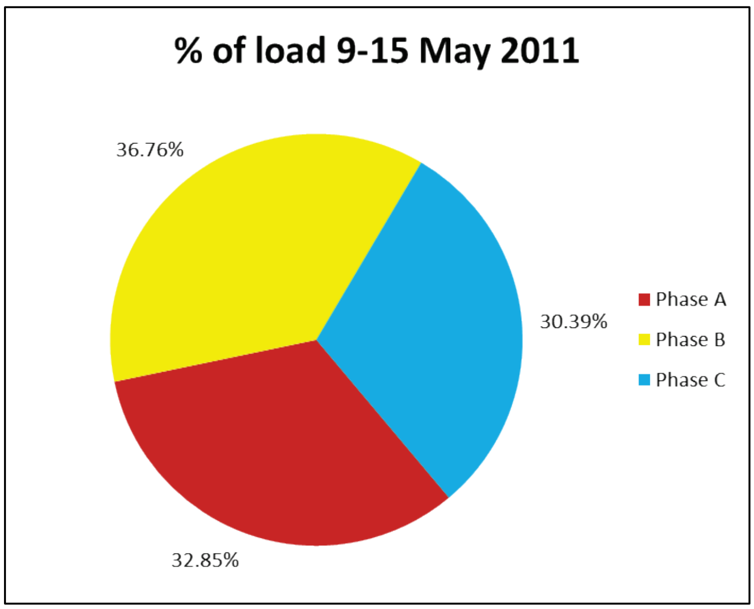

Figure B.5. The proportion of loading on each phase based on the aggregated load profile from 9th May to 15th May 2011.

Table B-1. Number of premises allocated on each phase.

	Phase A	Phase B	Phase C
% load	32.85	36.76	30.39
No. of premises	13	16	13
Total premises	42		

The number of premises allocated on each phase has been assumed based on the structure of the single line diagram shown in Figure 4.8. Two heavy load branches are assumed to be on different phase in order to get the most accurate loading on each phase, which has been validated by Scottish Power engineer. The premise No. 55 connects one of the two heavy loading service branches as shown in Figure single line diagram. Therefore, the phase allocation of premise No. 55 can be applied to other premises with the same service cable connection. In order to determine the phase of premise No. 55, the voltage profile has been analysed during the time period of the substation measurement profile. Figure B.6 shows the voltage profile of premise No. 55 and substation feeder between 1am and 5am.

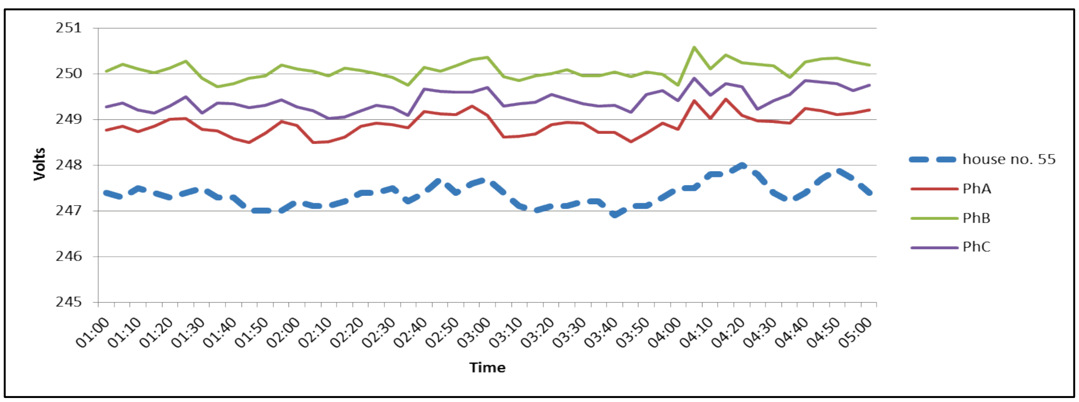

Figure B.6. Voltage profile of premise No. 55 and substation feeder between 1am and 5am.

The dashed line indicates the voltage measured at premise No. 55 and the red, blue, yellow lines are showing the voltage measured at substation feeder. It is clear that the voltage value of premise No. 55 is below the substation feeder voltages due to line loss and power consumptions. Another difference between these two sets of voltage profiles is the synchronisation of the measurement data as shown in Figure B.7. There is approximately one hour time difference between two voltage profiles. The synchronisation problem has been adjusted. The adjusted voltage profile of premise No. 55 compared with the substation feeder voltage profiles is shown in Figure B.8a, b, c.

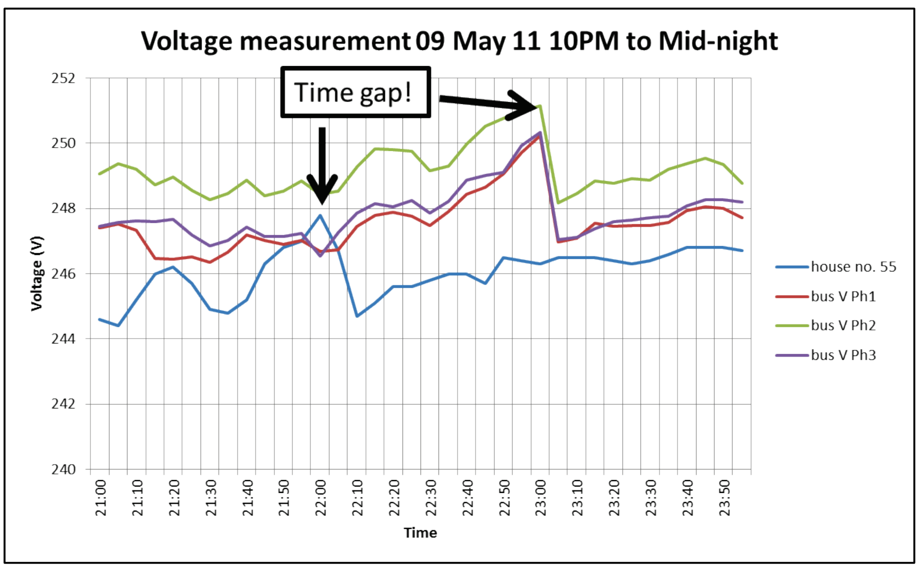

Figure B.7. Premise No. 55 monitoring data is not synchronised with the substation monitoring data.

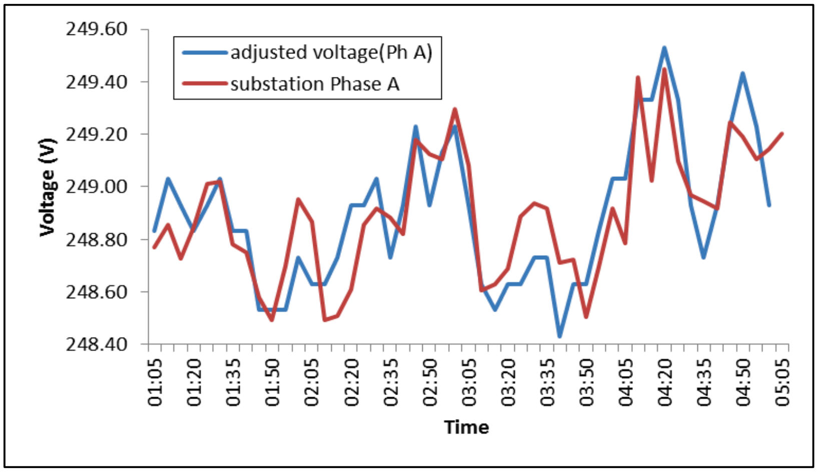

(a)

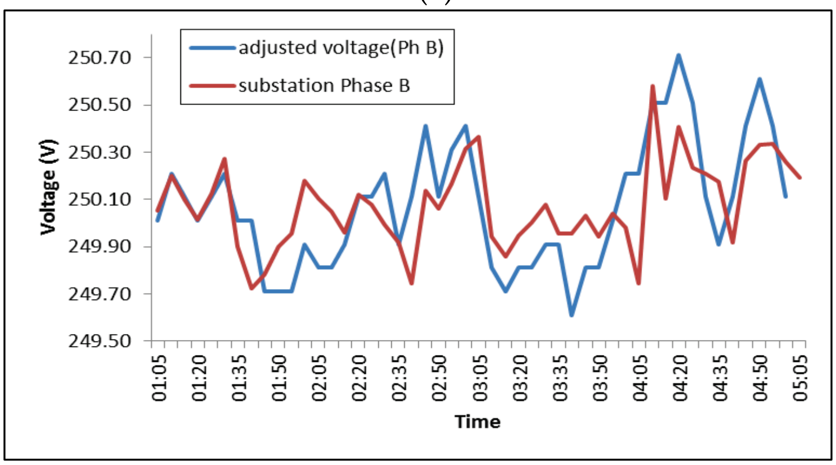

(b)

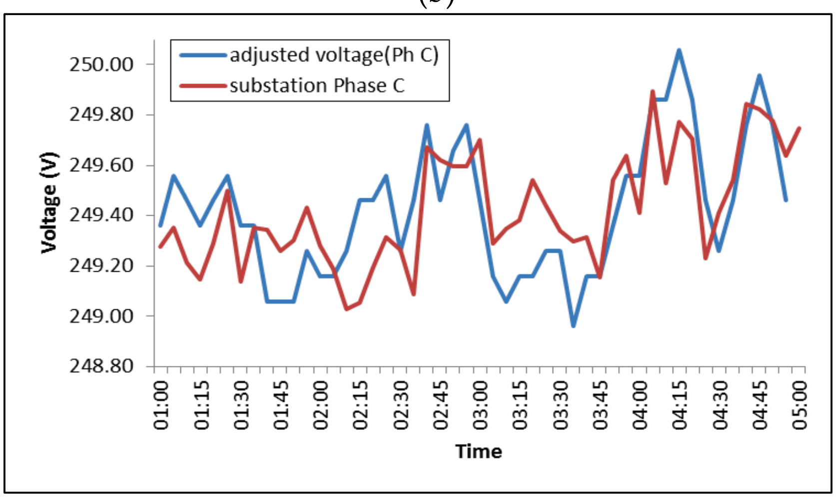

(c)

Figure B.8. Adjust premise No. 55 phase voltage compare with substation phase voltage. (a) Phase A; (b) Phase B; (c) Phase C.

From the Figure B.8a, it is obvious that premise No. 55 voltage is in phase with substation phase. Premise No. 55 is on the branch of 9 premises attached single phase service cable; therefore, that single phase service cable is in phase A. From the substation real power monitoring data as shown in Figure B.2. and Figure B.3, loads of Phase A and Phase B have higher compensation from the PV generation during daylight period than Phase C. Therefore, it is reasonable to assume that Phase A and Phase B have higher PV generation than Phase C.

Appendix C: Household Electricity Consumption Change Due to Car Use

The CREST model generates individual household electricity consumption based on active occupancies. The use of car changes the household active occupancies. Therefore, when the car departs from home or arrives back home, it also indicates that a person sets off or returns home at that specific time. It has been defined that '-1' means one person drives a car away from home, and '0; means one person drives a car back home. When integrating car use Monte Carlo model with household electricity consumption model, it has been assumed that active occupancies reduces by one if a car use is '-1' and remains unchanged when car use value is '0'. Therefore, the active occupancies for each time step reduces by one when there is a car departing from home; otherwise, the active occupancies remains the same. Figure C.1 shows the household electricity consumption change due to car use.

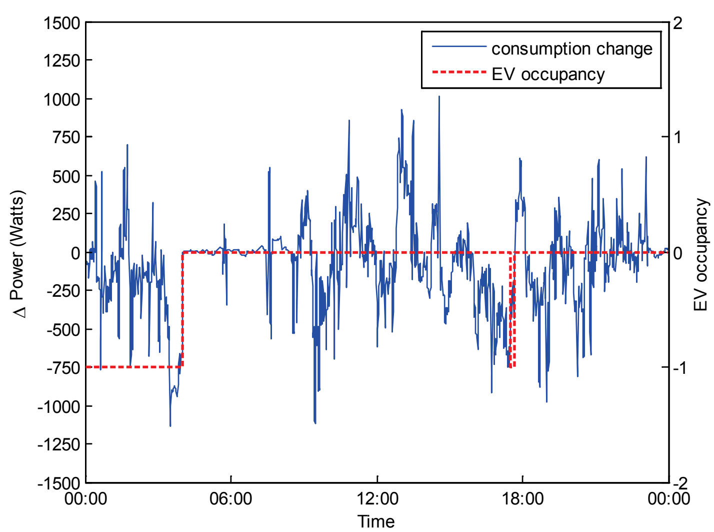

Figure C.1. Household electricity consumption change due to car use.

Appendix D: Power Flow Results for Cable Currents and Household Voltage Profiles

In Chapter 4 section 4.2.6, impact of electric vehicle charging has been assessed on the LV network. Feeder loading increased EV charging is presented in Figure 4.12 and maximum feeder loading is illustrated in Figure 4.13. Table D-1 gives the value of maximum feeder loading with EV penetration varying from 0% to 100%.

Table D-1. The maximum feeder loading as the power flow results.

EV penetration	Max Load of the day (kW)
0%	50.936
10%	57.177
20%	57.177
30%	64.961
40%	64.961
50%	67.479
60%	76.971
70%	83.517
80%	83.517
90%	91.509
100%	91.504

Voltage profiles at monitored household are shown in Figure 4.14 and 4.15. Table D-2 shows the value of minimum voltages at the monitored household with EV penetration varying from 0% to 100%.

Table D-2. The minimum voltage level at the monitored household.

EV penetration	Minimum voltage (p.u.)
0%	0.94344
10%	0.94344
20%	0.93276
30%	0.93716
40%	0.92772
50%	0.91188
60%	0.88052
70%	0.88052
80%	0.88052
90%	0.88052
100%	0.88052

EV charging creates a new peak load of 7.8 kW at household 52 from 11:30 to 12:05. For household 51, EV charging occurs three periods (04:25 to 05:19, 14:40 to 15:38, 17:20 to 17:27).

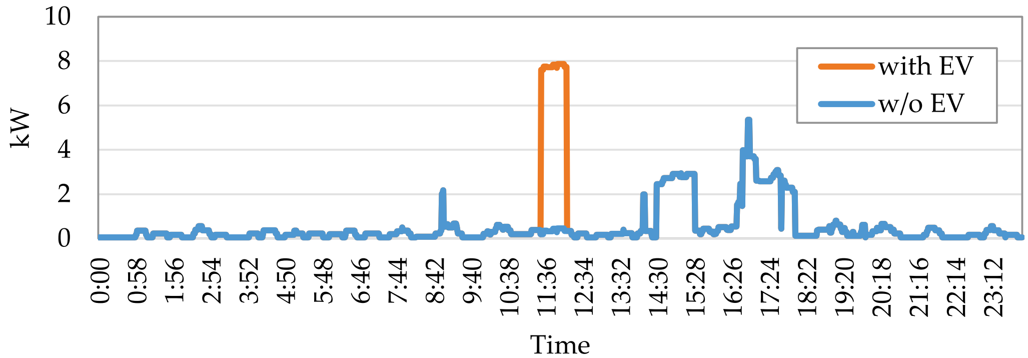

Figure D.1. EV charging impact on Household 52 electricity profile.

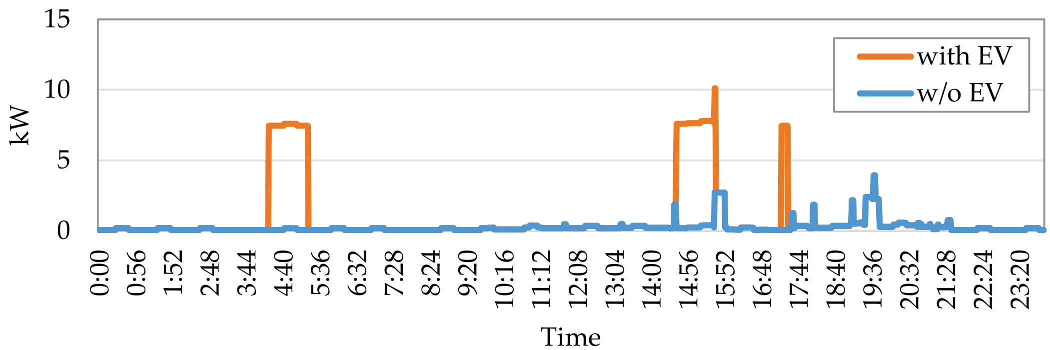

Figure D.2. EV charging impact on Household 51 electricity profile.

The peak load remains the same for 10% and 20% EV penetration level; however, for the 20% EV penetration level, the peak load has been increased when EV charging takes place.

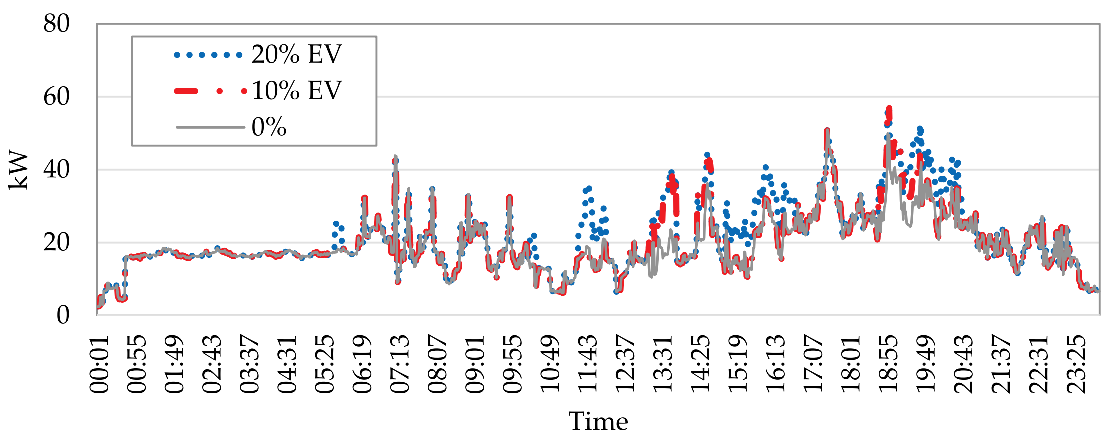

Figure D.3. Secondary substation feeder loading with EV charging.